Thermal Pollution in Urban Streams of the North Carolina Piedmont

by

Kayleigh A. Somers

University Program in Ecology
Duke University

Date:_____

Approved:

_____
Emily Bernhardt, Co-Supervisor

_____
Dean Urban, Co-Supervisor

_____
Martin Doyle

_____
Brian McGlynn

Dissertation submitted in partial fulfillment of
the requirements for the degree
of Doctor of Philosophy
in the University Program in Ecology
in the Graduate School
of Duke University

2013

ABSTRACT

Thermal Pollution in Urban Streams of the North Carolina Piedmont

by

Kayleigh A. Somers

University Program in Ecology
Duke University

Date:_____

Approved:

_____
Emily Bernhardt, Co-Supervisor

_____
Dean Urban, Co-Supervisor

_____
Martin Doyle

_____
Brian McGlynn

An abstract of a dissertation submitted in partial
fulfillment of the requirements for the degree
of Doctor of Philosophy
in the University Program in Ecology
in the Graduate School of
Duke University

2013

Abstract

Currently, cities comprise 52% of the Earth's land surface, with this number expected to continue to grow, as most of the predicted 2.3 billion increase in population over the next 40 years is expected to occur in urban areas (United Nations Population Division 2012). Urban areas necessarily concentrate food, energy, and construction materials, and as a result tend to be hotter and more polluted than the surrounding landscape. All urban ecosystems are thus quite altered from their pre-urban state, but urban streams are particularly impacted. As low lying points on the landscape, streams are subject to the degradation caused by urban stormwaters, which are transmitted rapidly from the surfaces of pavements, roofs, and lawns through stormwater infrastructure to streams.

The systematic changes seen in many urban streams have been described as the "Urban Stream Syndrome" (USS) and serve as an organizing conceptual framework for urban stream research (Walsh et al. 2005b). A primary symptom of USS is increased flashiness in hydrographs, as stormwater in urban areas is routed efficiently into streams (Booth and Jackson 1997, Konrad and Booth 2005). With this stormwater runoff comes intense scour leading to deeply incised channels, large amounts of contaminants and nutrients, and, as will be discussed in this thesis, heat surges (Booth 1990, Tsihrintzis and Hamid 1997, Walsh et al. 2005a, Nelson and Palmer 2007, Bernhardt et al.

2008). At baseflow, urban streams are contaminated by sanitary sewage leakages, are unable to exchange water with their floodplains due to incision and with groundwater due to lower water tables, and are warmer due to canopy loss and urban heat island effects (Paul and Meyer 2001, Pickett et al. 2001, Groffman et al. 2002, 2003). These baseflow and stormflow changes lead to the loss of sensitive taxa and increase in tolerant biota, as well as changes in ecosystem function, including carbon and nitrogen processing (Paul and Meyer 2001, Meyer et al. 2005, Imberger et al. 2008, Cuffney et al. 2010).

The urban heat island effect can increase air temperatures up to 10°C above those in surrounding, non-urban areas, while impervious surfaces can reach temperatures up to 60°C (Asaeda et al. 1996, Pickett et al. 2001, Kalnay and Cai 2003, Diefenderfer 2006). These changes are particularly troublesome, as research has shown that temperature is a controlling factor in aquatic systems for both stream biota and ecosystem processes (Allen 1995, Kingsolver and Huey 2008). Thermal changes control and can alter basic morphological features of biota, such as size and growth rates (Gibbons 1970, Kingsolver and Huey 2008). USS synthesis reports have called for further research into the processes by which urban areas influence the temperature of streams and the resulting effects on the ecosystems, but until recently have largely been ignored (Paul and Meyer 2001, Wenger et al. 2009). This dissertation explores the timing, magnitude, and pattern of thermal pollution for streams within urban heat islands, with the goal of understanding

what aspects of watershed development most strongly influence the thermal regimes of streams.

In order to explore thermal pollution in urban streams, I asked three overarching questions:

1) How much hotter are highly urban streams than streams in less developed watersheds?

2) How far do urban heat pulses propagate downstream of urban inputs?

3) How can development *configuration* mitigate or exacerbate development *amount* in mediating urban thermal pulses?

In Chapter 2, I explore the differences in baseflow and stormflow temperatures in 60 watersheds across the North Carolina Piedmont that ranged across a gradient of urbanization. I asked:

1) How do maximum temperatures at baseflow and maximum temperature surges at stormflow differ across watersheds with varying development intensity?

2) What reach- and watershed-scale variables are most correlated with these 2 aspects of stream thermal regimes?

3) Do stream management approaches (riparian buffers, channel restoration) address the links between these variables and stream temperature?

I found that the 5 most urban streams were on average 0.6°C hotter (within errors of measures) at baseflow than the 4 most forested streams. During a single storm event, urban streams showed an increase over five minutes of up to 4°C, while forested streams showed little or no thermal increase. Reach-scale characteristics, specifically canopy

closure and width, primarily controlled baseflow temperatures. These local factors were not important drivers of stormflow temperature changes, which were best explained by watershed-scale development and road density. Management that focuses on baseflow temperatures, such as riparian buffers and reach-scale restoration, ignores the intense urban impacts that occur regularly during storm events.

Next, in Chapter 3, I explore longitudinal temperature patterns in a single stream, Mud Creek, in Durham, North Carolina. Mud Creek's headwaters are suburban, and the stream travels through a number of housing developments before entering a 100-year-old forest. I placed 62 temperature loggers over a 1.5 km reach of this stream. To explore the mechanisms by which stormflow heat pulses dissipate along this stream reach, I asked:

1) What is the range of heat pulse magnitudes that occur over a year?

2) What is the maximum distance that a heat pulse travels downstream of urban inputs?

3) How do the magnitude and distance vary with storm characteristics, including antecedent air temperature and amount and intensity of precipitation?

I found that heat pulses with amplitude of greater than 1°C traveled more than 1 km downstream of urban inputs in 11 storm events over one year. This long dissipation distance, even in a best-case management scenario of mature and protected forest, implies that urban impacts across a developing landscape travel far downstream of the impacts themselves and into protected areas. Heat pulses greater than 1°C occurred in storms with

greater intensity of and total precipitation and greater time of elevated stormflow. Air temperature, flow intensity, maximum flow, and total precipitation controlled the magnitude of the heat pulse, while the distance of dissipation was controlled by the magnitude of the heat pulses and total precipitation. The importance of air temperature, flow, and precipitation metrics imply that both magnitude and distance of dissipation of heat pulses are likely to increase with climate change, as air temperatures increase and sudden, intense storms become more frequent. This translates to even greater ecological impacts in urban landscapes like Durham municipality, where the 98.9% of streams less than 1 km downstream of a stormwater outfall will become even more likely to be impacted by urban stormwaters.

In Chapter 4, I examine which aspects *about* development best explain thermal differences observed at baseflow and stormflow. To do this, I selected 15 similarly sized watersheds in the North Carolina Piedmont region within 45 to 55% development that varied in other development characteristics, specifically density of stormwater infrastructure and aggregation of development patches. I asked two questions:

1) How does the configuration and connectivity of development within a watershed influence baseflow and stormflow temperatures in receiving streams?

2) How do baseflow and stormflow temperatures vary with development characteristics?

I found that aspects of development varied greatly within this urban intensity subset, with ranges for some metrics nearly equal to the variation observed across all

watersheds in the landscape. Longer pipe lengths, shading from incised channels, and shaded impervious surfaces resulted in cooler baseflow temperatures. As in Mud Creek, stormflow metrics were influenced through two physical pathways: air temperature and either flow intensity, to explain overall thermal change, or antecedent flow, to explain intensity of thermal change. Greater sub-surface connectivity of development to the stream network increased thermal responsiveness to storms through faster delivery and greater amount of heated runoff. Greater proportions of forest in a watershed decreased the amount and temperature of runoff delivered to the stream, while development within the riparian zone throughout a watershed led to warm baseflow temperatures and lack of response to stormflow heat surges. By decreasing the connectivity of development to the stream network, thermal regimes of streams can be less impacted even in relatively urban watersheds.

Thermal pollution in urban streams is a problem that will only be exacerbated by predicted climate change and urban expansion. These findings imply that thermal pollution is a problem throughout urban landscapes, even far downstream of urban inputs and within protected areas, and must be managed as an important component of the USS. Future research should focus on the transferability of these findings to regions outside of the southeastern United States and to the movement of other urban pollutants, and on exploring the potential to manage these systems by decreasing sub-surface connectivity.

Dedication

To Robert Jay Somers, for telling me to always ask questions.

And to Matthew James Poland, for convincing me I could answer them.

Contents

List of Tables

List of Figures

Acknowledgements

It really does take a village to make a dissertation, and I am so thankful to everyone who played a part in my research and keeping me sane.

My advisors and committee members helped me through every step of this long and difficult process. My advisors, Drs. Emily Bernhardt and Dean Urban, supported me through all five years of my PhD and guided me to ask interesting questions and explore the implications of the answers. Dr. Urban taught me about landscape ecology, the importance of spatial processes, and the methods needed to wrangle large, multivariate datasets. Dr. Bernhardt guided me into the worlds of urban streams and biogeochemistry and taught me the most important aspects of stream ecology. Dr. Martin Doyle, one of my committee members, always kept me on my toes and helped me make sense of geomorphological data, especially for the research in Chapter 4. Dr. Brian McGlynn, another of my committee members, was essential to in helping me to think about how broader physical processes influence my questions and helped me use a number of new hydrologic tools in Chapters 3 and 4.

Many other researchers also helped me in completing this research. John Fay was always willing to help me turn rambling thoughts into ArcGIS models. Dr. Jim Heffernan provided suggestions and perspectives on multiple parts of my thesis and introduced me to many amazing researchers in his lab and beyond. As members of my

original committee, Drs. Curt Richardson and Justin Wright helped me in the first steps of formulating my research questions and considering how my questions fit into ecology as a whole. Dr. Dan Richter guided me in the process of learning about urban soils and sediments and considering connections to my work. Dr. Christine Hatch worked with me to install the ill-fated distributed temperature sensor mentioned in Chapter 3 and aided me in accessing and understanding the data it provided. Finally, Dr. Jim Grace of the United States Geological Survey was fundamental in understanding and utilizing structural equation models to explore datasets in Chapters 2 and 3.

I had the pleasure and advantage of working with amazing colleagues throughout my time at Duke University in the Bernhardt Lab. Lab technicians and managers, Brooke Hassett, Anna Fedders, and Medora Burke-Scoll, kept my field and lab work running like a well-oiled machine and were always willing to explain new methods. Post-docs in the lab, Drs. Ben Colman, Marcelo Ardon, and Ashley Helton all provided helpful guidance and reminded me that I would, in fact, complete my degree. My fellow PhD students in the Bernhardt and Urban labs kept me going and helped me in every way possible. Dr. Jen Morse provided many comments and thoughts on my early musings. Dr. Elizabeth Sudduth gave emotional and mathematical support even after leaving Duke for a teaching position. Dr. Brian Lutz begged the question: could he have more helpful suggestions? (With the answer being, no.) Dr. Alison Appling provided positive, helpful criticism on many manuscripts and presentations over the

years. Raven Bier asked me insightful questions about my own work and gave me many detailed comments that improved my manuscripts. Kris Voss provided me with huge amounts of statistical help, especially in terms of interpreting results correctly, in Chapter 4. Matt Ross helped me remain excited about my work and look at it from wholly new perspectives.

In Dean Urban's lab, I worked with a wide range of inspiring colleagues. Despite only overlapping one year, Dr. Joe Sexton has provided encouragement – and unique thermal and landcover data. Despite not overlapping at all with Dr. Nicki Cagle, I've had the pleasure of bouncing ideas off of her and learning even more about landscape ecology from her. Dr. Stephen Mitchell has been my only consistent companion in the lab over these years and kept me from taking myself too seriously. The newest addition, Brenna Forester, has proved to be as amazing as she seemed when she interviewed and has allowed me to borrow her talent in the field and in my thought processes. Though not technically in Dean Urban's lab, Danica Schaeffer-Smith showed me that it was not a mistake to share my cubicle, and has helped me in the field and the editing room.

In Jim Heffernan's lab, I've worked closely with Megan Fork and Anna Braswell, both of whom helped me by joining me in the field and reading and editing manuscripts. As a fellow urban researcher, Meredith Steele has inspired me with thoughtful comments and criticisms.

Many of the people above helped me in the field, at one point or another – some of them over long days in very hot weather. I also wanted to specifically thank those people who helped me most in the field. Malia Losordo spent three hot, North Carolina summers wading in streams with me and never complained, even under the worst of circumstances. Justin Garland helped me upload loggers monthly throughout an entire year, including cold and rainy days– and finally convinced me to learn to write loops in R. Abby Maciejewski got her first taste of fieldwork with me and did not immediately turn tail and run, which was extremely impressive. Mark Panny helped me to finish up fieldwork for Chapter 4 and also took over the mind-numbing process of translating raw data into usable data.

In addition to all of these scholarly helpers, I had so much moral support from my friends, many who overlap with the people listed above. Katie Grogan, my first fellow-football fan at Duke, reminded me to stay sane. Her small dog, Foxy, also helped to convince me that sanity is worthwhile. Basma Mohammad, my first roommate in Durham, suffered through a nerve-wracking first year with me and supported me with baked goods when needed. Amy Morsch provided a constant sounding board for my academic thoughts. Trevor and Haley Nace and their menagerie of animals were always a comfort to be around and introduced me to many amazing people in Durham. Alana Belcon provided me with constant maternal love and suggestions and strategies for how to make it through every stage of my research. Laura Johnson has as my sponsor,

constantly making suggestions for how to respond to problems and improve my work and myself. Simon and Laura Woodrup dealt with me on some of my worst days and still remained supportive, loving friends despite it all.

My father, Bob Somers, was an integral part to getting up and facing the day each and every day. Marlie Somers provided constant joking at my own expense, underlain with sincere concern whenever I needed it. Jordan Somers was always encouraging and on my side, no matter what. Antonia Taylor and her family constantly kept me in their prayers. My extended family supported me with kind thoughts and words throughout this process.

My second family, the Polands, have been just as amazing. Jeff Poland has planned and carried out vacations that have reminded me there is a world beyond my thesis. Lisa Poland never fails to inspire me and remind me that I can accomplish everything I want. Jenna Poland has been a constant cheerleader and wonderful friend. Judy and Jim Poland, the McDonalds, and the Stacks have all provided much needed pats on the back and nods of encouragement throughout this process.

Matt Poland, my fiancé, has been the primary reason that I am sane and happy. I cannot imagine how anyone has completed a PhD without him by their side, but I am happy that I did not have to try. Between himself, Annabel Somers, and Wilkie Poland, I have been constantly reminded just how lucky I am even in the most difficult moments of research.

1. Introduction

Currently, cities comprise 52% of the Earth's land surface, with this number expected to continue to grow, as most of the predicted 2.3 billion increase in population over the next 40 years is expected to occur in urban areas (United Nations Population Division 2012). Urban areas necessarily concentrate food, energy, and construction materials, and as a result tend to be hotter and more polluted than the surrounding landscape. All urban ecosystems are thus quite altered from their pre-urban state, but urban streams are particularly impacted. As low lying points on the landscape, streams are subject to the degradation caused by urban stormwaters, which are transmitted rapidly from the surfaces of pavements, roofs, and lawns through stormwater infrastructure to streams.

Urban stream syndrome

The systematic changes seen in many urban streams have been described as the "Urban Stream Syndrome" (USS) and serve as an organizing conceptual framework for urban stream research (Walsh et al. 2005b). A primary symptom of USS is increased flashiness in hydrographs, as stormwater in urban areas is routed efficiently into streams (Booth and Jackson 1997, Konrad and Booth 2005). With this stormwater runoff comes intense scour leading to deeply incised channels, large amounts of contaminants and nutrients, and, as will be discussed in this thesis, heat surges (Booth 1990, Tsihrintzis and Hamid 1997, Walsh et al. 2005a, Nelson and Palmer 2007, Bernhardt et al.

2008). At baseflow, urban streams are contaminated by sanitary sewage leakages, are unable to exchange water with their floodplains due to incision and with groundwater due to lower water tables, and are warmer due to canopy loss and urban heat island effects (Paul and Meyer 2001, Pickett et al. 2001, Groffman et al. 2002, 2003). These baseflow and stormflow changes lead to the loss of sensitive taxa and increase in tolerant biota, as well as changes in ecosystem function, including carbon and nitrogen processing (Paul and Meyer 2001, Meyer et al. 2005, Imberger et al. 2008, Cuffney et al. 2010).

The urban heat island effect can increase air temperatures up to 10°C above those in surrounding, non-urban areas, while impervious surfaces can reach temperatures up to 60°C (Asaeda et al. 1996, Pickett et al. 2001, Kalnay and Cai 2003, Diefenderfer 2006). These changes are particularly troublesome, as research has shown that temperature is a controlling factor in aquatic systems for both stream biota and ecosystem processes (Allen 1995, Kingsolver and Huey 2008). Thermal changes control and can alter basic morphological features of biota, such as size and growth rates (Gibbons 1970, Kingsolver and Huey 2008). USS synthesis reports have called for further research into the processes by which urban areas influence the temperature of streams and the resulting effects on the ecosystems, but until recently have largely been ignored (Paul and Meyer 2001, Wenger et al. 2009). This dissertation explores the timing, magnitude, and pattern of thermal pollution for streams within urban heat islands, with the goal of understanding

what aspects of watershed development most strongly influence the thermal regimes of streams.

Thermal ecology

Studies of stream and river temperature date back at least as far as a Napoleonic expedition of Egypt in 1799, when an explorer measured the temperature of the Nile river in addition to recording the size of the Pyramids, but these studies have truly gained attention in the last half century (Webb et al. 2008). In the 1960s, researchers and policy makers became concerned about the influence of heated discharge from power plants on aquatic ecosystems, including streams (Coutant 1970). This led to the creation of a field known as "thermal ecology", which focused on documenting and exploring the effects of thermal enhancement from a variety of sources (Gibbons and Sharitz 1974). In addition to power plant discharges, much of thermal ecology has focused on the effects of dams, which can be cooling if released from the bottom of the impoundment, and warming if released from the top (Poole and Berman 2001, Caissie 2006). The decrease in flow downstream of dams and consequent decrease in hyporheic exchange further decreases the ability of streams and rivers to regulate temperature (Ward and Stanford 1995).

Recent thermal ecological studies focus on areas where biotic effects are intertwined with economic incentives, especially areas with salmonids. For example, the Willamette Valley in the Pacific Northwest has begun to develop and enforce thermal

trading schemes (Cochran and Logue 2011). This program maintains a more natural thermal regime in the Tualatin River by offsetting heated wastewater with the planting of additional riparian shading. This trading scheme shows the potential to treat thermal pollution similarly to more commonly regulated pollution, such as nitrogen. As the scope of thermal pollution studies have expanded, research has also begun to focus on understanding the ecological implications of these changes.

Thermal changes in streams affect biota directly due to long-term thermal enhancements and through acute heat shocks on biota and ecosystem processes. Benthic macro-invertebrates exposed to temperatures outside of their optimal range typically showed sub-lethal effects, growing at slower rates and having lower fecundity and abundance (Branham et al. 1975, Vannote and Sweeney 1980, Ward and Stanford 1982). Behavioral changes, including decreased mating and feeding and increased vulnerability to predation, occurred due to both long-term and acute thermal changes (Coutant 1973, Salmela and Anderson 1978, Mesa et al. 2002, Hester and Doyle 2011, Carolli and Bruno 2012). Many sensitive species have strict thermal ranges and suffer fatalities when exposed to temperatures above their thermal thresholds (Bowler 1963, Nebeker and Lemke 1968, McCullough et al. 2009a). Increased water temperature also leads to hypoxia and anoxia, further stressing and potentially killing biota (Caissie 2006).

Decreased dissolved oxygen also changes redox status, which can alter the availability of some contaminants, including arsenic, manganese, and iron (Chae et al.

2008). This impact lasts longer than urban heat pulses themselves, which means that thermal pollution both accompanies and exacerbates other urban pollutants. Higher stream temperatures are also associated with higher rates of individual and cumulative metabolism, because most metabolic reaction rates increase with temperature (Clarke and Fraser 2004). Rates of ecosystem respiration and gross primary production, have been shown to be significantly, positively correlated with stream temperature (Bernot et al. 2010, Sudduth et al. 2011). Denitrification and nitrogen uptake rates were also positively correlated with stream temperature (Holmes et al. 1996, Inwood et al. 2005, Sudduth et al. 2011).

Despite the clear connections between increased temperatures in cities and the potential to affect urban streams through thermal regime alteration, relatively few studies exist that document the magnitude of these changes and explore the processes by which they occur.

Thermal pollution in urban streams

Urban stream studies often include the collection of air and stream temperature data, but are not the primary focus of research (e.g., Chadwick et al. 2006, Shields et al. 2010, Beaulieu et al. 2011). Many more studies have focused on the creation of models to predict potential stormwater runoff and stream temperatures with, at most, minimal validation in the field (LeBlanc et al. 1997, Webb et al. 2008). These models predict increases in baseflow temperatures with increased watershed urbanization, but do not

explore the spatial scale of these effects or the potential for propagation throughout the landscape (Krause et al. 2004). At stormflow, greater thermal pollution is predicted to occur when air temperature is greater than stream temperature, storms are short and intense, and watersheds have greater imperviousness (Van Buren et al. 2000, Herb et al. 2008). A limited set of studies has collected empirical data to test these predictions. At baseflow, mean urban stream temperatures in Long Island were found to be up to 8°C greater than forested streams, while stormflow heat pulses were up to 15°C warmer (Pluhowski 1970). Similarly, an urban stream in Washington, D.C. increased 5.8°C over 20 minutes during a storm event (Galli 1991). More recent studies have mirrored these results, documenting storm heat surges of more than 7°C (Nelson and Palmer 2007, Hester and Bauman 2013). The direct effects of these heat surges on stream biota are difficult to disentangle from the accompanying increases in stormflow intensity and sediment and chemical pollutant loads that are typically associated with urban runoff.

As climate change leads to increased air temperatures, streams have also become warmer, with the greatest increases in urban areas (Kaushal et al. 2010). Global warming and urban expansion are expected to collectively increase both the magnitude and spatial extent of thermal pollution in the coming decades. These predictions make the problem of thermal pollution increasingly relevant to urban watershed management.

Current state of the science

The study of thermal pollution in urban streams has largely remained the realm of engineers and hydrologists. This research focuses on simulation modeling across landscapes and watersheds (such as LeBlanc et al. 1997, Krause et al. 2004), using minimal field data, and at individual best management practice locations, sometimes using monitoring data (such as Herb et al. 2008, Jones and Hunt 2009, Winston et al. 2011). These studies address thermal pollution questions by focusing on a small number of sites, often just one. At these sites, scientists calculate full hydrological and energy budgets and gain an intense understanding of a single or small number of sites.

These studies typically describe the physical processes the lead to thermal pollution, but ignore the watershed-scale landcover metrics that impact the magnitude of thermal pollution. The research in this thesis trades the full hydrological knowledge of a limited number of sites for less intense knowledge of a much greater number of sites. Rather than provide a precise understanding of the physical processes occurring at each site, the studies in this thesis explore the landcover metrics that explain the variation in thermal pollution in streams across a landscape. The findings from this work provide guidelines for better management of entire urban landscapes, rather than suggestions for designs of single best management practices.

By incorporating the predictions and hypotheses of hydrological and engineering studies with the methods of landscape ecology, I explored the spatial patterns of

landcover within watersheds and the relationship between these patterns and the processes of heat transfer within stream networks. The research in this thesis embraces the thermal heterogeneity of stream networks in urban areas and attempts to explain the variability observed in field measurements through the patterns of urbanization in a watershed. This 'streamscape ecology of thermal pollution' provides a novel perspective on both urban streams and thermal pollution.

Dissertation outline

In order to explore thermal pollution in urban streams, I asked three overarching questions:

1) How much hotter are highly urban streams than streams in less developed watersheds?

2) How far do urban heat pulses propagate downstream of urban inputs?

3) How can development *configuration* mitigate or exacerbate development *amount* in mediating urban thermal pulses?

In Chapter 2, I explore the differences in baseflow and stormflow temperatures in 60 watersheds across the North Carolina Piedmont that ranged across a gradient of urbanization. I asked:

1) How do maximum temperatures at baseflow and maximum temperature surges at stormflow differ across watersheds with varying development intensity?

2) What reach- and watershed-scale variables are most correlated with these 2 aspects of stream thermal regimes?

3) Do stream management approaches (riparian buffers, channel restoration)

address the links between these variables and stream temperature?

I found that the 5 most urban streams were on average 0.6°C hotter at baseflow than the 4 most forested streams. During a single storm event, urban streams showed an increase over five minutes of up to 4°C, while forested streams showed little or no thermal increase. Reach-scale characteristics, specifically canopy closure and width, primarily controlled baseflow temperatures. These local factors were not important drivers of stormflow temperature changes, which were best explained by watershed-scale development and road density. Management that focuses on baseflow temperatures, such as riparian buffers and reach-scale restoration, ignores the intense urban impacts that occur regularly during storm events.

Next, in Chapter 3, I explore longitudinal temperature patterns in a single stream, Mud Creek, in Durham, North Carolina. Mud Creek's headwaters are suburban, and the stream travels through a number of housing developments before entering a 100-year-old forest. I placed 62 temperature loggers over a 1.5 km reach of this stream. To explore the mechanisms by which stormflow heat pulses dissipate along this stream reach, I asked:

1) What is the range of heat pulse magnitudes that occur over a year?

2) What is the maximum distance that a heat pulse travels downstream of urban inputs?

3) How do the magnitude and distance vary with storm characteristics, including antecedent air temperature and amount and intensity of precipitation?

I found that heat pulses with amplitude of greater than 1°C traveled more than 1 km downstream of urban inputs in 11 storm events over one year. This long dissipation distance, even in a best-case management scenario of mature and protected forest, implies that urban impacts across a developing landscape travel far downstream of the impacts themselves and into protected areas. Heat pulses greater than 1°C occurred in storms with greater intensity of and total precipitation and greater time of elevated stormflow. Air temperature, flow intensity, maximum flow, and total precipitation controlled the magnitude of the heat pulse, while the distance of dissipation was controlled by the magnitude of the heat pulses and total precipitation. The importance of air temperature, flow, and precipitation metrics imply that both magnitude and distance of dissipation of heat pulses are likely to increase with climate change, as air temperatures increase and sudden, intense storms become more frequent. This translates to even greater ecological impacts in urban landscapes like Durham municipality, where the 98.9% of streams less than 1 km downstream of a stormwater outfall will become even more likely to be impacted by urban stormwaters.

In Chapter 4, I examine which aspects *about* development best explain thermal differences observed at baseflow and stormflow. To do this, I selected 15 similarly sized watersheds in the North Carolina Piedmont region within 45 to 55% development that varied in other development characteristics, specifically density of stormwater infrastructure and aggregation of development patches. I asked two questions:

3) How does the configuration and connectivity of development within a watershed influence baseflow and stormflow temperatures in receiving streams?

4) How do baseflow and stormflow temperatures vary with development characteristics?

I found that aspects of development varied greatly within this urban intensity subset, with ranges for some metrics nearly equal to the variation observed across all watersheds in the landscape. Longer pipe lengths, shading from incised channels, and shaded impervious surfaces resulted in cooler baseflow temperatures. As in Mud Creek, stormflow metrics were influenced through two physical pathways: air temperature and either flow intensity, to explain overall thermal change, or antecedent flow, to explain intensity of thermal change. Greater sub-surface connectivity of development to the stream network increased thermal responsiveness to storms through faster delivery and greater amount of heated runoff. Greater proportions of forest in a watershed decreased the amount and temperature of runoff delivered to the stream, while development within the riparian zone throughout a watershed led to warm baseflow temperatures and lack of response to stormflow heat surges. By decreasing the connectivity of development to the stream network, thermal regimes of streams can be less impacted even in relatively urban watersheds.

Thermal pollution in urban streams is a problem that will only be exacerbated by predicted climate change and urban expansion. By exploring the streamscape ecology of urban streams, this research shows that thermal pollution is a problem throughout

urban landscapes, even far downstream of urban inputs and within protected areas, and must be managed as an important component of the USS. Future research should focus on the transferability of these findings to regions outside of the southeastern United States and to the movement of other urban pollutants, and on exploring the potential to manage these systems by decreasing sub-surface connectivity.

This dissertation has shown that:

- Reach-scale habitat factors control baseflow temperatures, while watershed-scale landcover factors control stormflow temperatures,
- Urban impacts can travel far downstream during storm events, even under the best-case management scenarios, and
- Sub-surface connectivity, via the rapid movement of stormwater into stream networks, is the primary control on magnitude and intensity of heat pulses in urban streams. Shading can lead to cooler streams at baseflow, but also to larger, more intense heat pulses during storm events.

2. Streams in the urban heat island: spatial and temporal variability in temperature[1]

Introduction

Cities create urban heat islands with air temperatures up to 10°C greater than surrounding areas (Pickett et al. 2001). The urban heat-island effect is mostly macroscopic and is described by comparing temperatures within a city to those in the surrounding areas. However, temperature is highly variable within urban areas and along a gradient of urban development. This local-scale variability in land cover and temperature should be reflected in local-scale variability in stream temperatures. Higher temperatures and greater developed surface area should lead to higher baseflow temperatures in streams and the potential for heat surges during stormflow (Walsh et al. 2005b, Violin et al. 2011). Thermal pollution is a result of several often interacting local- and watershed-scale influences, including hydrologic connections to impervious surfaces, increased radiation caused by decreased riparian canopy cover, decreased forested area in the watershed, and direct inputs of warm water via stormwater infrastructure (Wenger et al. 2009). The relative importance of local- and watershed-scale factors and their interactive effects on in-stream temperature is currently unknown.

---

[1] Somers, K. A., E. S. Bernhardt, J. B. Grace, B. A. Hassett, E. B. Sudduth, S. Wang, and D. L. Urban. 2013. Streams in the urban heat island: spatial and temporal variability in temperature. Freshwater Science.

The urban stream syndrome includes a variety of pathways by which urban development influences stream ecosystems in ways that can be synergistic (amplifying) or compensatory (negating) (Paul and Meyer 2001, Meyer et al. 2005). During storms, large amounts of water enter streams via overland flow and from stormwater pipes that discharge directly into streams. The force of the water alters the morphometry of the stream by incising the stream bed and disconnecting the stream from its floodplain so that even during major storms, water can no longer overflow the banks (Walsh et al. 2005b, Bernhardt et al. 2007). Bank overflow is biogeochemically important for both stream and riparian ecosystems because it transports and exchanges nutrients between the systems and helps to maintain stable banks (Lake et al. 2007, Sudduth et al. 2011). Urban streams become over-connected to their catchments via overland flow and stormwater inputs and under-connected to their riparian zones via channel incision and loss of riparian vegetation (Bernhardt et al. 2008). Local variability in stream temperature is one of many factors that affect urban streams, but changes in the thermal regimes of urban streams are less well studied than alterations in geomorphology, hydrology, and nutrients.

Small-scale variation in stream temperatures has been studied extensively in rural streams that have salmon and trout fisheries. These studies include reports of increases in stream temperatures caused by dams and loss of forested buffers (Johnson 2004, Jones et al. 2006, Olden and Naiman 2010). Some investigators have created

deterministic models that use meteorological data—especially air temperature—to describe or predict stream temperature (Mohseni et al. 1998, Caissie 2006, Kelleher et al. 2011). Changes in temperature caused by urbanization have been less studied. Thus, little is known about the magnitude and spatiotemporal patterns of thermal pollution in urban streams or the specific local and landscape factors that control them.

This knowledge gap is problematic because stream temperature and variability are ecologically important. Increased stream temperatures can cause dissolved O_2 (DO) limitation via increased microbial activity and O_2 demand and reduced O_2 diffusion and solubility. Stream temperature influences growth, metabolism, and reproduction of aquatic biota, and can be lethal if it exceeds thermal limits of aquatic fauna (Vannote and Sweeney 1980, Hester and Doyle 2011). Maximum temperatures at baseflow often are negatively correlated with taxon richness largely because higher temperatures are correlated with a loss of taxa sensitive to changes in DO or that are at the low-latitude or low-elevation boundaries of their distribution (Beitinger et al. 2000a, Sponseller et al. 2001, Wang and Kanehl 2003, Jones et al. 2006, Nelson and Palmer 2007). Higher temperatures can accelerate microbial activity, leading to higher rates of respiration and organic matter decomposition and causing subsequent changes in ecosystem metabolism and biogeochemical cycling (Hill et al. 2000a, Imberger et al. 2008). Thus, researchers and land managers need a better understanding of how local temperature variability affects stream thermal regimes.

Urbanization elevates water temperature at baseflow and can cause temperature surges during storms. Impervious surface in highly developed watersheds leads to high levels of runoff during storms (Dunne and Leopold 1978, Arnold and Gibbons 1996). The initial runoff from paved surfaces can reach extremely high temperatures because impervious surfaces can be as much as 50°C hotter than the air (Berdahl and Bretz 1997). The water that conveys the heat pulses also carries contaminants and nutrients and scours the stream bed. The effects of these heat pulses on organisms have been studied rarely, but they can briefly elevate stream temperatures above the maximum thermal tolerances of some sensitive organisms (Nelson and Palmer 2007). Temperatures near or above optimal thermal ranges, even for brief periods, can stress organisms and affect their development and behavior even when they do not increase mortality. Heat pulses can cause behavioral and physiological changes in some invertebrate and fish species (Salmela and Anderson 1978, Mesa et al. 2002).

We conducted a field study in the Piedmont of North Carolina, USA, in summer 2009 to examine the complex routes by which urban heating can affect water temperatures. We were interested in exploring how baseflow thermal regimes and storm-flow temperature surges are altered in urban streams and asked 3 specific questions: 1) How do maximum temperatures at baseflow and maximum temperature surges at stormflow differ across watersheds with varying development intensity? 2) What reach- and watershed-scale variables are most correlated with these 2 aspects of

stream thermal regimes? 3) Do stream management approaches (riparian buffers, channel restoration) address the links between these variables and stream temperature?

Methods

Study area

The Triangle region of the North Carolina Piedmont is framed by the cities of Raleigh, Durham, and Chapel Hill. Historically, the region was largely agricultural with a few industrial cities. After broad-scale abandonment of agriculture in the 1930s, the area underwent widespread reforestation to pines, which are now succeeding to hardwoods (Kirby 2006). The area is undergoing explosive population growth and now has a range of development intensity from heavily urbanized Raleigh in the east to more agricultural areas in the west (Fig. 1). State parks and large tracts of lands owned and protected by institutions provide remnant areas of natural vegetation with minimal impacts from recent development. The area is a macrocosm in which to study urbanization and its various trajectories and serves as a model landscape for other regions experiencing similar patterns of development.

Site selection

We conducted a synoptic survey of ~70 low-order streams distributed throughout the area and across a range of land covers (Figs 1, 2A–D) as part of a larger study of the urban stream syndrome. We compiled a list of potential sites that included streams previously monitored by the US Geological Survey (USGS) as part of the Effects

of Urbanization on Stream Ecosystems (EUSE) program, North Carolina's Department of Water Quality (DWQ), and Durham Storm Water (DSW), a series of ongoing research sites (Sudduth et al. 2011, Violin et al. 2011), and sites that had not been previously studied. We chose sites on the basis of land cover and ease of access. We worked with a time series of land-cover data created by Sexton et al. (in press) who used signature-extension methods to develop a classification scheme based on the 2001 National Land Cover Dataset (Homer et al. 2004) that could be extended with the same thematic resolution and accuracy to the entire Landsat Thematic Mapper archive. We extracted land-cover data (raster images at 30-m resolution) for 5-y increments (1985–2005). To select study sites, we analyzed 2005 land-cover data with moving-window averages to approximate proportions of development, agriculture, and forest in each candidate watershed to ensure that our sites would represent the full range of land-cover variation in the region. We used a geographic information system (GIS) (ArcGIS, version 9.3; Environmental Systems Research Institute 2008) to search for areas where streams crossed roads or ran beside them and used 2008 aerial photographs (NAIP 2008) to air-truth these sites. We eliminated sites that appeared to be ponds or lakes rather than streams, did not appear to have any body of water in the area, or appeared inaccessible.

We visited 118 potential sites and eliminated those that were on private property, extremely difficult to access, too deep to sample in chest waders, or so small that they were likely to dry early in the season. We deployed samplers at 74 sites on 19 May 2009

for 30 d. Each sampler consisted of temperature loggers anchored to large concrete blocks that were secured by rebar inserted into the stream bed. We stationed all samplers in runs or pools, so that they would remain covered by water as long as possible in dry conditions. Some samplers were lost or buried by floods, and some data loggers malfunctioned, leaving a final data set consisting of detailed channel measurements, watershed land-cover analysis, and continuous temperature data at 60 sites.

Temperature data

We used Onset HOBO® Temperature/Alarm (waterproof) Pendant® Data Loggers (UA-001-08) in the samplers to record temperature every 10 min from 20 May to 10 June. These loggers are accurate to ±0.54°C, so we will not describe trends and differences of a magnitude <1.08°C. We focused on 2 biologically relevant temperature variables: 1) maximum temperature surge during stormflow and 2) maximum temperature during baseflow. We began by isolating a 24-h period surrounding a major storm (1100 h 28 May–1100 h 29 May) and calculating the maximum temperature change that occurred over 10 min during stormflow. This change indicates the sudden and severe thermal surges that can occur in urban streams. To analyze differences in baseflow temperature among streams, we focused on the week surrounding this storm (24 May–1 June) to ensure that baseflow and storm-flow temperatures were comparable and to minimize the likelihood of major disturbances caused by sediment burial or low-to-nonexistent

baseflow. We calculated mean daily minimum, maximum, and mean temperatures during baseflow, mean observed change over any 24-h period (diel amplitude), and mean degree-days using the double-triangle method and a base temperature of 0°C (Sevacherian et al. 1977).

Habitat measurements

We measured canopy cover, stream channel depth, width, and incision, and streambed habitat diversity in a 100-m reach upstream of 42 of the 60 samplers between June and August 2009 and at the remaining 18 sites between June and August 2010 (Table 1). We counted the number of habitat transitions between pools, riffles, and runs in this 100-m reach. Reach-level description of habitat transitions may reflect watershed urbanization because streams in more urbanized environments typically have fewer habitat transitions consequent to scouring and incision caused by storms (Walsh et al. 2005b, Violin et al. 2011). We measured the wetted width and the depth in the center of the channel at each transition and every 10 m and calculated the minimum, maximum, and mean wetted width and depth for the reach. We surveyed cross-sections at 3 randomly chosen transects in each reach. We used a string level and measuring tape across the top of opposite banks to record bank-to-bank width and measured the height between the tape and a minimum of 7 points: top of left bank, bottom of left bank, left edge of water, thalweg, right edge of water, right bottom of bank, and right top of bank. We added points as needed to account for sandbars and other anomalies. We calculated

the incision of the stream as channel depth at thalweg divided by bankfull width at the 3 cross-sections. We measured canopy closure from the ground at the thalweg of the stream with concave forest densiometers (Forest Densiometers, Bartlesville, Oklahoma) (Lemmon 1957) at each cross-section to provide an estimate of canopy closure 100 m upstream of the temperature logger. Densiometer readings are subjective, so field canopy-closure measurements were made by 2 technicians who underwent extensive calibration to ensure their interpretations were consistent. We also calculated canopy closure from aerial photographs taken in 2008 (NAIP 2008). We created a 10- × 10-m grid in ArcGIS that covered the entire study area, overlaid satellite images of each stream reach with the grid, and visually analyzed cover 100 m upstream of the temperature loggers. We counted the grid cells in which the stream was not visible and divided this number by 10. For example, if the stream was clearly visible in 2 of the grid cells, we estimated canopy closure as 80%. These estimates were only slightly correlated with densiometer readings (adjusted $R^2 = 0.25$, $P < 0.05$), probably because of differences in sampling and photography dates and in resolution between densiometer readings and 30-m grids.

We were unable to measure habitat at 18 sites in 2009, so we revisited these sites in 2010 and used the same procedures to measure habitat indices in order to increase our sample size of sites with temperature, habitat, and landscape data to 60. We also revisited 13 sites (for which we had 2009 habitat data) that spanned the range of urban

development in our study region to test whether habitat variables differed between years. Only variables related to depth differed significantly between years (paired *t*-tests), primarily because of differences in weather between years. Therefore, we did not use minimum, maximum, and mean depth measurements in the model.

Land cover

We used ArcGIS tools to delineate the watershed upstream of each sampler based on 30-m light detection and ranging (LiDAR)-derived digital elevation model (DEM) data (North Carolina Department of Transportation 2007). We imported global positioning system (GPS) coordinates for each sampler and calculated the elevation (range 60–197 m asl) and orientation of each study reach because these variables affect light availability in rivers (Julian et al. 2008). We used a flow-accumulation raster layer to hand-edit the sites by shifting their locations into the nearest cells of highest flow accumulation. This manipulation created a set of pour points from which the GIS could delineate the watershed for the area upstream of each sampler. We checked each watershed with the DEM and aerial photographs and rectified obvious errors.

For each watershed, we computed a set of indices to represent land cover (Table 1). We calculated % developed land in 1985, 1995, and 2005 and % forest and % field in 2005. We addressed potential differences between older development and newer development, such as differing age and types of stormwater infrastructure and best management practices (Kaushal and Belt 2012) by calculating the proportion of

development observed in 2005 that occurred between 1985 and 2005 and between 1995 and 2005. We did not use the amount of watershed classified as "field" in our analyses because this classification is difficult to assess. In agricultural areas, field indicated crops and pasture, but in urban areas, field represented golf courses, lawns, or cemeteries.

We calculated several variables that incorporated the effects of land cover on streams. We began by assuming that land-cover effects were inversely proportional to their distance from the stream (King et al. 2005a). This approach took into account surface connectivity between the stream and watershed, but did not account for the effects of subsurface connectivity created by stormwater infrastructure. Many of the watersheds in our study were outside of municipal boundaries in areas where storm-water infrastructure or information on the location of storm-water infrastructure do not exist. Attempts to estimate these connections would have been extremely haphazard. We chose to estimate connections between development and streams via natural flow paths because storm-water infrastructure tends to follow these flow paths. Thus, our methods provide a first-cut understanding of the effects of land cover in urban watersheds.

We used developed land cover as a proxy to calculate effective development for each watershed. We used the DEM to calculate the distance along a hydrologic flow path from each grid cell with developed land cover to the nearest grid cell containing the stream. This distance was an estimate of the actual distance to the stream along the

flow path. We weighted this distance by the relative infiltration capacity of land covers encountered along the flow path based on the curve number method (U.S. Department of Agriculture 1986). We calculated curve numbers based on hydrologic soil groups from SSURGO soils data (Soil Survey Staff United States Department of Agriculture 2010) and land cover (natural vegetation has high infiltration rates, developed land has low infiltration rates). We used calculated curve numbers to estimate effective resistance to infiltration. Thus, water flowing over land with natural vegetation with high infiltration capacity effectively traversed a longer distance than water flowing over developed land because it had more time to infiltrate. In contrast, impervious surfaces led to shorter effective distances along the flow path. We expected sites farther from the stream along these flow paths to have less effect on the stream than nearby sites, so we modeled the relationship between the distance from the stream and the effect on the stream as a negative exponential decay function. The rate at which this decay should occur and the distance at which the effect of a cell on a stream should be effectively null were not known. Therefore, we selected a range of distances (50–2000 m) over which we could expect the effect of the cell on the stream to become arbitrarily small (1%) and calculated an exponential decay rate based on each distance. We computed infiltration-weighted distances from the stream along surface flow paths for each cell with developed land cover to produce a range of effective development variables with different decay rates. In this approach, a grid cell with developed land cover was down-

weighted if it was far from the stream, not in the flowpath, or if water would pass over cells with land-cover with high infiltration capacity before it reached the stream. We calculated the average of these values in each watershed. To calculate effective weighted development, we weighted the land-cover classes low-density developed, medium-density developed, and high-density developed (corresponding to NLCD classes 22, 23, and 24, respectively) by relative impervious indices of 33, 66, and 100% (Homer et al. 2004) and used the procedures described above for effective development.

We calculated effective forest as for effective development but with forested land cover. The result was an estimate of buffering land cover, weighted by hydrologic proximity to the stream. We expected effective forest to be most important over short distances (e.g., 50–100 m), whereas effective development would be important at longer distances (≥1000 m). Because we computed both indices over a range of distances, we were able to assess these scaling relations directly in exploratory data analysis.

We calculated % connected development as the percentage of the watershed with developed land cover that was closely connected to a stream (based on distance to stream). We calculated % developed land within 100 m of a stream and divided this area by the total watershed area, so that this variable was comparable between watersheds. Dividing by total area in the watershed also placed % connected development in the context of the larger watershed, while weighting it higher than land cover further from the stream.

We indexed the effects of roads and traffic volume on streams by methods described in previous studies of the relationship between roads, traffic volumes, and runoff. We began by computing the Euclidean distance from each raster grid cell in each study watershed to the nearest road. We assumed that road effects decreased rapidly with increasing distance. We log(x)-transformed these distances with a distance–decay constant based on the results of a study of the dissipation of heavy metals with increasing distance from roads (Lygren et al. 1984). We weighted this distance–decay relationship based on estimates of traffic volume provided by North Carolina Department of Transportation (North Carolina Department of Transportation 2007). Inverse-distance-weighted traffic volume estimated road effects mediated by traffic and is correlated with road size (Mayer et al. 2011). For example, the heavy metals deposited by car exhaust are directly proportional to traffic volume on nearby roads. Roads that are more heavily trafficked are generally larger. We also computed road density in each watershed to gauge whether cumulative effects might be more important than the influence of the nearest roads (Kratzer et al. 2006). We summed road effects in the watershed as total m of road/ ha of watershed. We calculated the mean number of road/stream intersections in each watershed/km of stream to estimate the effect of routing stormwater from roads directly into streams (Jones et al. 2000).

Variable selection

Our goal was to select variables that would best represent paths by which urbanization might affect baseflow and storm-flow stream water temperatures (Fig. 3). We used exploratory data analysis to select predictor variables and to assess possible interaction pathways. We classified the variables as reach or catchment scale and grouped them within scales into categories that might describe mechanisms affecting stream temperature (Fig. 3). Catchment-scale variables described forest, road, and development land cover, and reach-scale variables described physical habitat or light. We used simple correlations to test for relationships between each habitat and land-cover variable and the 2 thermal variables, maximum temperature at baseflow and maximum temperature surge during stormflow. Reach orientation was the only categorical variable, so we used a *t*-test to compare each thermal variable between north–south oriented streams and east–west oriented streams and found no difference between orientations. Except for orientation, we retained the variable in each group with the strongest simple correlations with the response variables to reduce the potential for confounding. For example, we retained a single road-effect variable (road density) and a single light-effect variable (canopy closure from aerial photographs). We also used these correlations to select the most appropriate decay distances for effective development and effective forest. We selected effective forest calculated with a decay distance of 50 m because it was most strongly correlated with the temperature variables.

Percent developed area in 2005 was more strongly correlated with the temperature variables than effective development, so we removed effective development.

We used regression tree analysis (Breiman et al. 1984) to explore the possibility that response variables might be affected by alternative causal pathways expressed in different branches of a regression tree (Urban 2002). This procedure also allowed us to screen for confounding variables that could be highly correlated with both explanatory and response variables in the model. We included these relationships in structural equation models (SEMs) via indirect pathways and intermediate variables, which take into account confounding relationships. For example, the final SEM showed that canopy closure was an intermediate variable between development and maximum temperature, revealing that canopy closure affected maximum temperature but was affected by development. We used the reduced set of predictors and the pathways suggested by regression trees and our knowledge of urban streams to develop an SEM.

SEM

We used SEM (Amos, version 16.0, SPSS 2007; Grace 2006, Grace et al. 2010) to evaluate hypotheses about the mechanisms connecting predictors and responses of interest. SEM can be used in a variety of ways (Grace et al. 2012), but our focus was on evaluating and discovering network connections in the system. The conceptual metamodel used to explore the influences of catchment- and reach-level alterations on temperature changes in urban streams (Fig. 3) represented many possible SEMs that

could be evaluated with our data. These models included both watershed- (road density, % development) and local-scale variables (stream width, canopy closure, distance-weighted forested area). This conceptual model also suggested possible indirect pathways. For example, % development could affect maximum temperature directly or by association with reduced canopy closure, which also affects maximum temperature. We developed SEMs, evaluated multivariate expectations against our data, and made necessary modifications to pose alternative models. Thus, our use of SEM can be considered a model-building application (Joreskog 1982).

In model fitting, we used goodness-of-fit variables for the overall model and tests of significance for individual path coefficients to revise the initial model sequentially. We considered removing links in the model if the data suggested they lacked explanatory power. This pruning continued until all path coefficients retained in the model were significant ($P < 0.05$) or our biophysical understanding of the system required that the variable be retained (Grace 2006a). At the same time, we assessed overall model fit after each iteration with the goal of achieving a model that produce results that did not differ from the data (i.e., model–data consistency). We assessed potential violations of the stringent assumptions of maximum-likelihood estimation by fitting this model using the Bayesian estimation procedures (Arbuckle 2007). The methods produced nearly identical standardized regression weights, indicating that maximum-likelihood-estimation methods produced a robust solution.

Longitudinal surveys

We conducted intensive temperature mapping in 4 of the 60 streams in August 2009 to document spatial variability in baseflow temperature. These streams had a range of development and % connected development. Portions of the study reaches of all 3 of the urban streams had been recently restored. The air temperatures during this study were some of the hottest in the year, providing an optimal period in which to examine maximum baseflow temperature and to observe extremes. We used a YSI Model 30 handheld conductivity and temperature probe (Yellow Springs Instruments, Yellow Springs, Ohio) to measure the temperature every 50 m and above and below any pipe outfalls or tributaries. We walked upstream and continued until we had data for a ≥1-km-long section of stream. We calculated summary statistics for each stream and used *t*-tests to compare stream temperatures in shaded versus unshaded locations. We used these analyses to corroborate conclusions drawn from the synoptic survey data.

We did all analyses except SEMs in R (version 2.10.1; R Development Core Team 2008) and the packages *tree* (Ripley 2009) and *ecodist* (Goslee and Urban 2007).

Results

Watershed land cover

Watersheds had from 0% to 99% developed land (Table 1; Fig. 4A). Some watersheds were almost entirely developed (99% in 2005), whereas others were nearly completely forested (96% in 2005) (Fig. 4B). Other aspects of development varied greatly

among watersheds (e.g., % fields; Fig. 4C). Road density ranged from 0 to 60 m/ha (Table 1, Fig. 4D). Even among the 10 most-developed watersheds, road density ranged from 12 to 60 m/ha. The number of road/stream intersections varied from 0 to 4 km of stream (Fig. 4E), and % connected development ranged from 0 to 100% (Fig. 4F).

Inverse-distance-weighted land-cover variables

Only 2 inverse-distance-weighted land-cover variables were related to the temperature variables. Effective weighted development had the 4th-strongest correlation with minimum temperature. Percent development was the best descriptor of temperature variables in the SEM. Effective forest performed better than % forest and was included in the SEM. These variables describe the surface connectivity to streams of both development and forest (King et al. 2005a).

Stream thermal regimes

The wide range in development was accompanied by wide variation in stream thermal regimes (Fig. 5). Baseflow temperatures ranged from an absolute minimum of 12.4°C to an absolute maximum of 33.2°C, with an average across all sites of 17.2°C (Table 2). Storm-flow changes ranged from decreases of 3°C to increases of 4.2°C, but mean decreases and increases in temperature were <1°C across all sites. Temperature variables describing minimum, mean, and maximum temperatures, maximum temperature surge during stormflow, and degree-days were all significantly higher in the 10 most-developed watersheds than in the 10 most-forested watersheds (1-tailed

unpaired *t*-test, $\alpha = 0.05$). The only thermal variable not significantly different between the 2 groups was the mean diel change in temperature.

Correlates of stream baseflow temperatures

Baseflow minimum, maximum, and mean temperatures were each strongly correlated with different explanatory factors (Table 3). At the reach scale, warmer baseflow temperatures were associated with wider streams, whereas cooler baseflow temperatures were associated with greater riparian canopy cover and more habitat transitions. At the watershed scale, warmer temperatures occurred in watersheds with higher road densities, and cooler temperatures occurred in watersheds with higher % forest. Reach-scale factors were often stronger correlates with baseflow temperature than were watershed land-cover attributes. Many of these watershed and reach-scale factors were correlated. For example, % development was highly correlated with road density ($r = 0.51$) and with canopy closure from aerial photographs ($r = –0.47$). Other factors had opposing effects on temperature, e.g., % development and % forest.

The final SEM included 5 explanatory variables and explained 47% of the variation in baseflow maximum temperatures across streams ($\chi^2_{5df} = 1.655$, $P = 0.976$) (Fig. 8). Maximum temperature appeared to be most strongly influenced by canopy closure via a direct negative path and by mean width of the channel by a direct positive path. Percent developed land cover and road density significantly influenced maximum temperature via a direct path. A significant indirect path indicated that shading effects

of % canopy cover dampened the positive relationship between % developed land and stream baseflow temperatures

Baseflow temperature varied by as much as 10°C along a 1-km stretch of urban Goose Creek and as little as 2°C along a 1-km stretch of forested Stony Creek (Table 4). Temperature was spatially variable in the 2 narrower urban streams (Goose Creek and Rocky Branch) but was more uniform (and warmer) in a wider urban stream (North Gate) (Fig. 6A–C). The highest temperatures in the narrower urban streams were associated with canopy gaps (1-tailed unpaired *t*-test, $\alpha = 0.05$). Much of the spatial heterogeneity in Goose Creek and Rocky Branch was a result of variation in riparian shading. Temperatures were significantly lower in sections of the stream with closed canopies than in sections with canopy gaps (1-tailed unpaired *t*-test, $\alpha = 0.05$). Stormwater outlets had inconsistent effects on baseflow temperature. The highest temperature (29.5°C) observed during the longitudinal survey was in a well-shaded section of Rocky Branch immediately below a stormwater outlet, whereas the coldest temperature (22.7°C) was in an unshaded section of Goose Creek below piped tributary.

Controls of storm-flow temperature surges

Thermal responses of streams to storms were related to watershed land cover but also varied greatly among streams in watersheds with similar land cover (Fig. 7). Maximum temperature surge during stormflow was significantly greater in the 10 most-urban streams than in the 10 most-forested streams (1-tailed unpaired *t*-test, $\alpha = 0.05$).

Urban stream temperatures increased intensely and suddenly during storms, whereas forested stream temperatures responded gradually to stormflow and often showed only a small increase or a cooling effect in response to summer storms. Maximum temperature surge during stormflow was more strongly correlated with catchment- than with reach-scale variables. Percent development was positively correlated and % forest was negatively correlated with maximum temperature surge during stormflow (Table 3). Maximum temperature surge during stormflow was greater in reaches with greater channel incision and less canopy cover, factors that were highly correlated with % development.

The final SEM explained 44.8% of the variance in maximum storm-flow temperature surge (Fig. 8). The strongest effect was the positive direct path between % development and the maximum temperature surge during stormflow. Maximum temperature surge during stormflow also was influenced by stream width via a direct negative path. The model also identified a significant indirect path by which road density and % development negated some of the cooling effect of % canopy closure on maximum temperature surge during stormflow.

Discussion

Impervious surfaces can be up to 50°C hotter than air temperatures (Berdahl and Bretz 1997). Our results showed that differences in thermal regimes at the watershed scale are propagated to stream channels during stormflow, but the magnitude of

warming is dampened at baseflow. Minimum, maximum, and mean baseflow temperatures were consistently >1°C warmer in the 10 most-urban than in the 10 most-forested streams. However, the magnitude of the diel temperature range did not differ between urban and forested streams (as reported in review of the literature; Walsh et al. 2005) because nighttime minimum and midday maximum temperatures were similarly elevated in urban watersheds. Stormflows resulted in rapid stream warming by as much as 4°C in just 10 min. Our SEM suggests that these stormwater-derived thermal surges are not effectively mitigated by typical management efforts to preserve or restore forested riparian buffers. Our results suggest that the magnitude of storm thermal surges is greatest in well-shaded urban streams, which have cooler baseflow temperatures in advance of the delivery of large quantities of hot urban stormflows.

How much difference do a few degrees make?

The hottest temperature observed in our survey was 28.5°C, a temperature above the critical thermal maxima for Salmonidae and Cottidae, among other families (Beitinger et al. 2000a). For most North American freshwater fish species, the critical thermal maxima fall within the range of 32 to 40°C (Beitinger et al. 2000a). In most cases, even during summer thunderstorms, our urban streams did not enter this range. Thus, we found little evidence to suggest that urban stream heating will lead to fish mortality. However, temperatures that exceed the thermal optima of aquatic organisms can lead to slower rates of development or growth (reviewed by Hester and Doyle 2011). The higher

temperatures in the urban streams in our study have the potential to be stressful for in-stream biota and are likely to exacerbate and extend zones of hypoxia and anoxia in benthic sediments and to speed biogeochemical reactions. Quantifying the biological effects of the baseflow temperatures observed in our study streams is difficult because so little is known about this topic.

Thermal surge during stormflow

The effect of temperature surges as high as 4°C on stream biota are poorly understood (Nelson and Palmer 2007). In laboratory studies of thermal tolerance, temperature changes typically are gradual. Thus, results of these studies may have little relationship to outcomes of the temperature surges in urban watersheds. In urban areas, storms result in high flows, intense scouring, and large inputs of pollutants and nutrients in streams. Thus, the effects of heat surges are entangled with a large suite of changes that occur during storms. The extent to which heat shock might contribute to the biological degradation that accompanies flashy urban-stream flow regimes is unclear. However, the sudden and intense temperature surges observed in our study conclusively demonstrate rapid conveyance of heat from impervious surfaces into streams and are an effective indicator of the degree of connectivity between impervious surfaces (and their associated contaminants) and nearby streams. The rapidity of the response highlights the role of storm-water infrastructure in connecting the entire watershed during storm events. Our results are a convincing demonstration of the

capacity of the watershed to absorb and dissipate urban heat. Even our most-extreme observations of storm-flow temperature increases of 4°C in 10 min involved only a small fraction of the heat stored watershed-wide in impervious cover.

Management implications

Surface-connected development, described here by effective development, was an ineffective predictor of thermal regimes in streams. This result emphasizes the importance of including storm-water infrastructure and % developed land in the entire watershed in management practices, rather than focusing on the state of the riparian zone (for further discussion, see Walsh et al. 2005a, Bernhardt et al. 2008b). Baseflow temperatures strongly influenced the magnitude of the temperature surge during stormflow. This result also has important management implications. Local managers could effectively maintain cooler baseflow by increasing canopy cover in riparian areas and by altering stream width, but these efforts are unlikely to effectively mitigate storm-flow heat surges. Riparian cover can reduce baseflow temperatures, but urban streams with high canopy cover may experience much larger temperature increases during storms than those with low canopy cover because large volumes of hot stormwater enter the stream during stormflow. Thus, the difference between baseflow and storm-flow temperature is likely to be greater in a cooler than in a warmer stream. These findings reinforce the importance of considering the entire catchment and its effects when

designing local conservation and restoration projects and when considering how changes in local variables will interact with largely unchanged landscape variables.

Future research

Documentation of temporal and spatial variations in temperature of urban streams is an important first step in understanding how urbanization influences the thermal regime of streams. Our study provides a detailed starting place for research designed to identify the extent of thermal changes caused by urbanization in warm-water streams in other areas. Our descriptions of thermal changes in urban streams and the variables that best explain them are likely to hold true for warm-water streams in urban areas across the world. However, the strength of the relationships is likely to change depending on the specific landscape and the local context of the site. Our work also provides a basis for using temperature as a tracer of urban effects on streams, especially for contaminants and nutrients likely to enter the stream during stormflow.

More research is needed to explore the thermal variability observed in watersheds with moderate amounts of development. For example, we observed an almost 5°C difference between the minimum and maximum mean temperature of streams across the landscape. The thermal variability in moderately developed watersheds was not well explained by the model and many mechanisms were left unclear. Within this moderate range of development, storm-water management, specifically subsurface infrastructure and best management practices, are likely to have

intense effects on the thermal regimes of streams. Researchers need more accurate descriptions of locations and conditions of stormwater pipes. We suspect that the lack of explanatory power of our hydrologically nuanced indices of surface connectivity reflect the reality that these effects are overridden by subsurface connectivity in urban watersheds. Incorporation of fine-scale effects of canopy cover and imperviousness into models also is essential for understanding urban stream ecosystems. Last, more in-depth longitudinal studies with increased spatial and temporal resolution will increase understanding of the influences of variables like outfalls and canopy openings on baseflow and stormflow and will enable researchers to better understand controls on the thermal regimes of urban streams.

Tables

Table 1. Habitat- and watershed-scale variables used in our study. Variables with significant relationships with thermal variables and those used in the structural equation model (SEM) are noted. * = not significant, ** = significant, but not selected for model, * = used in SEM, Min = minimum, Max = maximum, N/A = not applicable.**

Variable	Spatial scale	Description	Min	Max	Analysis
Habitat transitions	Reach	Number of flow habitat transitions per stream reach	1	40	**
Orientation	Reach	N–S vs E–W oriented streams	N/A	N/A	*
Mean width	Reach	Mean wetted width (m)	0.39	13.85	***
Minimum width	Reach	Minimum wetted width (m)	0.05	8.3	*
Maximum width	Reach	Maximum wetted width (m)	2.3	24	**
CV of width	Reach	Coefficient of variation of width	0.09	2.16	**
SE of width	Reach	Standard error of width	0.07	1.15	**
CV of depth	Reach	Coefficient of variation of depth	0.07	2.63	*
SE of depth	Reach	Standard error of depth	0.31	57.03	*
Mean channel incision	Reach	Mean channel incision	0.04	0.44	**
SD of channel incision	Reach	Standard deviation of channel incision	0.002	0.18	*
CV of channel incision	Reach	Coefficient of variation of channel incision	0.008	0.7	*

Canopy closure from ground	Reach	Percent of canopy closure measured at site with spherical densiometer	13	100	*
CV of canopy closure	Reach	Coefficient of variation of canopy cover	0.002	1.16	*
SE of canopy closure	Reach	Standard error of canopy cover	0.09	28.6	*
Canopy closure from aerial photograph	Reach	% canopy closure estimated using 2008 NAIP air photographs	5	100	***
1985 % development	Catchment	% developed land in the watershed in 1985	0	93	*
1995 % development	Catchment	% developed land in the watershed in 1995	0	97	*
% development	Catchment	% developed land in the watershed in 2005	0	99	***
Development since 1985	Catchment	% watershed developed between 1985 and 2005	0	54	*
Development since 1995	Catchment	% watershed developed between 1995 and 2005	0	29	*
Older development	Catchment	% 2005 development present in 1985	0	100	*
% forest	Catchment	% land classified as forested in the watershed in 2005	1	96	*

% field	Catchment	% land classified as field in the watershed in 2005	0	82	*
Effective development	Catchment	See Methods	0	465	**
Effective weighted development	Catchment	See Methods	0	315	*
Effective forest	Catchment	See Methods	0	165	*** (50 m)
Inverse-distance-weighted traffic volume	Catchment	Mean traffic volume per area of watershed weighted by distance to stream	0	48,285	**
Road density	Catchment	Road density (m/ha); total road length in watershed divided by watershed area	0	60	***
Road/stream intersections	Catchment	Number of road/stream intersections/stream km in watershed	0	4	*
% connected development	Catchment	% watershed development directly connected to the stream	0	100	*
Zonal temperature	Catchment	Mean skin temperature of watershed, May 2005 thermal mapping satellite data	20	27	*

Table 2. Mean minimum (min) and maximum (max) values for thermal variables for all streams, 10 most-developed streams, and 10 most-forested streams. Average min and max temperature (temp), mean temp, mean diel range, and degree-days describe the period from May 24 to June 1. Max temp increases and decreases were calculated over 10 min during a 24-h period surrounding a storm. * indicates changes of a magnitude <1.08°C, reflecting the instrument loggers' temperature accuracy of ± 0.54°C.

	Mean min temp (°C)	Mean temp (°C)	Mean max temp (°C)	Max temp increase (°C)	Max temp decrease (°C)	Mean diel range (°C)	Degree-days
Min all streams	17	18.6	20.2	*	*	1.1	19.4
Max all streams	21.4	23.5	26.9	4	-2.5	5	25
Min 10 most-developed streams	17	18.6	22.2	*	*	1.2	21.7
Max 10 most-developed streams	21.4	23	26.1	4	-2.5	4.5	24.6
Min 10 most-forested streams	17.3	18.7	20.2	*	*	1.5	19.4
Max 10 most-forested streams	18.8	21.7	25.1	*	*	3.3	23.5

Table 3. Correlations between thermal variables and landscape and habitat variables of synoptic survey sites, ordered by correlation with mean temperature. Maximum positive and negative correlations for both reach- and catchment-scales are bolded. Minimum and maximum temperature describe the period from May 24 to June 1. Maximum temperature surge over 10 min was calculated during a 24-h period surrounding a precipitation event. Landscape variables were calculated for the watershed of the study site. Habitat variables were calculated for a 100-m reach above the samplers at each site.

	Min temp (°C)	Mean temp (°C)	Max temp (°C)	Diel range (°C)	Degree-days	Max temp surge (°C)
Mean width	0.5212	**0.6022**	**0.4219**	0	**0.4611**	0
Minimum width	0.4284	0.5127	0.3516	0	0.3904	0
SE of depth	**0.5249**	0.5014	0.3384	0	0.4076	0
SE of width	0.3508	0.4131	0.3176	0	0.3208	0
Maximum width	0.2859	0.3575	0.3216	0	0.3111	0
Road density	0.2385	**0.3386**	0.4421	**0.4467**	**0.4564**	0.3073
Inverse-distance-weighted traffic volume	0.271	0.3315	**0.4717**	0.2326	0.406	0.406
Road/stream intersections	0.2198	0.3187	0.3791	0.2169	0.3406	0
2005 development	0.3763	0.2424	0.4066	0	0.3933	**0.6008**
Development since 1985	0	0.2381	0.3174	0	0.3563	0.4085
Development since 1995	0	0.217	0.3003	0	0	0.441
CV of width	0	0	0	0	0	0
CV of depth	0	0	0	0	0	0
Mean channel incision	0	0	0	**0.2479**	0	**0.3877**
SD of channel incision	0	0	0	0	0	0
CV of channel incision	0	0	0	0	0	0

CV of canopy closure from ground	0	0	0	0	0	0
SE of canopy closure from ground	0	0	0	0	0	0
1985 development	0.3536	0	0.3069	0	0.3456	0.4705
1995 development	0.3637	0	0.3491	0	0.3563	0.5171
Older development	0	0	0	0	0	0
2005 field	0	0	0	**–0.2455**	0	–0.3104
Effective development	0.3695	0	0.3229	0	0.3242	0.4798
Effective weighted development	**0.4051**	0	0.2728	0	0.3269	0.438
% connected development	0.3451	0	0.3317	0	0.3336	0.5652
Zonal temperature	0.3412	0	0.3381	0	0.3548	0.469
Effective forest	–0.3356	–0.2513	–0.224	0	–0.3268	0
Canopy closure from ground	–0.3511	–0.3171	–0.2589	0	–0.2879	0
2005 forest	**–0.4133**	**–0.3220**	**–0.4475**	0	**–0.4658**	**–0.4539**
Canopy closure from aerial photograph	–0.4139	–0.4014	–0.4236	0	**–0.4033**	**–0.2487**
Habitat transitions	**–0.4196**	**–0.4933**	**–0.3256**	0	–0.3522	0.2398

Table 4. Results of longitudinal survey of 4 stream reaches. Mean air temperature is air temperature over the time of the survey. The number of observations (*n*) and total distance surveyed differs among stream. Min = minimum, max = maximum, temp = temperature, SD = standard deviation, CV = coefficient of variation.

Stream	Mean air temp (°C)	Min temp (°C)	Max temp (°C)	Mean temp (°C)	SD	CV	*n*	Total distance (m)
Goose Creek	28.8	22.7	28.7	25.4	1.4	0.06	40	1047
Stony Creek	30.3	22.9	25.4	24.2	0.5	0.02	32	1150
Rocky Branch	30.5	23.6	29.5	26.6	1.6	0.06	70	2089
North Gate	28.9	26.5	27.8	27.1	0.3	0.01	45	1700

Figures

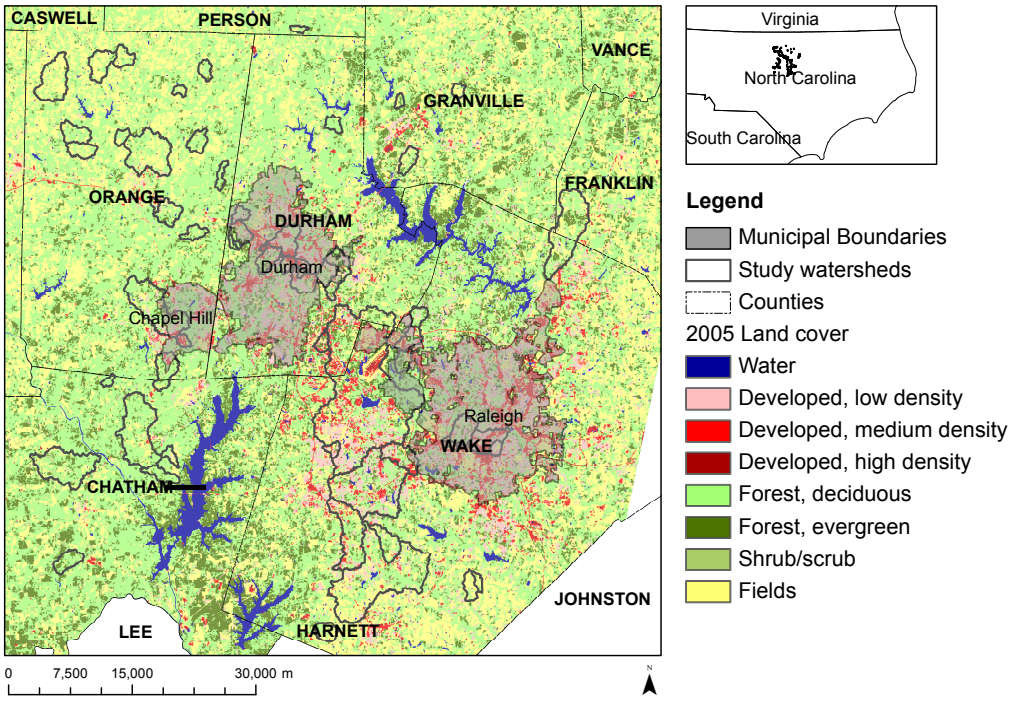

Figure 1. Map of land cover across study area with study watersheds delineated. County names are shown in all capitals.

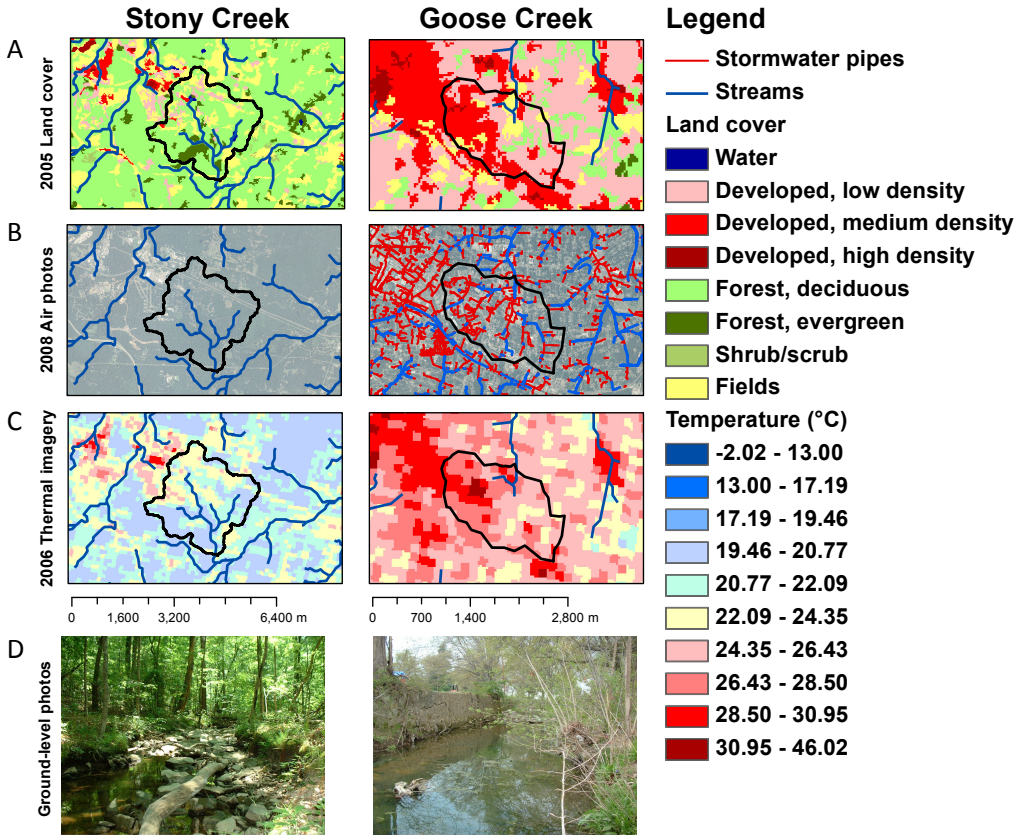

Figure 2. Comparison of Goose Creek (83% development, 5% forest) and Stony Creek (7% development, 73% forest) showing the intensity of stormwater piping and stream burial that occurs in developed watersheds (A), land cover from aerial photographs (air photos) (B), watershed-scale thermal regime, as shown by skin temperature from satellite data (C), and ground-level photographs of the study reaches (D).

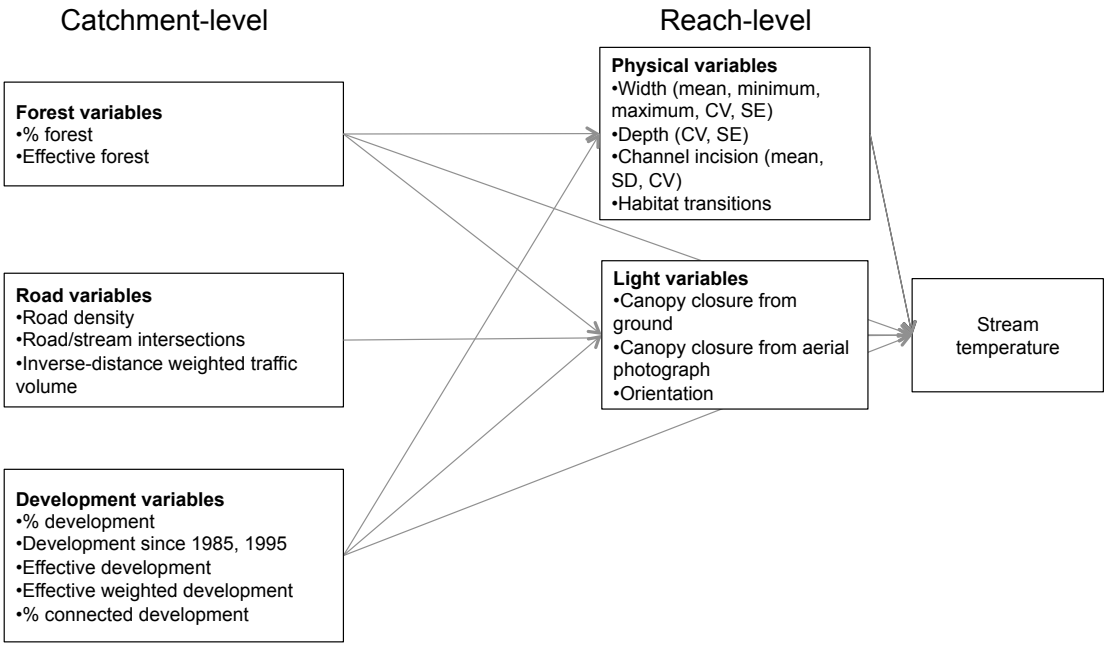

Figure 3. Conceptual metamodel (Grace et al. 2010) showing influence of watershed- and reach-level variables on stream temperature. Each box includes a list of potential variables to describe the given category. This diagram reflects our understanding of the system and was used to select variables to include in the structural equation model. Arrows show direction of effects.

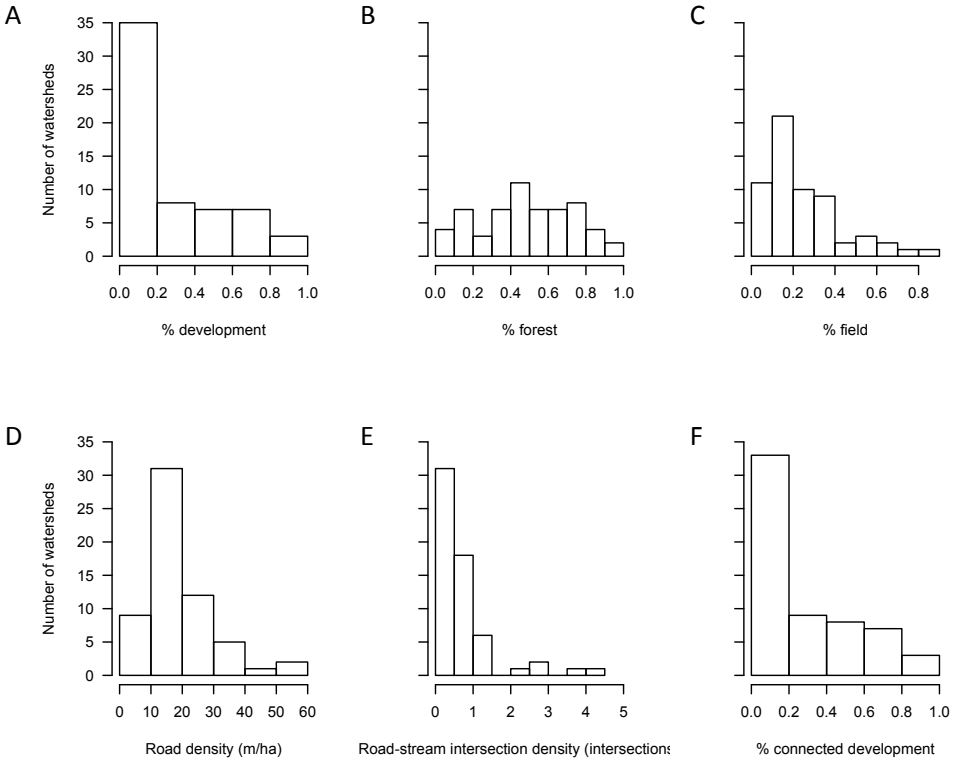

Figure 4. Histograms showing the distributions of % development (A), % forest (B), % field (C), road density (D), road–stream intersection density (E), and % connected development (F) across watersheds. See Table 1 and Methods for descriptions of variables.

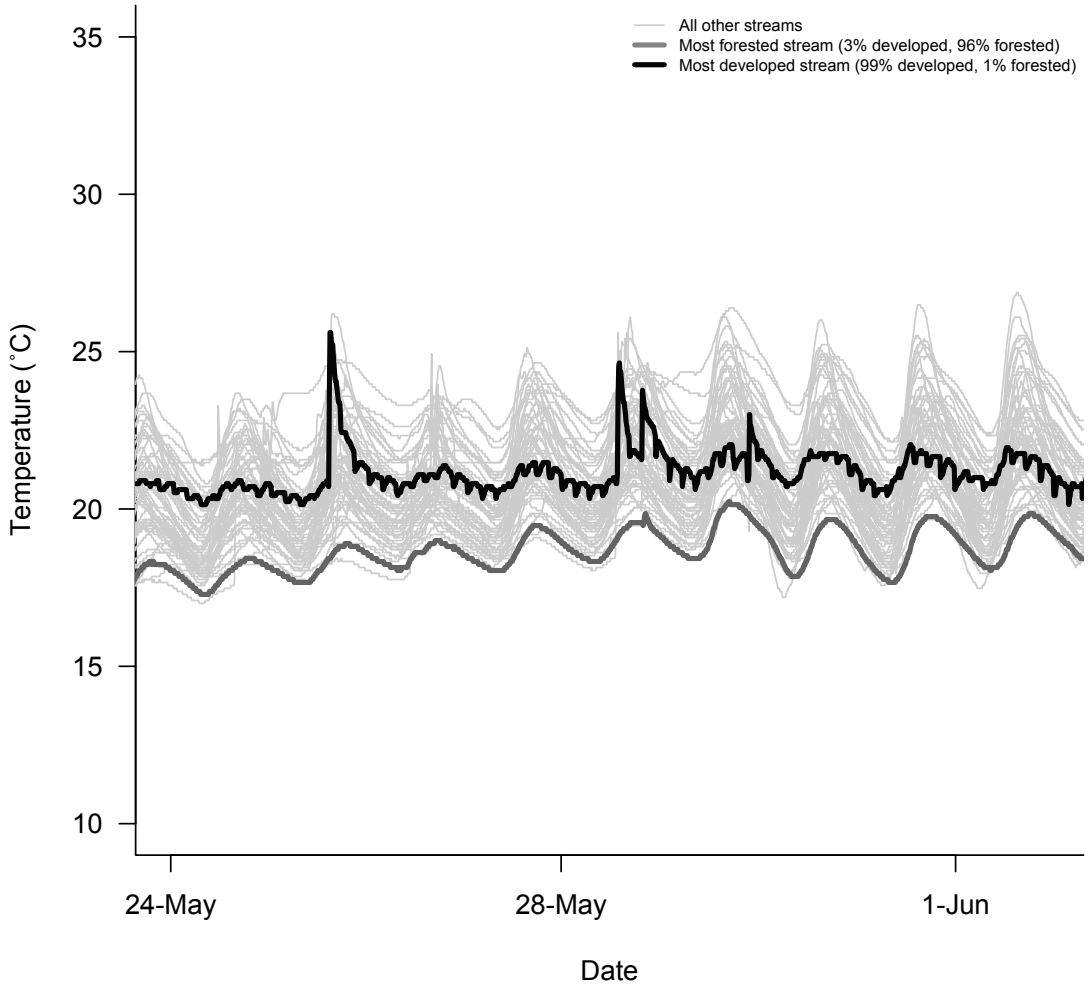

Figure 5. Temperature data from synoptic survey. Lines are color-coded by the primary land-cover category in the watershed. Temperature accuracy is ±0.54°C.

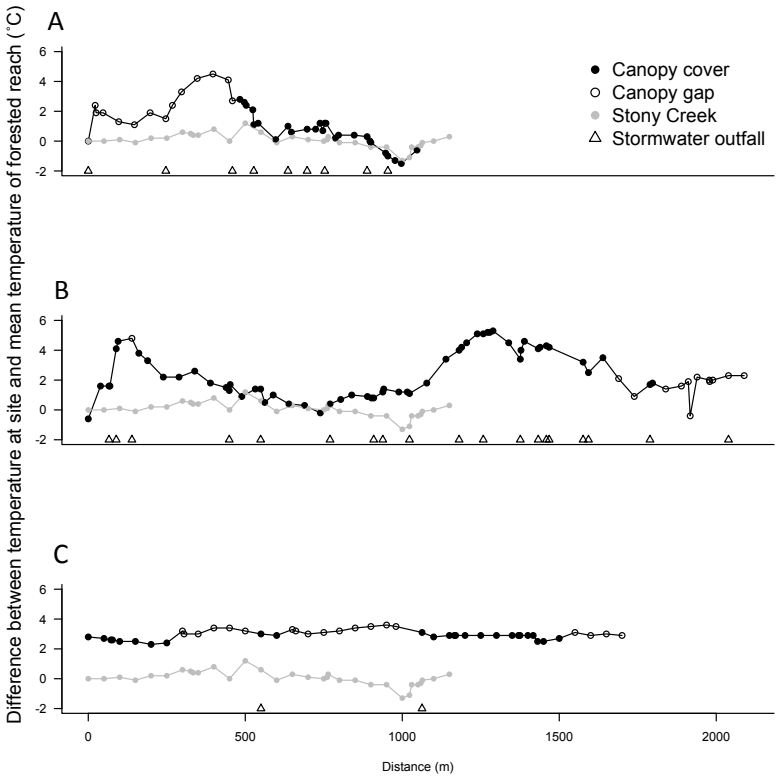

Figure 6. Longitudinal thermal profiles of 3 urban streams: Rocky Branch (A), North Gate (B), and Rocky Branch (C) compared to a forested stream (Stony Creek). Distance at 0 m represents the upstream beginning of the study reach and the measurements move from upstream to downstream along the *x*-axis. Stony Creek has no outfalls in the study reach.

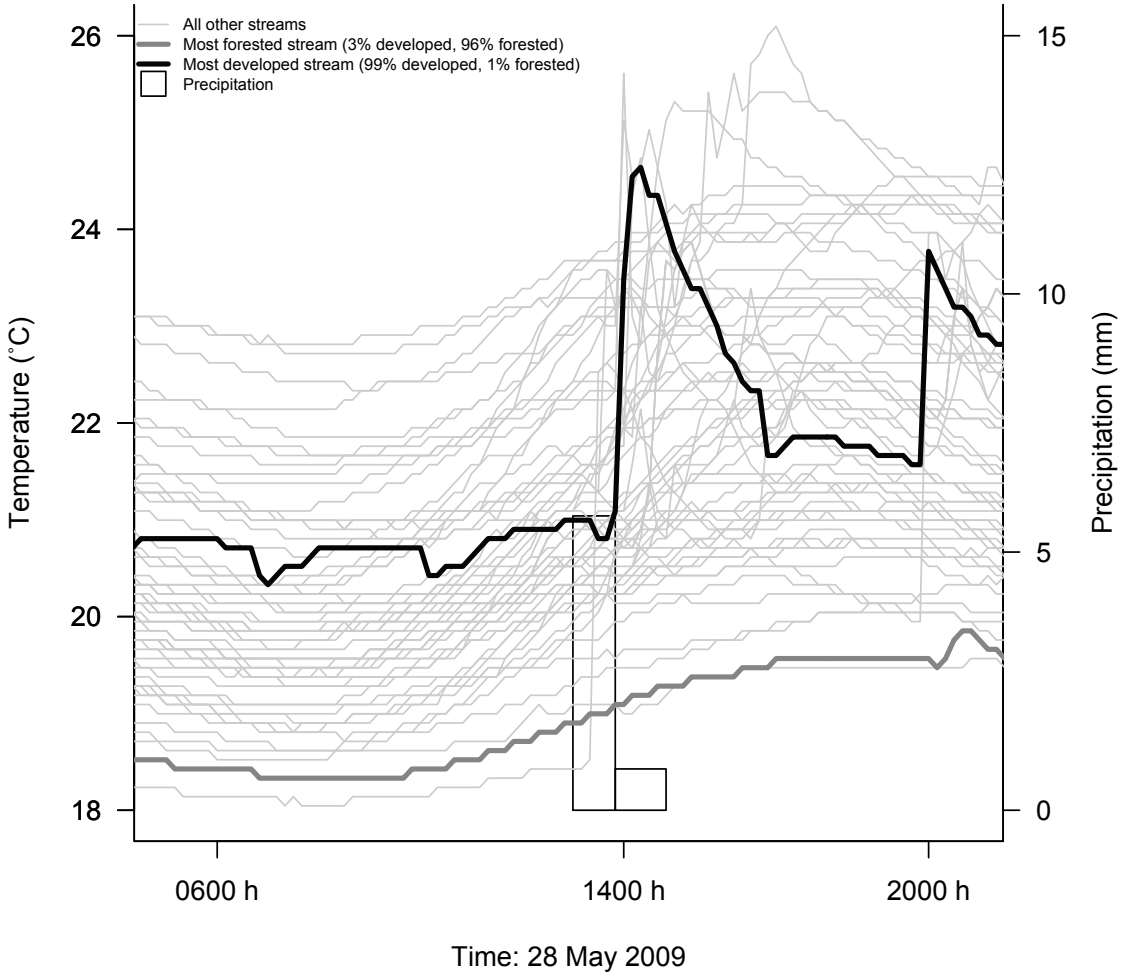

Figure 7. Thermal responses of different streams to the same storm. Lines are color-coded by the primary land-cover category in the watershed. Bar graphs show precipitation, measured on the alternate *y*-axis. Temperature accuracy is ±0.54°C.

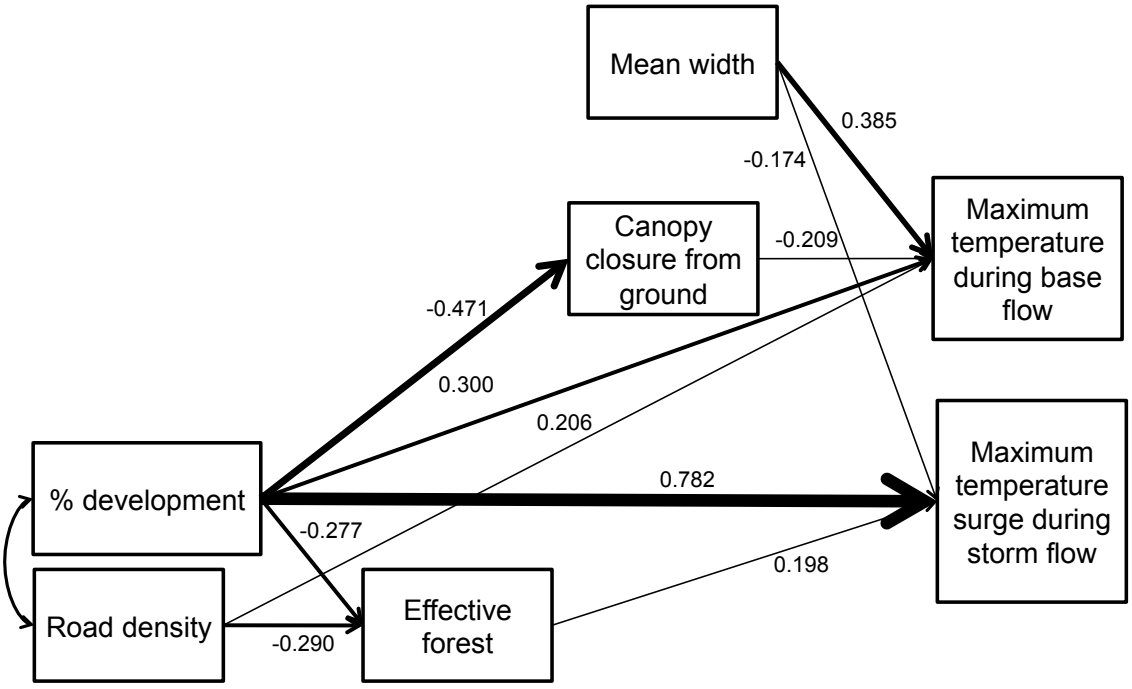

Figure 8. Final thermal structural equation model (SEM) showing standardized regression weights. The SEM was fit simultaneously with 2 focal response variables, maximum temperature during baseflow and maximum temperature surge during stormflow. Arrows show direction of effects. Arrow line weight indicates strength of the path. See Table 1 and Methods for descriptions of variables.

3. Downstream Dissipation and Management of Stormflow Heat Pulses: A Case Study and its Implications

Introduction

Although all freshwaters are experiencing gradual warming, streams in cities are much warmer than their non-urban counterparts (Kaushal et al. 2010). Increased heat-absorbing surfaces and decreased canopy cover in developed areas result in urban heat islands, with some air temperatures more than 10°C above those in surrounding areas (Oke 1973, Pickett et al. 2001, Kalnay and Cai 2003). As urban watershed infrastructure routes precipitation directly off of heat-absorbing impervious surfaces, receiving streams can experience stormflow heat pulses of greater than 7°C (Van Buren et al. 2000, Nelson and Palmer 2007, Somers et al. 2013). The localized warming of both baseflow and stormflow due to urbanization far exceeds the more subtle impacts of global climate change, but global warming is likely to further exacerbate these local heat effects, particularly for regions where climate models predict increasingly frequent and more severe storms (Nelson and Palmer 2007, Kaushal et al. 2010).

Changes in stream thermal regimes threaten the quality and availability of in-stream habitat for aquatic biota and alter the rates of many ecosystem processes (Imberger et al. 2008, Deitchman and Loheide 2012). Sensitive taxa often have clearly defined thermal maxima, above which temperatures prove fatal (Beitinger et al. 2000b, McCullough et al. 2009b), and higher temperatures exacerbate problems of hypoxia in eutrophic waters (Matthews and Berg 1997). Below lethal levels, high temperatures and

sudden thermal changes stress many biota, and may alter their behavior or fitness (Salmela and Anderson 1978, Mesa et al. 2002, McCullough et al. 2009b, Hester and Doyle 2011). Thermal changes also affect microbial activity, increasing the rates of ecosystem processes, including litter breakdown and microbial respiration (Hill et al. 2000b, Imberger et al. 2008).

In unmanaged watersheds, streams' thermal regimes result from direct radiation, heat exchange with air and streambed materials, and diffusion and advection within the water column (Figure 9A). At baseflow, heat enters a stream ecosystem via direct radiation, when sunlight reaches the stream directly, and diffuse radiation, when sunlight is deflected before eventually reaching the stream (Boughton et al. 2012). When air temperatures are higher than stream temperatures, streams gain heat through convection; the opposite can also be true (Caissie et al. 2007). Evaporation and subsequent evaporative heat flux is a primary pathway for heat leaving stream ecosystems (Caissie 2006). Convective heat exchange with streambed sediments and groundwater can also lead to heat gain or loss (Poole and Berman 2001). The temperature of upstream water provides the base temperature for subsequent diffusion of heat from these many sources and longitudinal dispersion through advection (Webb and Zhang 1997). In less modified systems, stormflow heat budgets differ from baseflow primarily via cooling provided by precipitation and decreased radiation (Figure 9B). Direct and diffuse radiation, as well as subsequent longwave radiation, are typically

minimal due to cloud cover, often resulting in decreased air temperature before a storm event (Caissie 2006).

Urban streams are typically hotter at baseflow, due to convection with air warmed by urban heat islands and increased direct radiation resulting from decreased canopy cover (Kalnay and Cai 2003, Walsh et al. 2005b) (Figure 9A). During storms, a much larger proportion of the heat absorbed by impervious surfaces is directly transported into stream channels, overwhelming baseflow heat pathways (Figure 9B) (Somers et al. 2013). Heated run-off from pavement adds an intense stormflow pathway to urban systems that increases stream temperature, negating the cooling effects of precipitation observed in less impacted streams (Herb et al. 2008). To explore the mechanisms by which stormflow heat pulses dissipate in Mud Creek, we asked:

1. What is the maximum distance that a heat pulse travels downstream of urban inputs?
2. How does this distance vary with storm characteristics, including antecedent air temperature and amount and intensity of precipitation and flow?

We created a conceptual model to describe the aspects of a storm that influence the magnitude of a heat pulse in an urban stream and the distance to which it disperses longitudinally (Figure 10). We hypothesized that, the greater the magnitude of the heat pulse, the greater the distance it will travel downstream before dissipating, so that these two metrics are highly correlated. We expected that air temperatures preceding individual storms directly control the size and dissipation distance of a heat pulse, by

influencing the amount of heat entering the stream. Specifically, air temperature impacts the temperature of precipitation as well as the amount of heat absorbed by land surfaces. Precipitation also influences the amount of heated run-off entering the stream, again increasing a heat pulse's magnitude and distance to dissipation. The intensity of a storm—characterized by large amounts of precipitation over a short period of time and large and sudden changes in flow—will also increase the magnitude of the heat pulse and the distance downstream it travels. Dilution, the amount of antecedent flow in the stream that can reduce heat from run-off, will decrease both the initial magnitude of the heat pulse and its dissipation distance. Similarly, as average flow during the storm increases, less heated run-off dilutes heat delivered to the system, decreasing the magnitude of the heat pulse and the distance it travels.

Study Area

To better understand the magnitude of stormflow heat pulses, the potential for these pulses to travel downstream, and the aspects of storms that influence the size and distance to dissipation of these pulses, we used Mud Creek in Durham, North Carolina as a case study (Figure 11). Mud Creek is 11% impervious, according to 1-m resolution landcover based on color infrared National Agricultural Imagery Program (NAIP) aerial photo mosaics (United States Department of Agriculture 2009) and described fully in Beck et al. (*in prep*). The stream originates from a series of stormwater drains and ephemeral channels within a 1980s era residential development, before flowing for ~2

km through a protected research forest (Figure 11). This gradient allows us to track the downstream dissipation of stormflow heat pulses in a relatively controlled setting.

Although habitat metrics in the downstream portions of Mud Creek are similar to more forested, less impacted streams, Mud Creek shows lower levels of sensitive macroinvertebrates and higher levels of tolerant macroinvertebrates than these same forested watersheds (Violin et al. 2011). One hypothesis for this mismatch between habitat and biodiversity is the influence of upstream urbanization, including stormflow heat pulses. Given the relatively low amount and intensity of development upstream and the high quality of downstream management, this research aims to understand how thermal impacts propagate and dissipate from the upper, urban watershed into the protected stream reach. This study helps us to better understand the potential for urban impacts to travel downstream and the aspects that control these impacts. Further, by using a best-case management scenario, we can calculate conservative estimates of downstream longitudinal impacts.

Methods

Data collection

We instrumented a 2 km reach of Mud Creek for one year, from May 2011 to April 2012 (Figure 11). This reach flows through a suburban development into a protected forest. Sixty-one stream temperature loggers (Onset HOBO® Temperature/Alarm (waterproof) Pendant® Data Loggers (UA-001-08); accuracy

±0.54°C) were deployed throughout the study reach, focusing loggers above and below all stormwater pipe outfalls and canopy openings. In addition, we collected temperature data using a distributed temperature sensor from CTEMPs (Center for Transformative Environmental Monitoring Program) for approximately 7 weeks along 1.5 km of this same reach. However, storms repeatedly moved large sections of the cable out of the water. Despite weekly maintenance of the cable, the resulting data were far too noisy to be used with confidence. We also placed 8 air temperature loggers (Onset HOBO® Pro Series Temperature Data Loggers; accuracy ±0.2°C) along Mud Creek, at 300, 1300, 1650, and 2140 m downstream of the start of the study reach. At each location, we placed one logger on the ground and one at breast-height on a tree. Water level was recorded using a pressure transducer (Solinst Levelogger Silver, Model 3001) at the downstream portion of the study reach. We also placed a precipitation gauge at the upper end of the study reach (Onset Data Logging Rain Gauge RG3).

Calculation and statistical analysis of air temperature and baseflow metrics

Our research questions focus primarily on stormflow metrics, but we were also interested in thermal differences at baseflow. We performed analyses to identify differences in both stream and air temperature between the urban and forested portions of the study reach. After removing days containing storm events and periods where the stream was dry, we calculated a number of metrics to quantify stream and air temperature along the study reach (Table 5).

For each air temperature logger, we calculated daily minimum, median, and maximum temperatures, as well as daily degree-days using the double-triangle method and a base temperature of 0°C (Sevacherian et al. 1977, Roltsch et al. 1999). Degree-days are a useful way to describe the cumulative heat experienced in an area, by including both maximum and minimum temperatures over a 24-hour period, rather than reducing this variation by calculating the average temperature over a day (Sevacherian et al. 1977). We then used paired, two-tailed *t*-tests to compare the air temperatures at both ground and breast-height at the upper, urban end of the reach to the air temperatures at the lower, forested end of the reach.

For baseflow stream temperature, we calculated daily degree-days and cumulative monthly daily degree-days at each logger. To assess the greatest potential differences, we grouped the loggers into those in the upstream third, most urban portion of the reach and in the downstream third, most forested portion of the reach. We removed loggers within or directly downstream of canopy gaps to remove canopy effects. For reference, we also compared these to a forested tributary feeding into Mud Creek. Although this stream is much smaller, this tributary provides a fully forested system under the same climate and storm conditions to Mud Creek. This qualitative comparison emphasizes the changes caused by urbanization to the thermal regime and ensures that patterns are not natural. Across these three groups (urban, forested

downstream of urban, and completely forested), we used paired two-tailed *t*-tests to compare these metrics over the entire year and the summer.

Identification of storms and calculation of stormflow metrics

To calculate flow from water level, we created a rating curve of the level to flow relationship based on salt slug dumps during storm events, following Hongve 1987 and Kite 1993, with a maximum flow measured of 3150 L/s. We did not include stormflows greater than this amount in our analyses (leading to a loss of data for 10 storms from the 12 month record). We defined storms as events when flow reached greater than 10% of antecedent baseflow following measurable precipitation. We defined storm event start times as the start of precipitation and end times as the time when flow returned to within <10% of antecedent baseflow or, for storms in a series, when flow was at a minimum before increasing with a new storm event.

To describe the magnitude of heat pulses, we considered a number of metrics, including maximum temperature, maximum temperature increase, area under the curve, duration of elevated temperature, and amplitude (Figure 12). However, we focused on storm amplitude at each thermal logger as the best description of overall temperature changes caused by stormflow. In the calculation of amplitude, maximum positive amplitude was calculated as the temperature after the highest positive change in temperature minus the minimum temperature before this positive change in temperature. If no positive change occurred, maximum amplitude was recorded as zero.

To quantify the heat pulse across the study reach, we calculated the maximum amplitude that occurred across the entire reach over the storm event as well as the distance at which the amplitude decreased to less than 1°C.

We characterized individual storms by their duration, peak flow, and cumulative flow and considered antecedent flow and the proportional increase in flow as potential modifiers of storm effects. We calculated the duration of elevated flow as the time from minimum flow in the first half of the storm to the time of minimum flow in the second half. Cumulative flow over the storm was calculated as the area under curve of elevated flow, as defined above. Antecedent flow was calculated as the average flow over 24 hours before the start of the storm event. The dilution of stormflow by antecedent flow was calculated as the difference between maximum and antecedent flow and as the percent increase in flow, quantified as the maximum flow divided by the antecedent flow. Flow intensity was calculated as the maximum change in flow over 1 minute. Flow over the storm event was further quantified as the mean and maximum flow over the storm event and mean flow over the first hour of the storm event.

We characterized the precipitation regime surrounding each storm by the average and total precipitation over each storm event. We calculated precipitation intensity as the maximum precipitation rates during the storm event over 5 and 60 minutes, as well as the precipitation rate over the first hour of the storm event. Air temperature prior to each storm was calculated over the 30, 60, and 120 minutes prior to

the storm event. We also considered the cumulative heat before a storm by calculating the sum of degree-hours using the double-triangle method and a base temperature of 0°C over 2, 3, 4, 5, and 6 hours before the storm event (Sevacherian et al. 1977).

Statistical analyses of stormflow metrics

First, we were interested in assessing the storm conditions in terms of precipitation, flow, and air temperature under which an amplitude greater than 1°C occurred. We grouped storms into those that showed no amplitude greater than 1°C; amplitude greater than 1°C; amplitude greater than 1°C 1 km downstream of urban inputs; and amplitude greater than 1°C only at a canopy opening in the forested portion of the reach. We removed the final category from further analyses. Although 1°C is near the threshold for overall accuracy of the loggers, the amplitude measured here consists of the difference between the maximum and minimum temperatures over the storm rather than the overall, absolute temperature. By selecting a cutoff threshold near the margin of error, we err on the side of analyzing all storms that likely showed heat pulses.

Second, we were interested in assessing, for storms during which an amplitude greater than 1°C occurred, which storm conditions could best explain the magnitude of the maximum amplitude along the reach and the distance at which the amplitude became less than 1°C. We first selected the variable from each category in our understanding of the system that was most highly correlated with the response variables

of heat pulse amplitude magnitude and distance to dissipation (Figure 11). To interpret the effects of individual variables and avoid conflation of correlations and collinearity between variables, we chose to use structural equation modeling (SEM) following our conceptual diagram and using the most highly correlated variables within each category (Grace et al. 2010). Unlike heat equations and other methods, SEMs allowed us to include and analyze direct pathways between precipitation metrics and the thermal response variables as well as indirect pathways via flow variables. After fitting the initial model based on our path diagram, we used a step-down procedure, iteratively removing the weakest pathway and then re-fitting the model until all pathway *P*-values were < 0.1 (Grace 2006b).

Landcover analyses

To assess the implications of heat pulses that travel more than 1 km downstream of urban inputs, we calculated the amount of stream within the municipal boundaries of Durham, North Carolina that was less than 1 km downstream of a stormwater outfall. To do so, we analyzed NHDPlus Version 1 flow lines (U.S. E.P.A. 2006), as a network dataset based on flow direction, and Durham Municipal stormwater infrastructure (Durham Storm Water 2007) using a geographic information system (ArcGIS, version 11; Environmental Systems Research Institute 2008, Redlands, California). We also assessed these metrics within land defined as "managed areas" by North Carolina's Natural Heritage Program (Department of Environmental and Natural Resources 2012). We

calculated the percent of stream length potentially impacted by stormwater outfalls in the entire municipality as well as within managed areas of the municipality.

Results

Air temperature

Across all sites, air temperatures ranged from -7.9 to 44.9°C over the course of the year, with the maximum average daily temperature, 29.1°C, occurring at the ground surface logger in the upper portion of the sub-catchment. There were no differences in the minimum, median, or maximum air temperatures between our upper urban sub-catchment and the downstream, forested area. However, daily degree-days at the ground surface over the year were typically 2.1°C greater in the upper urban sub-catchment than in the downstream forested reach (unpaired, two-tailed *t*-test, $\alpha = 0.05$). There were no statistically significant differences between these metrics for temperature loggers installed at breast-height.

Baseflow

Across all sites, water temperatures ranged from -5 to more than 32°C over the course of the year, with maximum temperatures observed in canopy gaps during periods of extremely low flow. We observed the greatest mean daily stream temperature, 28.9°C, within the forested reach but directly below the largest canopy gap in the study reach. Diel variation ranged from less than 1 to almost 20°C across all loggers in Mud Creek. Again, some of these maximum diel ranges may be explained by

either direct radiation or thermal anomalies, but changes of this magnitude were recorded at multiple logger locations and across multiple days. The coolest average temperature over the study was observed within the urban reach, below a small tributary, and the warmest average temperature over the study was observed in the upstream portion of the forested reach, in a pool below a debris dam. The daily degree-days of water temperatures throughout Mud Creek were consistently greater than 1°C warmer than the surface waters of a nearby, fully forested tributary.

Stormflow

Our loggers captured temperature data for 54 storms from May 2011 to April 2012 (Table 6; Table 14 in Appendix A; Figure 13). Storms ranged from showing no heat pulse (amplitude of less than 1°C) across the entire reach to showing a heat pulse of greater than 1°C 1 km downstream of urban inputs, the end of the study reach (Figure 14). In 42 of these storms, we observed heat pulses with amplitude greater than 1°C. Amplitude of greater than 1°C at only a single location in the reach occurred in only 8 of these storms, and the maximum amplitude was greater than 1.2°C in four of these storms. Nineteen of these storms showed a heat pulse of amplitude greater than 1°C only directly below the inputs of the upper, urban watershed, while three storms showed heat pulses of amplitude greater than 1°C only downstream of a large canopy gap within the protected forested area. Finally, 11 storms showed heat pulses of amplitude greater than 1°C transported at least 1 km downstream of urban inputs. For

the same population of storms, only 1 showed amplitude greater than 1°C in the forested tributary (Figure 15). The maximum amplitude of any heat pulse across all storms and the entire study reach was 5.4°C; the maximum amplitude downstream of urban inputs was 5.3°C.

Storms that resulted in heat pulses greater than 1°C differed significantly from storms that did not generate heat pulses (Figure 16). Storms with a heat pulse amplitude greater than 1°C anywhere in the reach had significantly greater precipitation in the first hour, total precipitation, and maximum precipitation rates over 5 minutes and 1 hour (unpaired, two-tailed *t*-tests, $\alpha = 0.05$). Additionally, these storms had significantly greater elevated stormflow duration and area under the stormflow curve (unpaired, two-tailed *t*-tests, $\alpha = 0.05$). However, there were no differences between pre-storm thermal metrics. Storms with heat pulse amplitudes greater than 1°C greater than 1 km downstream of urban inputs compared to storms with heat pulse amplitude less than 1°C had greater total precipitation, difference between maximum and antecedent flow, maximum change in flow, and maximum flow, as well as lower antecedent flow (unpaired, two-tailed *t*-tests, $\alpha = 0.05$). Further, these storms had greater mean air temperature 30 minutes before the storm event. Storms that only showed heat pulse amplitudes of greater than 1°C at the canopy gap in the forested area, compared to storms that showed no heat pulse amplitude greater than 1°C, had greater flow duration and lower antecedent flow (unpaired, two-tailed *t*-tests, $\alpha = 0.05$).

We also explored which storm characteristics best explained both the magnitude of the heat pulse amplitude and the distance along the study reach at which the heat pulse dissipated to less than 1°C. We analyzed the 26 storms in which a heat pulse greater than 1°C occurred in locations other than downstream of the large canopy gap and for which no data were missing. Among all candidate explanatory variables, we found significant positive correlations between response variables of maximum amplitude and distance of dissipation and explanatory variables of air temperature, flow, and precipitation (Table 14 in Appendix A). We found no negative correlations with the response variables.

We found that maximum amplitude was strongly correlated with all air temperature metrics, with the greatest correlation with the sum of air temperature degree-hours over 2 hours preceding the storm (r = 0.5). Maximum amplitude also showed high correlations with all precipitation variables, the greatest of which were precipitation intensity over one hour (r = 0.48) and the first hour of the storm (r = 0.45). Finally, maximum amplitude showed the highest correlations with flow variables describing intensity over 1 minute (r = 0.45) and dilution, measured as difference between peak stormflow and antecedent baseflow (r = 0.43).

Maximum distance of amplitude of more than 1°C was mostly highly correlated with precipitation metrics, with the greatest correlation with total precipitation (r = 0.79) and maximum intensity per hour (r = 0.77). Maximum distance was also highly

correlated with a number of flow metrics, the greatest being with dilution, calculated as the percent increase in flow during the storm (r = 0.74). The magnitude of the amplitude of the heat pulse also highly correlated with the distance the heat pulse traveled (r = 0.65). Finally, air temperature showed high correlations with maximum distance, the greatest with cumulative degree-hours over 2 hours preceding the storm (r = 0.63).

We selected the most highly correlated variable in each category and created an SEM following the structure and pathways of our conceptual model (Figure 17). We then fit and stepped down this model using maximum likelihood estimates, iteratively removing the pathway with the greatest *P*-value and re-fitting the model until all pathways were significant (α = 0.1). The aim here is to find a final model consistent with the data; that is, to *fail* to reject the null hypothesis that the model and data are consistent. The final model had 6 degrees of freedom, a Chi-square of 5.517, and a probability level of 0.479 (Figure 17). This model allowed us to explain 75% of the variation in the distance of dissipation of the heat pulse and 41% of the variation in the magnitude of the heat pulse (Table 7).

Two variables we had hypothesized as important were removed from the model: precipitation intensity, calculated as maximum precipitation rate over 5 minutes, and dilution of stormflow by baseflow, calculated as the maximum flow divided by the antecedent flow. Total precipitation affected distance directly and positively (total direct effect = 0.627), while no flow variables influenced distance. Alternately, maximum

amplitude was influenced by precipitation only indirectly via flow variables (total indirect effect = 0. 121). Flow intensity had a direct positive effect (0.937) on maximum amplitude, while maximum flow had a direct negative effect (-0.722) on maximum amplitude. Maximum amplitude was directly influenced by air temperature (0.470), but distance was affected by air temperature only indirectly through the maximum amplitude of the heat pulse (0.192). The most significant pathways that influenced the heat pulse distance were from both maximum amplitude and precipitation ($P < 0.001$). The strongest total effects on maximum amplitude were a positive effect from flow intensity and a negative effect from maximum flow ($P < 0.001$). The strongest total effects on distance of dissipation were positive effects from total precipitation, maximum amplitude, and flow intensity (Table 8).

Landcover analyses

Durham municipality entails 223.8 km^2 and contains 200.1 stream km and 8,329 mapped stormwater outlets (Figure 18). In total, only 2.2 km of stream length (1.1%) within the city are greater than 1 km downstream of a stormwater outfall. 38.4 km of the total 40.4 km (95%) of stream length within North Carolina Natural Heritage Managed Areas are less than 1 km downstream of an outfall or outlet.

Discussion

Summary of findings

Heat pulse size in Mud Creek is most greatly influenced by air temperature preceding a storm, flow intensity, and dilution of stormflow. Additionally, heat pulses are the most likely to penetrate far downstream when a storm occurs with a large amount of precipitation and when heat pulses show large amplitudes. In 11 events in one year (20% of storm events observed), heat pulses of amplitude greater than 1°C traveled more than 1 km downstream of urban inputs, into and within a best-case scenario management area. This case study shows that, even in a modestly developed watershed, urban stormwaters routinely penetrate more than 1 km downstream of stormwater outfalls.

Mud Creek as a best-case scenario in urban landscapes

The vast majority of stream networks in developing regions are less than 1 km downstream of a stormwater outfall and thus highly susceptible to the frequent urban stormwater pulses we have described here in Mud Creek. We have emphasized the thermal pollution problems associated with these storms, because temperature effects are relatively inexpensive to monitor at high spatial and temporal frequencies. However, it should be equally clear that many pollutants, including trace metals and polycyclic aromatic hydrocarbons (PAHs), are also delivered from urban surfaces to streams during storms. They are likely to be transported much further than heat, which

dissipates rapidly due to exchange with groundwater and air. Thermal findings in Mud Creek emphasize the potential for stream degradation not only directly downstream of urban inputs, but across the entire urban landscape.

Although the study reach contains no best management practices (BMPs), Mud Creek's watershed contains relatively low development and a large amount of protected forest. Results from Mud Creek represent a best-case scenario for urban streams in the North Carolina Piedmont, which makes estimates about the distance that heat pulses can travel rather conservative. The magnitude of heat pulses in Mud Creek and their potential to travel far downstream of urban inputs emphasizes the need for studies that focus on downstream propagation of urban impacts and explore how these findings differ across regions and across watersheds.

Thermal management

Thermal pollution in urban streams at baseflow is now actively regulated in areas that contain economically important, and thermally sensitive, fish populations, such as salmonids in the Pacific Northwest of the United States of America (Jones et al. 2006). For example, Clean Water Services in the Willamette Valley, Oregon, USA has established thermal total maximum daily loads and begun temperature trading schemes throughout the watershed (Cochran and Logue 2011). This type of stream management often focuses on maintaining baseflow conditions at unimpacted levels (Figure 9C), while ignoring the potential for sudden, intense stormflow changes (Figure 9D) (Walsh

et al. 2005a, Bernhardt and Palmer 2007). Some progressive areas require settling ponds for cooling water and decreasing suspended sediment (Tsihrintzis and Hamid 1997) (Figure 9D). However, older development and areas without such regulations continue to pipe urban stormwater directly into streams (US EPA 1999, Kaushal and Belt 2012). As governments and companies begin to invest in maintaining baseflow temperatures, these same ecosystems face unaddressed, intense thermal changes during stormflow that can potentially travel far downstream of inputs.

Stormwater management focuses on changing the timing and delivery of stormflow to streams, allowing time for heat to dissipate through convection with air temperature and suspended solids to settle out of the water column (Figure 9D) (Barrett 2008, Herb et al. 2009). This can occur by increasing infiltration, for example through grassy swales and pervious surface, or by capturing stormwater in detention and retention systems, such as stormwater ponds, wetlands, or basins, before it enters the stream network (United States Environmental Protection Agency 1999, Dietz 2007). The distance required to dissipate large heat pulses via diffusion and convection with air temperature in Mud Creek implies that BMPs that decrease the initial amplitude of the heat pulse will also decrease the distance downstream the heat pulse travels, potentially protecting downstream systems from the worst impacts of stormflow.

By strategically placing stormwater BMPs upstream of managed areas, managers can explicitly consider downstream and watershed-level implications and better restore

stream sections currently protected from baseflow thermal alterations through riparian buffers and mature forest (Barrett 2008). Even with these practices in place, heat pulses can still occur in streams due to intense storms that overwhelm these engineered structures (Jones and Hunt 2009). Structures, such as large stormwater ponds, with little canopy cover and much direction radiation, can simply displace heat pulses from sudden, intense shocks during stormflow to constant, raised baseflow temperatures (Jones and Hunt 2010). By incorporating reach- and site-scale baseflow and stormflow management techniques throughout a watershed, the hydrology and thermal regimes of urban streams could be restored to a less modified state.

Future research

This research emphasizes the importance of exploring the movement of heat within urban stream networks. In this study, SEMs calculated both negative and positive relationships and their interactions, allowing us to go beyond the more simple relationships of a heat equation. However, many additional questions arise that could not be answered by the methods used in this study. Hydrologists and engineers have explored the thermal heterogeneity of stream reaches at this level, but typically focus on baseflow and ignore the temporal dynamics of sudden heat pulses. Applying baseflow heat and water budgets and models to stormflow heat pulses in urban stream networks would allow researchers to confirm the hypothesized mechanisms by which stream water gains and loses heat along a reach.

This study could gain from increasing the precision of loggers and including their accuracy more explicitly in statistical analyses. Additionally, we did not perform calibration of sensors to improve accuracy or to correct for drift (up to 0.1°C per year, according to Onset). Future research should use more accurate loggers and correct for drift as well as performing further sensitivity analysis to increase precision in measurements and more confidence in conclusions derived from results.

Looking forward: climate change and development

For Mud Creek, the aspects that we found most likely to influence the magnitude of heat pulse amplitudes greater than 1°C were high air temperature before storm events, precipitation, and flow intensity. High maximum flow, alternately, showed a negative effect on heat pulse magnitude and dissipation distance. Climate models for the southeastern United States predict hotter temperatures (annual air temperatures up to 2°C greater in 2020 compared to those in 1990), more intense and sudden storms, and more droughts, likely to combine to result in larger heat pulse amplitudes (Bernstein et al. 2007, Sun et al. 2009). Greater maximum amplitudes and precipitation will also increase heat pulse dissipation distances. As climate change worsens, heat pulses will likely increase in size and penetrate further into urban landscapes.

Currently, 51% of the world's population lives in these developed landscapes, and urbanization is projected to continue to increase internationally (Population Reference Bureau 2012). For example, researchers expect that urban populations will

nearly double over 40 years, increasing from 3.1 billion in 2010 to 5 billion in 2050 (Seto et al. 2011). Stormwater infrastructure hyper-connects these developed landscapes by moving water quickly from impervious surfaces into stream ecosystems (Kaushal and Belt 2012). Our findings imply that long-term downstream thermal urban impacts can, and often do, travel into protected, managed areas. Other urban pollutants, such as heavy metals and pesticides, likely propagate more than 1 km downstream far more frequently (for example, Grimm et al. 2005, Kaushal and Belt 2012).

With a population of approximately 233,000, Durham municipality provides an example of the small- to mid-sized cities that make up more than half of the world's urban population (United Nations Population Division 2012, United States Census Bureau 2013). Even in this moderately developed landscape, urban stormwater potentially impacts 98.9% of streams regularly. As climate change worsens and development increases, urban impacts to streams will increase and propagate even further downstream. Stream management in developed landscapes must focus on decreasing storm pulses that enter stream networks by assessing development connectivity and configuration and utilizing BMPs that address both baseflow and stormflow thermal pollution.

Tables

Table 5. Definitions of storm metrics calculated, including conceptual category.

Metric	Units	Description	Category
Air temperature degree days	Degree days	For each logger, at ground and breast height. Calculated daily and cumulative over each month.	Air temperature
Stream temperature daily degree days	Degree days	For the top and bottom third of the reach, as well as a forested tributary. Calculated daily and cumulatively over each month.	Baseflow stream Temperature
Antecedent flow	L/s	Average flow 24 hours before storm	Dilution of stormflow
Flow difference	L/s	Difference between maximum and antecedent flow	Dilution of stormflow
Flow percent	%	Percent increase in flow, quantified as the maximum flow divided by the antecedent flow	Dilution of stormflow
Average flow	L/s	Mean flow over storm event	Average flow
Average flow in 1st hour	L/s	Mean flow over first hour of the storm event	Average flow
Maximum flow	L/s	Maximum flow over storm event	Average flow
Maximum change in flow	L/s	Maximum change in flow over 1 minute	Flow intensity
Duration of elevated flow	Minutes	Duration of elevated flow, calculated as the time from minimum flow in the first half of the storm to the time from minimum flow in the second half of the storm	Stormflow duration
Area under flow curve	Liters	Area under curve of elevated flow curve	Cumulative stormflow
Maximum precipitation rate	In /time	Over 5 and 60 minutes; over first hour	Precipitation intensity
Average precipitation	In	Over entire storm event	Average precipitation
Total precipitation	In	Over entire storm event	Average precipitation
Mean air temperature	˚C	Over 30, 60, and 120 minutes before storm	Stormflow air temperature
Sum of air temperature degree-hours	Degree hours	Over 2, 3, 4, 5, and 6 hours before storm	Stormflow air temperature
Maximum amplitude of heat pulse	˚C	Across entire reach	Heat pulse
Distance of dissipation of heat pulse	Meters	Distance at which amplitude <1˚C	Heat pulse

Table 6. Selected storm characteristics for 54 storms, averaged across season, for which we collected air and stream temperature, precipitation, and flow data. Note that some air temperature data is missing from February to April 2012. Definitions of each metric are described in Table 1. All storm characteristics for each storm are listed in Table 14 in Appendix A.

Time	Num storms	Max flow (L/s)		Max flow intensity (L/s)		Total precip (in.)		Air temp (˚C)		Max amp. (˚C)		Dissipation distance (m)	
		Min	Max	Min	Max	Min	Max	Min	Max	Min	Max	Min	Max
May 2011 to Aug 2011	10	55	53060	3	7976	0.01	1.41	40	51	0.19	5.59	0	2168
Sept 2011 to Nov 2011	19	62	36533	4	8747	0.07	1.75	5	47	1.33	5.79	294	2168
Dec 2011 to Feb 2012	13	73	30694	6	5937	0.06	1.11	0	30	1.07	4.68	0	2168
Feb to Apr 2012	4	45	344	2	31	0.16	0.3	NA	NA	1.91	4.19	0	2168

Table 7. Strength and significance of pathways of fitted structural equation model.

Pathway	***P*-value**	**Standardized regression weight**
Total precipitation on maximum flow	< 0.001	0.712
Total precipitation on maximum change in flow	< 0.001	0.678
Air temperature on maximum amplitude	0.004	0.47
Maximum change in flow on maximum amplitude	0.03	0.937
Maximum flow on maximum amplitude	0.097	-0.722
Maximum amplitude on distance of dissipation	< 0.001	0.409
Total precipitation on distance of dissipation	< 0.001	0.627

Table 8. Direct, indirect, and total effects of stormflow metrics on maximum amplitude and distance of dissipation in fitted structural equation model.

Metric	Standardized direct effect on maximum amplitude	Standardized indirect effect on maximum amplitude	Standardized total effect on maximum amplitude	Standardized direct effect on dissipation distance	Standardized indirect effect on dissipation distance	Standardized total effect on dissipation distance
Max amp	NA	NA	NA	0.409	0	0.409
Max flow	-0.722	0	-0.722	0	-0.295	-0.295
Max change in flow	0.937	0	0.937	0	0.383	0.383
Total precip	0	0.121	0.121	0.627	0.049	0.676
Air temp	0.47	0	0.47	0	0.192	0.192

Figures

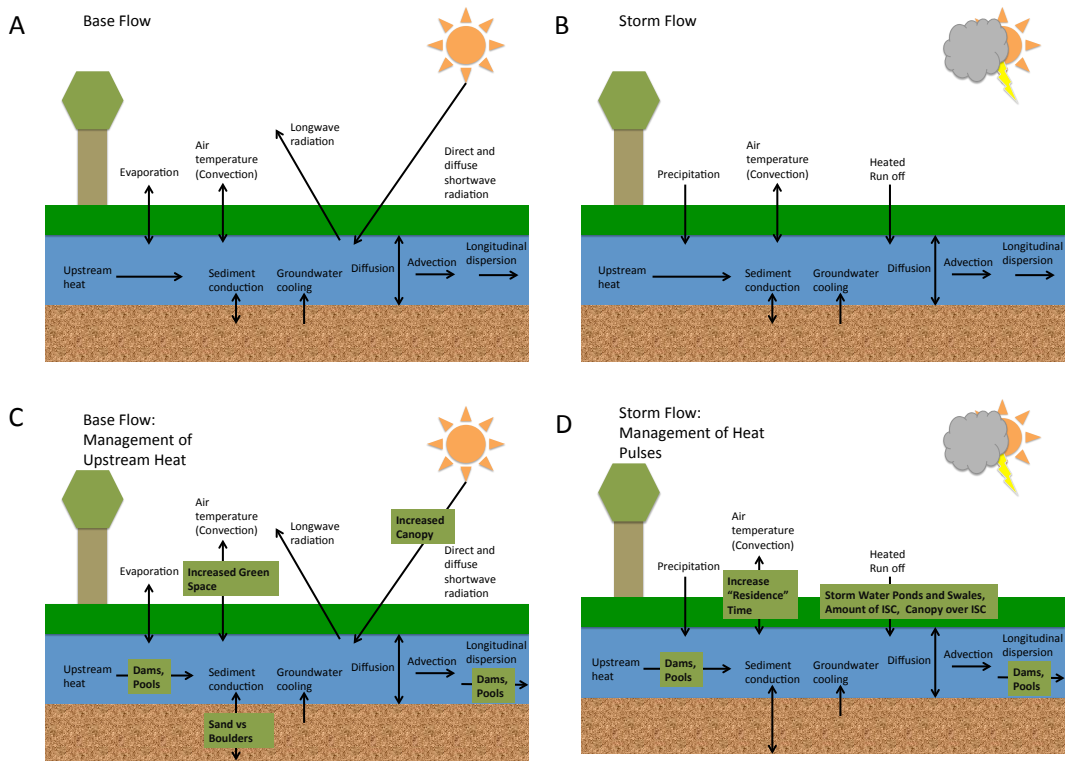

Figure 9. Heat budget of an urban stream ecosystem at baseflow (Panels A and C) and stormflow (Panels B and D). Panels C and D show, in green boxes, the potential for management to decrease incoming heat to the system and increase outgoing heat to the system, to maintain a more natural thermal regime.

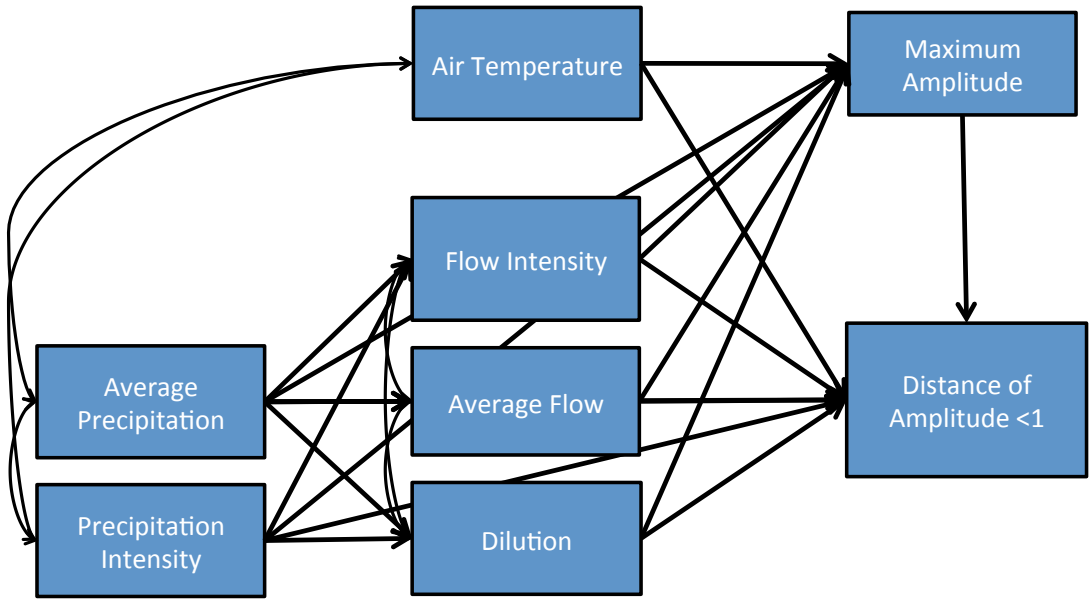

Figure 10. Conceptual diagram showing the relationships between storm metrics and the maximum amplitude of and distance travelled by a heat pulse in Mud Creek. Double-headed arrows show correlation, while single-headed arrows show directions of effects. All boxes other than the response variables of maximum amplitude and distance of amplitude more than 1°C represent groups of potential variables.

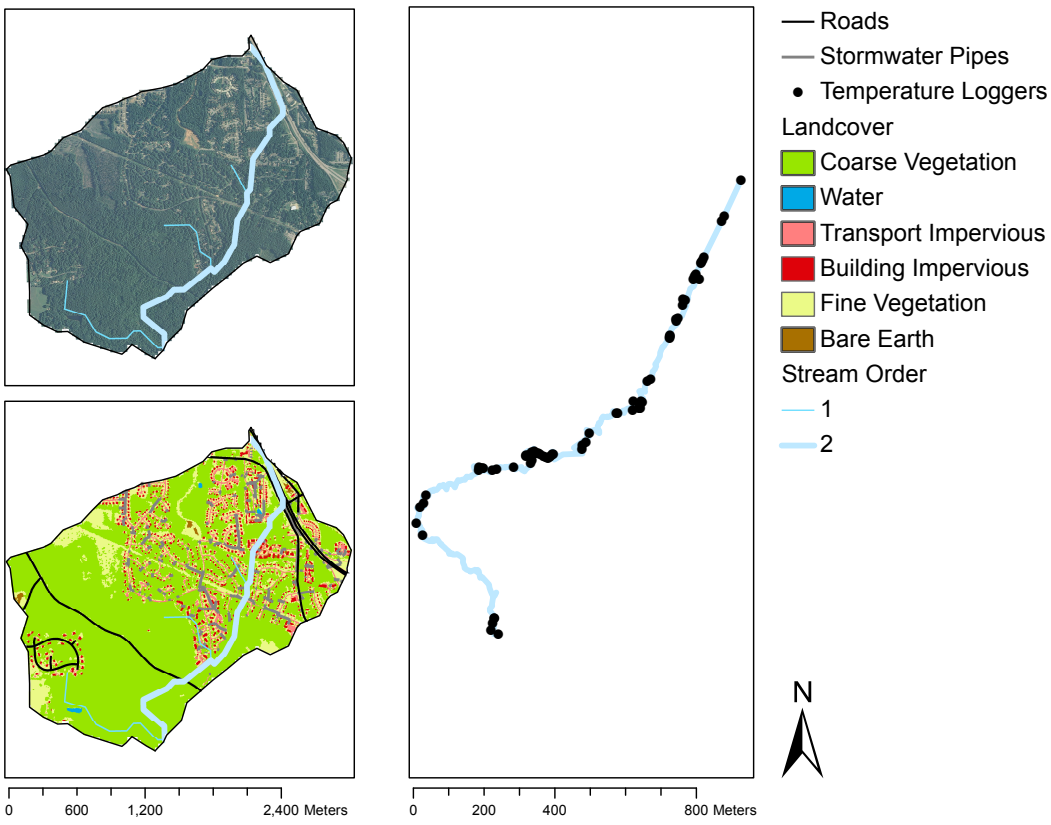

Figure 11. Mud Creek in Durham, North Carolina flows from stormwater infrastructure and residential developments into protected forest. The watershed's landcover gradient is clear using both aerial photography (Panel A) and 1-m resolution landcover (Panel B). The study reach, including placement of temperature loggers is inset (Panel C).

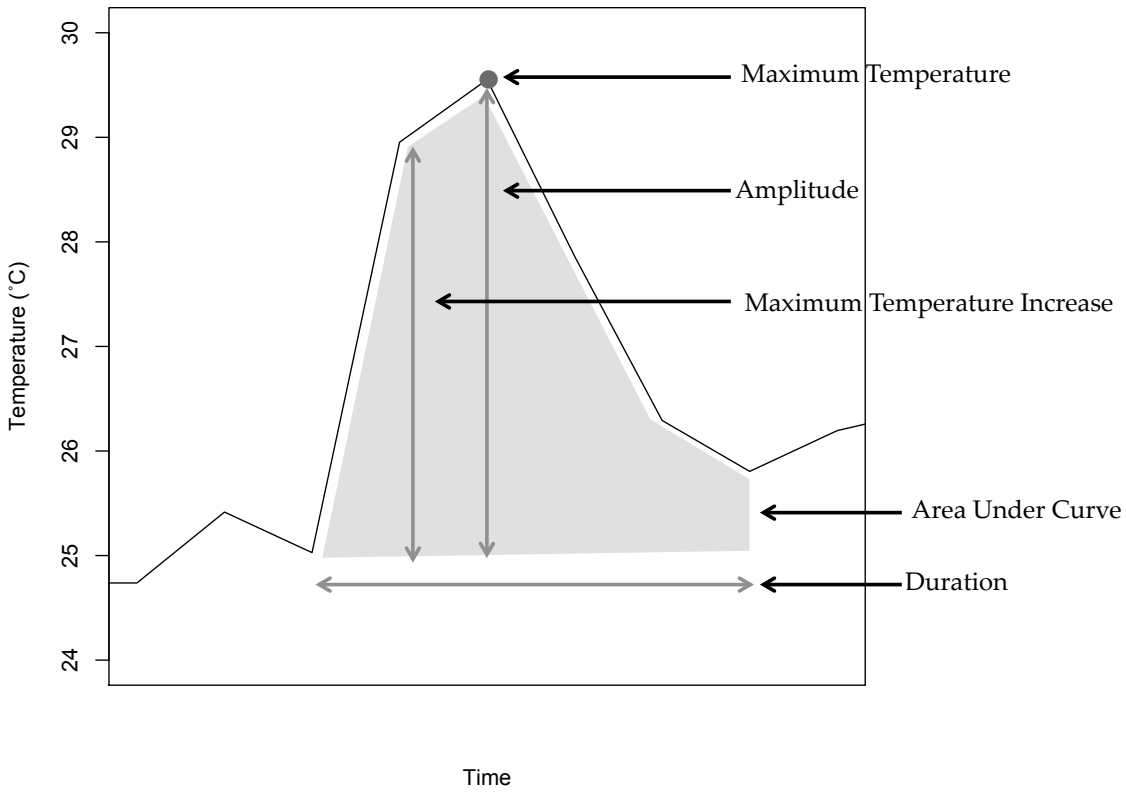

Figure 12. Example of thermal storm metrics calculated for heat pulse at each temperature logger during each storm.

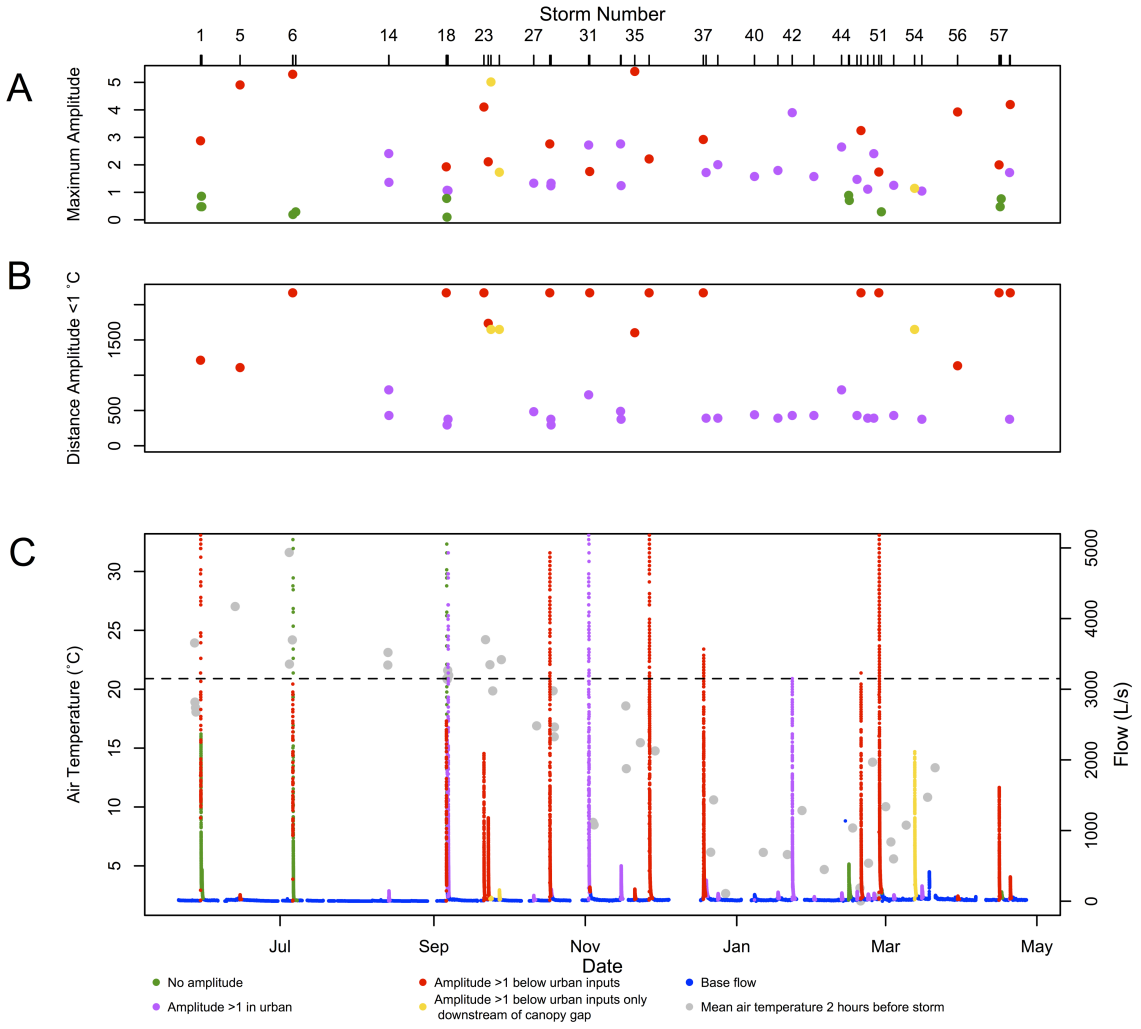

Figure 13. All 54 storms observed over one year at Mud Creek, including maximum amplitude across study reach and distance at which amplitude became less than 1°C. Dotted line in Panel C represents maximum flow measured using level-flow relationship. Storm id numbers listed in Table 14 in Appendix A are shown on the top y-axis. 33 storms occurred in warm weather (mean air temperature > 20°C).

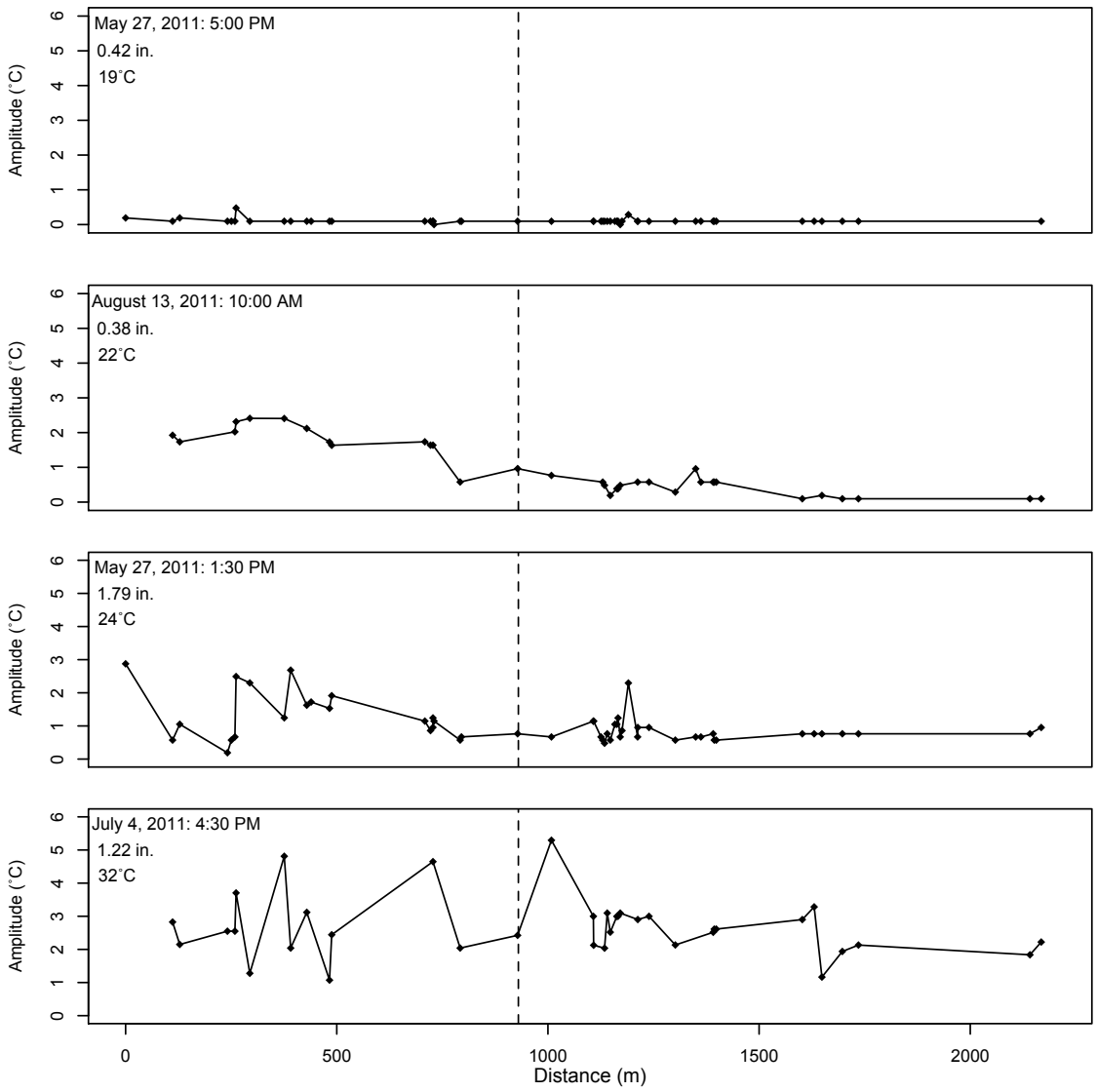

Figure 14. Differences in longitudinal patterns of heat pulse amplitudes along 2 km of Mud Creek for 4 storms, each in a different category of heat pulse amplitude and distance traveled by heat pulse. The date and time of the storm event, total precipitation, and average air temperature 2 hours before the storm are shown in the upper left. The dotted line at 970 meters shows the end of urban inputs to the system. The pattern of dissipation is not clear along the entire reach, partially due to showing the amplitude (difference between maximum and minimum temperature over the storm), which reflects baseflow and maximum temperature. Noise in the pattern also reflects the thermal logger accuracy of ± 0.54°C.

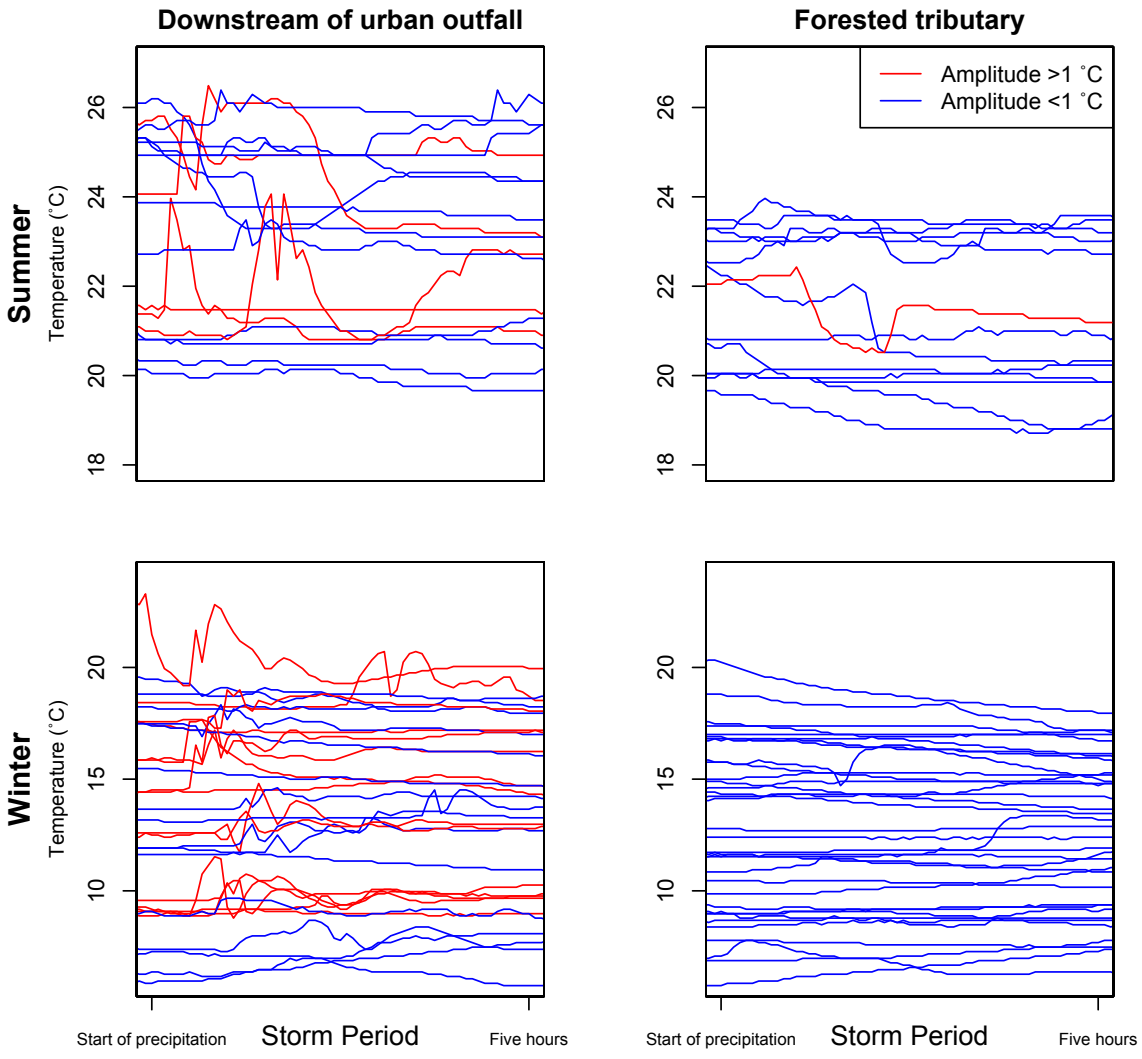

Figure 15. Differences in thermal responses to the same set of storms between just downstream of a stormwater outfall draining a parking lot and a forested tributary, over both summer and winter storms. Twenty storms showed amplitude more than 1°C below the stormwater outfall, while just one storm in the forested tributary did. Fewer storms are shown in the forested tributary in the summer due to lack of flowing water in the tributary. Thermal logger accuracy is ± 0.54°C, which is less than the overall patterns of differences across sites and within a site over a storm.

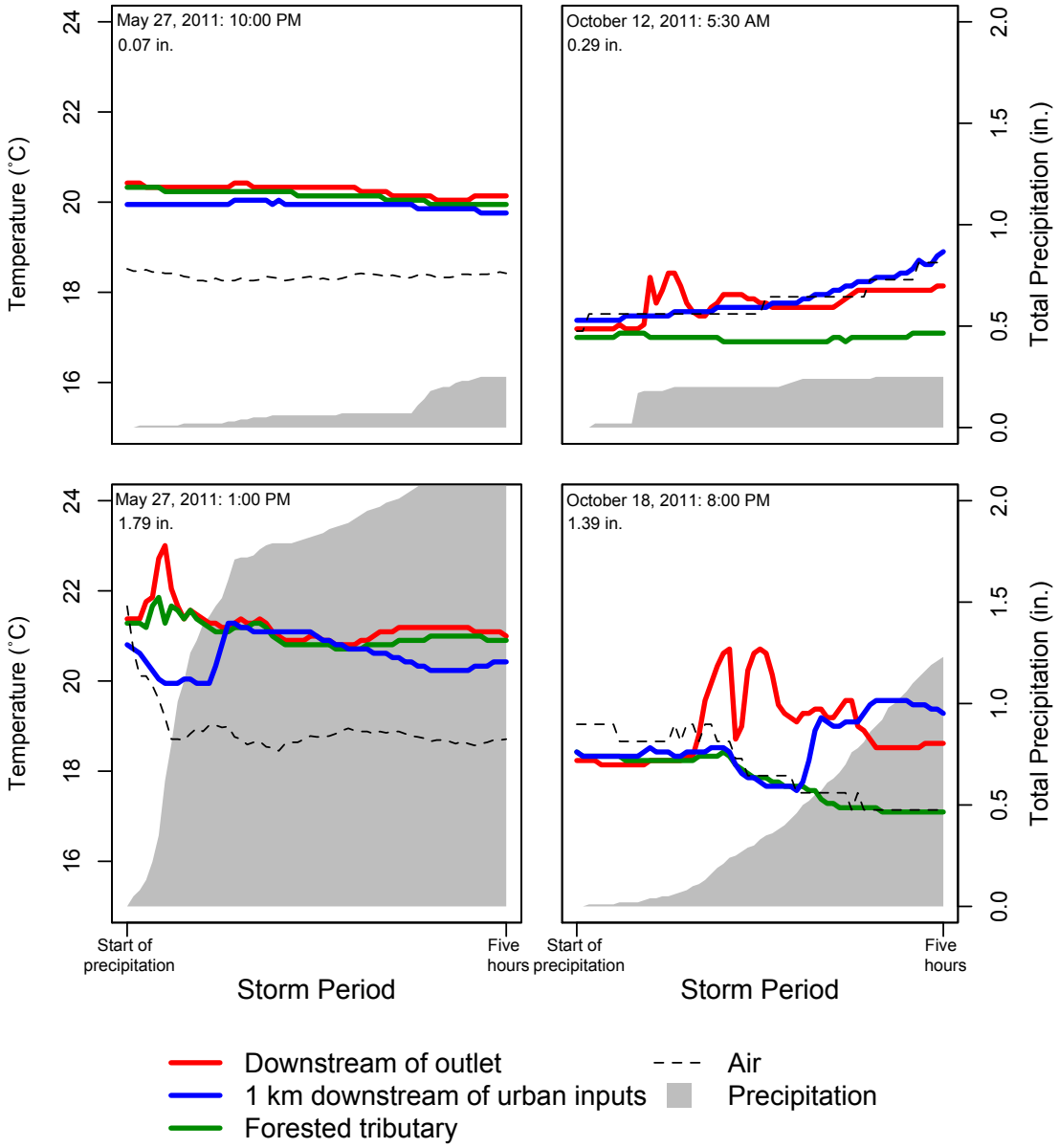

Figure 16. Thermal responses across the study reach of storms with (A) no heat pulse of amplitude more than 1°C, (B) heat pulse of amplitude more than 1°C only within urban inputs, (C) heat pulse more than 1°C below urban inputs that dissipates before end of study reach, and (D) heat pulse 1°C 1 km downstream of urban inputs. Storms with lower total precipitation are less likely to result in heat pulses. Note that the forested tributary generally decreases, or increases only slightly, for these same storms. Thermal logger accuracy is ± 0.54°C.

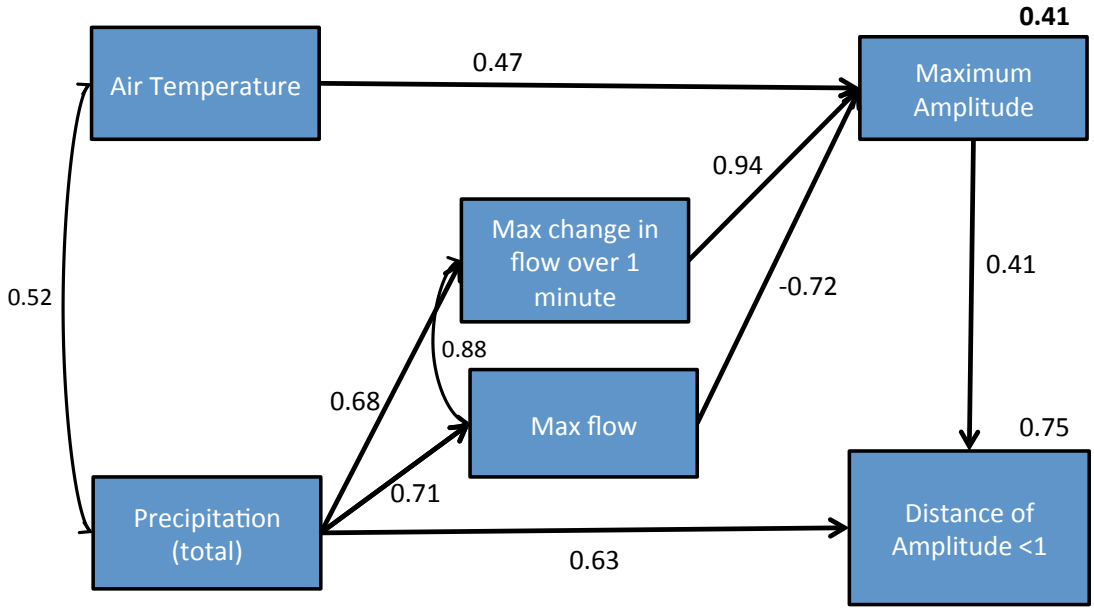

Chi-square: 5.517; P: 0.479; DF: 6

Figure 17. Fitted structural equation model showing standardized regression weights of the influence of storm metrics on the magnitude of heat pulse amplitude and distance to dissipation of heat pulse. Double-headed arrows show correlations; single-headed arrows show direction of effects.

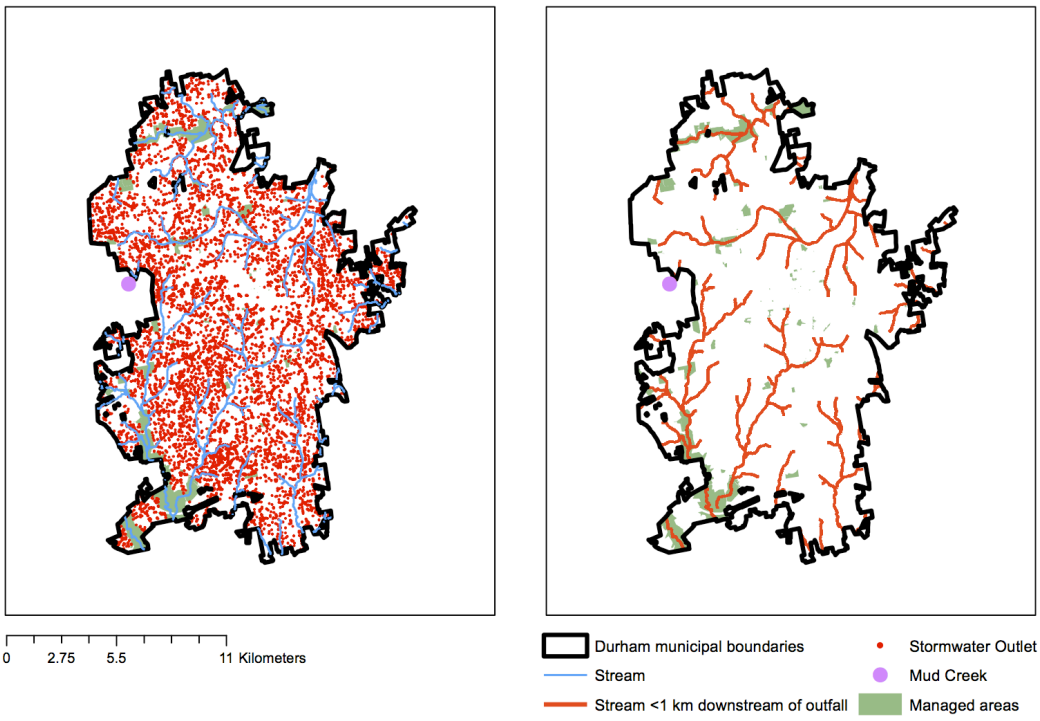

Figure 18. Stormwater outfalls, streams, and managed areas in Durham municipality (Panel A) and streams less than 1 km downstream of stormwater outfalls (Panel B). 98.9% of streams are potentially impacted by the 8,329 outfalls in Durham municipality.

4. All Pavement is not Created Equal: Examining the Effects of Development Configuration and Connectivity on Thermal Pollution to Streams

Introduction

Urbanization continues to alter the world's ecosystems, with projections showing that by 2050 the urban population will be equal to the world's population in 2002 (United Nations Population Division 2012). This growing urban population threatens freshwater ecosystems across the globe, especially as research has shown significant biological degradation of streams even at extremely low levels of development (Cuffney et al. 2010). In order to effectively manage these systems, we must find ways to decrease the impacts of urbanization.

In urban systems, storm events rapidly connect large amounts of runoff, containing heat and other pollutants, to stream networks. Along with baseflow stressors, these regular and intense stormwater impacts lead to streams with increased hydrograph flashiness, pollutants, stream incision, and tolerant benthic taxa: a suite of impacts described as the urban stream syndrome (USS) (Walsh et al. 2005b). Thermal pollution can serve as an inexpensive tracer of the magnitude and intensity of these impacts. Additionally, temperature serves as an important indicator of ecosystem health in its own right: warmer baseflow and heat pulses during stormflow contribute to the myriad stressors for biota in urban streams (Wenger et al. 2009). Warmer waters also hold lower levels of dissolved oxygen, promote microbial activity and algal

proliferation, and lead to significant physiological stress for macroinvertebrates and fish (Jones et al. 2006, Imberger et al. 2008, Hester and Doyle 2011). As an inexpensive and ecologically-relevant tracer of urban impacts, thermal pollution provides a starting point to move beyond describing urban streams to exploring the pathways that lead to their degradation.

Urban stream research typically focuses on development gradients or simple comparisons of undeveloped and very highly developed watersheds, such that the ends of the spectrum drive the observed variation (Wang and Kanehl 2003, Moore and Palmer 2005, Roy et al. 2005, Cuffney et al. 2010, Bernot et al. 2010). Between forested and urban endpoints, the conditions of streams subjected to similar levels of development vary greatly, and researchers do not understand what attributes of urbanization best explain the variation. Our previous work highlights the thermal variability that can occur *within* a development gradient in addition to *along* the gradient. We found that the most urban streams were warmer at baseflow and showed greater heat pulses at stormflow compared to the most forested streams (Somers et al. 2013). However, this pattern showed a large amount of variation; for example, the most urban stream in the study was both one of the coolest streams at baseflow and one of the most thermally responsive at stormflow due to large amounts of underground piping (Somers et al. 2013).

The USS serves to describe the degradation observed in urban streams and highlights differences between relatively unimpacted and highly impacted streams. At the same time, as described above, studies based in the conceptual model of the USS have shown that simple development metrics do not have straightforward, linear relationships with urban impacts. The variation in these relationships may be explained by differences in development characteristics: configuration, arrangement, and surface and sub-surface connectivity of development in a watershed. However, many development characteristics co-vary to some degree with one another and with development amount (King et al. 2005b, Walsh et al. 2005b, Wenger et al. 2009). For example, as the proportion of development in a watershed increases, the pipe density also generally increases. In order to disentangle the impacts of development characteristics from the impacts of proportion of development, landscape ecology theory suggests holding the proportion of landcover, p, in the study areas or watersheds constant (Gardner et al. 1987, Tischendorf et al. 2003, Gardner and Urban 2007). Further, studies show that the impacts of development characteristics are the most important and clear at moderate levels of p (Gardner and Urban 2007). Within a limited range of moderate levels of development, each study watershed provides a sample whereby differences in the configuration, age, and connectivity of landcover, rather than simply its amount, can be explored (Gardner and Urban 2007, Hatt et al. 2004, Dietz and Clausen 2008, Kaushal and Belt 2012, Pickett et al. 2013). Identifying the development

characteristics that are associated with the most extreme and measurable impacts on receiving streams will help us understand the extent to which the impacts of the absolute amount of impervious cover can be mitigated by the arrangement and connectivity of imperviousness within watersheds.

In this study, we move beyond the forest-to-urban gradient approach to explore urban impacts to streams in a fundamentally different way, focused on development characteristics rather than amount. Specifically, we asked (1) How much variability do we see in reach- and watershed-scale development characteristics and thermal metrics within a subset of development intensity? and (2) Which reach- and watershed-scale development characteristics can explain the variability in these thermal impacts? The answers to these questions disentangle the effects of development amount from development characteristics, providing pathways for mitigation of urban impacts while allowing for the existence of development in a watershed.

Methods

From May to October 2012, we collected temperature and flow data for 15 streams in similarly sized and moderately urbanized (45-55% developed) watersheds in the municipalities of Durham and Raleigh in the North Carolina Piedmont region. Although they contained similar amounts of development, these watersheds varied in terms of multiple development characteristics, including configuration, connectivity, and age.

Watershed selection

In order to select watersheds of similar size and proportion development across the Piedmont of North Carolina, we delineated watersheds of the 235 first-order streams for which stormwater infrastructure data was available within the municipal boundaries of Chapel Hill, Carrboro, Durham, and Raleigh, North Carolina (Figure 19). These streams provide the best approximation of headwater, first-order streams possible in an urban environment. However, researchers have noted that first-order streams are the most likely to be buried and piped in urban areas, so it is important to note that these streams were defined as first-order using available stream data and did not include piped stream tributaries (Roy et al. 2009).

For each watershed, we calculated landcover statistics based on 30-m data from the 2001 National Land Cover Dataset (Homer et al. 2004, Sexton et al. 2013). From this coverage, we calculated the proportion developed in 2005 for all 235 watersheds. Development intensity ranged from 2 to 94% in a given watershed; the average watershed in the dataset was 50% developed in 2005. For our intensive watershed-scale landcover analysis, we selected the 63 watersheds within the dataset that were within 5% of this average proportion of development.

We were specifically interested in comparing watersheds with variation in subsurface connectivity, in terms of stormwater infrastructure, and development configuration. We calculated pipe density using stormwater infrastructure data from

each municipality (Durham Storm Water 2007, City of Carrboro 2009, City of Raleigh Public Works 2009, City of Chapel Hill 2011) (Figure 19). We used FragStats v.3 to calculate a "clumpiness index", hereafter referred to as "development aggregation" (McGarigal et al. 2002). This metric ranges from -1 for a completely disaggregated "salt and pepper" landscape to 1 for a completely aggregated landscape (all impervious cover in a single large clump), with 0 indicating a random distribution of patch sizes of the landcover of interest. For example, a watershed with a development aggregation close to 1 would have only a few large patches of pavement, with very few additional small patches scattered across the watershed (Figure 20, Panel D).

From the original set of 63 moderately developed watersheds, we ultimately selected a subsample of 27 watersheds that captured the full range of variation in development aggregation and subsurface pipe density (e.g. Table 9; Figures 19 and 20). In May of 2012, we ground-truthed all sites and placed data-logging water-level and temperature sensors in 15 moderately developed streams. Several of our original candidate streams were not selected following field visits as we decided not to deploy equipment on private land, in areas where level-loggers could not be securely attached, or locations that were immediately downstream of large impoundments. To provide context for interpreting our moderately developed stream records, we also deployed loggers in two undeveloped watersheds and two highly urbanized watersheds that have

been the subject of prior study (Sudduth et al. 2011, Violin et al. 2011, Wang et al. 2011, Somers et al. 2013).

Categorizing thermal metrics

To focus our analyses of thermal pollution, we grouped reach- and watershed-scale predictor variables into four categories: direct radiation to the stream, convective watershed heatload, configuration of heatload, and transmission of heatload (Table 10, Figure 21). Because many of the metrics we calculated could fit into more than one category, we structured our analysis using loose, rather than definitive or exclusive categories. For example, we categorized metrics describing the amount *and* connection of impervious surfaces to the stream network as watershed heatload metrics because they describe the overall amount of heat absorbed across the watershed and go beyond describing the potential to transmit that heat into the stream network through convection with air and movement of runoff. Using these four categories, we described the thermal regime of an urban stream as a function of direct solar radiation received on the stream's surface together with its watershed's ability to absorb and transport heat to the stream.

For the 15 moderately developed, 2 forested, and 2 intensely developed watersheds, we performed additional, more-detailed analyses to describe development characteristics. First, we used available stormwater infrastructure data to assess the accuracy of watershed boundaries based only on digital elevation models (DEMs). For

some sites, we slightly altered delineations to include or exclude areas based on stormwater infrastructure moving water across natural watershed boundaries. Within these sewershed boundaries, we classified 1-m resolution landcover data, which is described fully in Beck et al. *in prep*. Briefly, color infrared National Agricultural Imagery Program (NAIP) aerial photo mosaics (United States Department of Agriculture 2009) were used to generate high-resolution (1m) land-cover classifications for Orange, Durham, and Wake Counties into six discrete land-cover classes: (1) coarse vegetation (trees and large shrubs); (2) water (ponds, lakes, and rivers); (3) transportation/pavement impervious surfaces (roads, driveways, sidewalks, and parking lots); (4) building impervious surfaces (houses, buildings, and structures); (5) fine vegetation (grass); and (6) bare earth. We then re-calculated all metrics described above using these more precise boundaries and high-resolution landcover data.

Direct radiation metrics

Channel width and incision and canopy closure are the primary determinants of the amount of direct radiation that reaches and heats a stream. Wider streams have greater surface area and the potential to absorb more heat (Caissie 2006), while streams shaded by incised channel banks and closed canopies receive less radiation and associated heat (Imholt et al. 2012). In the field, we calculated average stream width and incision along the study reach (described below). We used satellite imagery from NAIP

(United States Department of Agriculture 2009) to calculate the percent of canopy closure over a 100-m reach upstream of the monitoring point (as in Somers et al. 2013).

Watershed heatload metrics

Watershed heatload metrics consist primarily of traditional descriptions of urban landcover in urban stream studies, such as proportion developed and imperviousness and road density, which describe the potential for a watershed to absorb heat. Previous gradient research has shown that watersheds with greater proportions of urban landcover and road densities are broadly warmer and tend to show larger heat pulses during storms (Somers et al. 2013). We also calculated more innovative metrics of the watershed heatload, using 1-m resolution landcover and including the proximity of development to the stream along both natural and sub-surface flowpaths, to create a more comprehensive description of the heatload in a watershed.

To estimate the amount of heat absorbed across the newly-delineated sewersheds, we re-calculated the proportion of development in 2005 from 30-m landcover as described above, as well as the proportion forested in 2005 and impervious in 2006 (Fry et al. 2011). Using the high-resolution landcover described above, we also calculated more detailed metrics, including the proportion impervious (including separate calculations of transportation and building imperviousness) and the proportion vegetation (including separate calculations of coarse as compared to fine vegetation).

To quantify the amount of development in a watershed that is likely directly connected to streams simply by proximity to the channel, regardless of stormwater infrastructure, we calculated the amount of development within a 50-foot buffer of the stream, which is the legal requirement for current development in North Carolina (North Carolina Department of Environment and Natural Resources 1999). To compute the effects of development directly connected to stream by sub-surface connectivity, we calculated the development in a watershed connected to the stream by surface and sub-surface flowpaths, weighted by distance to channel and infiltration capacity of intervening landuse and hydrologic soil group. To do this, we used the methods of Somers et al. (2013) but rather than calculating distance to stream channel, we calculated distance to either a stream channel or a stormwater pipe (Figure 22). We used a tail distance of 10,000 meters, such that the decay rate (k) in an exponential equation was equal to 0.0005: this high tail distance means that even development very far from the stream along piped flowpaths still has a large effect on the stream in an urban watershed. In this way, we recognized that urban watersheds are hyper-connected, so that the effect of development decreases very slowly with distance from stream. We then calculated the proportion of effective development directly connected to the stream or pipe network across the watershed.

We computed road length densities and the effects of traffic volume using North Carolina Department of Transportation data (2009) and following the inverse-distance

weighting methods described in Somers et al. 2013. Briefly, this consisted of calculating the Euclidean distance from each road length to the nearest stream and weighting the effects of roads by this distance, transformed using a negative exponent, distance-decay constant, and multiplied by the volume of traffic on the road. This measurement takes into account the dissipation of road effects as distance from road increases and the increased heating effects of additional traffic.

Heatload configuration metrics

Configuration of heat-absorbing surfaces across the watershed accounts for the arrangement and aggregation of heat in a watershed. Larger aggregation and patches of development with greater surface area and are likely to be less shaded, resulting in greater amounts of direct radiation. This results in large heat masses on the landscape, which transmit greater amounts of heat into stream.

We calculated the arrangement of heat absorbing surfaces (imperviousness) using development aggregation metrics in FragStats as described above (McGarigal et al. 2002). We calculated an additional aggregation metric, correlation length, in each watershed to capture the average extensiveness of development across the watershed (McGarigal et al. 2002). Correlation length represents the average distance that one could travel from a random point, in a random direction, within a development patch before reaching the end of the patch (Keitt et al. 1997). To assess the effects of patch size across the watershed, we computed the mean development patch size and the "largest patch

index", which is the percent of the watershed represented by the largest developed patch the watershed contains (McGarigal et al. 2002).

Heatload transmission metrics

Finally, we describe the transmission of this heat to the stream network using stormwater infrastructure metrics. The connectedness of impervious cover to stream channels may be as or more important than its amount. As subsurface connectivity in urban watersheds increases, the heat stored in the watershed has a much greater potential to reach and pollute the stream network.

We calculated the density of stormwater infrastructure and the ratio of stream-to-stormwater-pipe length, as well as the density of intersections between stream channels and stormwater pipes. We also calculated the average and maximum lengths of all stormwater pipe sections in each watershed and the upstream distance from each monitoring point to the nearest pipe-stream intersection.

We assessed the changes in stormwater piping regulations over time by calculating the proportion of development in 1985 and 1995, as well as the proportion of development that had occurred since 1985 and the proportion of development present in 2005 that was present in 1985. Pre-1985 development were not regulated by National Pollutant Discharge Elimination System (NPDES) Phase I laws and pre-1995 development was not regulated by NPDES Phase II laws (US EPA 1999). Phase I laws focused on managing stormwater pollutants from industrial complexes and cities with

populations of at least 100,000, while Phase II laws addressed stormwater pollutants from smaller municipalities and construction sites (US EPA 1999). Because of this, older development is much more likely to be directly connected to streams.

Field data collection

At each site, we selected a shady pool or run for our monitoring station. We did this to avoid direct radiation effects on our measurements and to ensure the stream would continue running at the monitoring point for as long as possible over the summer. Pressure transducers (Solinst Levelogger Silver, Model 3001; Solinst Levelogger Gold, Model 3001; or Onset HOBO® Water Level Data Logger U20-001-01) were placed in a protective PVC casing and secured in each stream with rebar. Stream temperature loggers (Onset HOBO® Temperature/Alarm (waterproof) Pendant® Data Loggers UA-001-08) were co-located with the pressure transducers. We did not correct for drift in the temperature loggers (up to 0.1°C per year, according to Onset). Air temperature loggers were installed on nearby trees at each site at approximately breast height, facing north to avoid direct radiation. We installed barometric loggers (Solinst Barologger Gold, Model 3001) on trees at one site in Durham and one site in Raleigh to record barometric pressure, ensuring that barometric pressures were recorded within 30 km of all other loggers, as suggested by manufacturers. Pressure transducers and barometric loggers recorded every minute, and stream and air temperature loggers

recorded every 5 minutes. We returned to these sites multiple times to upload and re-launch loggers from May 2012 until the end of September 2012.

We used a laser level (Impulse 100LR) to measure geometric cross sections at the location of each logger within all study reaches. We laid a measuring tape along the cross-section between both leveled-off sides of the bank. We then measured the horizontal distance, inclination, and azimuth from the station. We calculated detailed cross-sections (measurements at every 20 cm along the measuring tape) at the location and approximately 10 m upstream of the monitoring station. We performed 2 additional, less-detailed cross sections at representative locations upstream of the monitoring station. At these sites, we recorded the horizontal distance and inclination from the station at the top and bottom of both banks, the edges of water on both sides, and the thalweg.

We estimated Manning's *n* for the stream and floodplain, based on vegetation and flow, and performed surveys to calculate the slope of a 100-m reach (Chow 1959). After laying a measuring tape along the thalweg, 50-m upstream and downstream of the monitoring station, we recorded the gradient, vertical distance, and horizontal distance using the laser level and the habitat (run, riffle, or pool) at every meter along the tape measure. We then calculated slope for the reach by plotting absolute elevation against distance for selected representative sections, from the top of one riffle to the top of the next riffle.

HEC-RAS and flow calculations

We entered cross-section, slope, and estimated Manning's *n* data collected in the field into HEC-RAS v.4.1, a hydrologic modeling software (U.S. Army Corps of Engineers 2010). We calculated flow over a reach length of five times the width of the cross-section, with cross-sections interpolated at 4 points along this length in order to allow the iterative process to converge on a solution at the most downstream station of the reach. We performed steady flow analyses using mixed (sub- and super-critical) flow regimes and normal depth at 21 discharges, ranging from 0.001 to 10 m^3/s. We then fit a power equation to the relationship between depths at the pressure transducer and calculated discharges. After compensating for barometric pressure using the barologgers, we calculated the depth of water above the pressure transducer at the cross section for each data entry. Using the power equation calculated from HEC-RAS, we used this compensated depth to calculate stream discharge for every depth measurement.

Baseflow separation and storm event identification

In order to separate baseflow from stormflow, we first performed a 3-pass digital filter using R package EcoHydRology (Fuka et al. 2012), with a filter parameter of 0.999 (based on Nathan and McMahon 1990). In order to identify the start and end of individual storm events, we defined the start of a storm as having greater stormflow than baseflow and the end of a storm as having equal stormflow and baseflow or greater

baseflow than stormflow. We further defined storm events as lasting at least 60 minutes and showing a greater maximum flow over the storm period than the mean baseflow over a 24-hour-period before the start of the storm. Additionally, we defined a storm as having a maximum watershed-area-normalized yield greater than 4 mm/hour based on yields observed during known storm events. Some storms appeared to have an unreasonably large yield, which we believe to have resulted from the damming effects of water infrastructure, such as culverts, at very high flows. This is likely due to some loggers being located in deep pools, so that the level recorded reflects standing water and is much higher than the amount of actual flow occurring. To account for this difficulty in estimating high flows, we used equations from USGS StreamStats NC to calculate the maximum flow and yield for storms of recurrence intervals of 2, 5, 10, 25, 50, and 100 years for each site (Weaver et al. 2012). Storms with yields greater than the 5-year recurrence interval (33 storms in total) were removed from analyses of stream thermal responses to ensure that unlikely, mis-calculated flows were not included.

Baseflow metrics

Our research questions focus primarily on stormflow pulses, but we were also interested in the baseflow temperature differences across these sites, because they impact the magnitude of thermal stormflow changes. Because some loggers failed for one or more weeks of their deployment and several streams dried during the study period, we focused on a week of baseflow temperatures in June, to include the greatest

number of sites that were not dry. After removing storm events, we calculated median daily minimum, mean, and maximum stream temperatures.

For each of these temperature measurements, we calculated regression equations within each of the 4 heat metric categories, described above (Table 10, Figure 21). Within each category, we selected all significantly correlated ($\alpha = 0.1$) variables and ordered them in a regression equation by decreasing correlation weight. If the equation was significant at $\alpha = 0.1$, we retained all variables. If not, we performed backwards stepdown until the regression was significant at $\alpha = 0.1$. We then repeated this process across all categories, rather than within each category.

Stormflow metrics

We calculated two thermal response metrics for each storm. First, we calculated the maximum positive amplitude as the difference between the temperature after the highest thermal increase and the minimum temperature afterwards, before an additional increase in temperature. If no positive change occurred, we did not analyze the storm's amplitude. This metric reflects the overall delivery of stormwater to a stream and the thermal change observed over a storm event. Second, we calculated heat pulse intensity as the maximum temperature increase over 5 minutes; if no temperature increase occurred, we did not analyze the storm's heat pulse intensity. To control for changes in variance of heat pulse intensity, we log-transformed the data before analysis. This metric reflects the rate of delivery of stormwater to a stream and the rate of thermal change in

the stream. Removing cooling or lack of thermal response allowed us to focus on the mechanisms by which storm and reach- and watershed-scale variables control the magnitude and variability in heat pulses.

Air and flow metrics were previously shown to explain large amounts of variation in the magnitude of heat pulses (Somers et al. *Chapter 3*). For air temperature before each storm event, we calculated the mean air temperature over 30, 60, and 120 minutes and the sum of degree-hours over 2, 3, 4, 5, and 6 hours before the storm event using the double-triangle method and a base temperature of 0 (Sevacherian et al. 1977).

We quantified the flow over each storm event in several ways. We calculated elevated stormflow duration as the time from minimum flow in the first half of the storm to the time of minimum flow in the second half of the storm. We also calculated the cumulative stormflow as the area under curve of elevated flow. To capture the capacity for baseflow to dilute heat during stormflow we calculated the antecedent flow as the average flow 24 hours before the storm event. We then calculated the difference between maximum stormflow and antecedent flow, as well as the percent increase in flow, quantified as the maximum flow divided by the antecedent flow. To analyze the effects of flow intensity, we calculated the maximum increase in flow over 1 minute during the storm event. Finally, we broadly described flow over the storm using additional calculations, including the mean and maximum flow over the entire event and the mean flow in the first hour of the event.

Hierarchical linear models

Previous work has shown that air temperature and flow metrics before and during a storm explain most of the variation in heat pulse size and dissipation rate within one urban stream (Somers, *Chapter 3*). In this study, we observed a wide range of variation in heat pulse metrics both across storms within individual watersheds and across watersheds. Our aim therefore was to decompose the relative importance of storm-level variables (e.g., air temperature and flow intensity) and watershed-level variables (e.g., pipe density and mean development patch size) in this inherently nested dataset. The variation in storms within and across watersheds result in unique combinations of storm and landcover metrics.

We used hierarchical linear models to embrace and simultaneously explain the variation in thermal metrics using a combination of both storm and reach- and watershed-scale predictors across the 45 to 55% developed sites. We were especially interested in exploring the degree to which development attributes modulate the relationship between storm and thermal response metrics (Figure 23: Arrows C and D). This analysis calculates the relationships between storm predictor and heat pulse response metrics for each watershed and then assesses the extent to which development metrics can explain the variation in these relationships across sites (Gelman and Hill 2006, Reckhow et al. 2009, Qian et al. 2010). In this way, we were able to use all of the collected data and separate the variability across storms and watersheds in a manner

faithful to the nestedness in our data, rather than solely focusing on the mean response of all storms within each site or all storms across all sites.

Hierarchical linear models increase the statistical power of our analyses by weighting the relationship observed at each site with the relationship across all sites. To do so, the hierarchical regression line for each site represents a weighted average between the least squares regression lines for all sites combined and for each site individually. The model explicitly accounts for variation in magnitude and rate of heat transfer to storm events across sites, while also borrowing strength from the magnitude and rate of heat transfer observed for all sites combined. Specifically, we fit models in which we allowed both intercepts ($\beta_{0,j}$) and slopes ($\beta_{1,j}$) of regressions of thermal response metrics (y_{ij}) on storm metrics (x_{ij}) to vary as linear functions of land cover metrics (LC_j):

$$y_{i,j} = \beta_{0,j} + \beta_{1,j} x_{i,j} + \epsilon_{i,j}$$

$$\beta_{0,j} = \gamma_{0} + \gamma_{1} LC_j + \epsilon_{\beta_0}$$

$$\beta_{1,j} = \delta_{0} + \delta_{1} LC_j + \epsilon_{\beta_1}$$

where the subscript i represents a storm nested within watershed j. This enabled us to determine those reach- and watershed-scale variables that explained variation in the regression slope (i.e. $\beta_{1,j}$) across watersheds as well as the strength and direction of that relationship.

We assessed two key results from the hierarchical linear models we fit. First, we determined which reach- and watershed-scale variables produced a fitted model that

best explained the variation in the *heat pulse metric itself* – the positive amplitude or the maximum thermal increase over 5 minutes. Second, we explored which reach- and watershed-scale variables produced a fitted model that best explained the variation in *the slopes of the relationships between storm (air and flow) and heat pulse metrics* (Figure 23: Arrows C and D). We refer to this slope ($\beta_{1,j}$, Figure 23: Arrows A and B) as the stream's magnitude of heat transfer (in relation to positive amplitude) and the rate of heat transfer (in relation to maximum thermal increase intensity). For example, we would interpret a strong positive relationship between pipe density and the slope between air temperature and positive amplitude as meaning that pipe density increases the magnitude of heat transfer of the watershed and that streams with greater pipe density are likely to have heat pulses of greater positive amplitude when air temperature is higher. The fitted models then inform us about both the ability of reach- and watershed-scale variables to improve the amount of variation explained in the heat pulse metric and the impact of reach- and watershed-scale variables to influence the magnitude and rate of heat transfer to the stream.

Fitting hierarchical linear models

The process of variable selection for inclusion in hierarchical models is an area of active research (Gelman and Hill 2006). Many researchers advise caution in assessing variables and models using traditional *P*-values, due to the inclusion of random effects and variation within the model (Gelman and Hill 2006). Here, we used R^2 values

primarily to compare and select the best explanatory variables. We constructed the hierarchical model by following a two-phased screening process for including predictors (i.e. x_{ij} and LC_j) in the model. First, we chose the single air temperature and flow predictor (x_{ij}) that was most highly correlated with the positive amplitude and heat pulse intensity responses (y_{ij}) (Figure 23: Arrows A and B). Because we observed high correlation among predictors (average absolute correlation for air temperatures = 0.90; average absolute correlation for flow metrics = 0.54), we did not include other air temperature or flow metrics as predictors in the model.

To select reach- and watershed-scale predictors (LC_j) for inclusion in the model (Figure 23: Arrows C and D), we fit all possible hierarchical models using each reach- or watershed-scale variable, for the chosen air and flow metrics, separately. For inclusion in the model, we chose the reach- or watershed-scale variable that best explained variation (i.e. highest R^2) in the slope ($\beta_{1,j}$) of the regression between each predictor (x_{ij}: air and flow metrics) and each heat pulse response (y_{ij}: amplitude and intensity) within each of the heat categories described above, as well as overall across all categories. We then fit a final model separately for the two heat pulse responses (y_{ij}: amplitude and intensity), by including the best storm (x_{ij}) and reach- and watershed-scale predictors (LC_j) identified in the two-stage screening process. In this final model, which included more than one predictor, R^2 values at the watershed-scale level often changed due to predictor correlation.

We assessed the ability of each model to explain the variation in the data itself (amplitude or intensity) and the variation across the groups, in each watershed's relationships between storm and thermal metrics. We calculated magnitude and rate of heat transfer as the relationships between either the air temperature or flow metric and the amplitude or intensity. In this way, each model consists of three R^2 values at the level of the data and the level of the group (Gelman and Pardoe 2006): (1) the ability of the model to explain the data, (2) the ability of the model to explain the relationship between air temperature and thermal metrics at the group level, and (3) the ability of the model to explain the relationship between flow and thermal metrics at the group level. The group-level R^2 values assess the mean response across all watersheds, rather than the more variable responses at the data level. Because of this, R^2 values at the group level of magnitude or rate of heat transfer are often high compared to R^2 values at the level of the data.

Significance of each hierarchical model was assessed by comparison to a null model which included only a random intercept ($\beta_{0,j}$) but no predictors. At each level of the model, we calculated R^2 by dividing the requisite regression sum of squares by the total sum of squares (Gotelli and Ellison 2004). All statistical analyses were performed in R v. 15.1 (R Development Core Team 2008b), and hierarchical models were fit using the lmer function from the lme4 package (Bates et al. 2012).

Results

How much does stream shading vary?

Many metrics describing direct radiation varied across the 15 sites of similar development intensity as much or more than across the endpoints of the gradient. Canopy closure varied little across the 15 sites, from 80 to 100%, because we strategically deployed instruments in shaded areas (Appendix B Table 16). The urban endpoint, dc_gc, was the least shaded at 70%, while both forested endpoints had 100% closed canopy (Appendix B Table 16). Mean width across the 15 sites was more variable, ranging from 0.18 to 3.82m; the urban and forested endpoints were within this range (Appendix B Table 16). Mean incision as depth-to-width ratio ranged more across the 15 moderately developed streams, 0.23 to 0.92, than across the endpoints, 0.32 to 0.63 (for width-to-depth ratio, the more common metric in hydrology and geomorphology, the incision ranged from 1.09 to 4.35 within the moderately developed streams and 1.60 to 3.13) (Appendix B Table 16).

How much does watershed landcover vary?

We delineated 235 watersheds across our study landscape, ranging from 2 to 94% developed in 2005 (Table 9). Of these watersheds, 63 fell within the selected range of interest, 45 to 55% developed (Table 9). Despite narrowing of the variation in proportion developed across these watersheds, these 63 watersheds showed a wide range in other development characteristics (Figure 24, Table 9). Some watershed heatload metrics

showed ranges in this subset similar to that across all watersheds in the landscape. For example, road density ranged from 0 to 5.4 km km^{-2} in our subsample (as compared to 0 to 7.96 km km^{-2} in the full dataset) (Figure 24, Panel D). Configuration of this development showed similar patterns: development aggregation, for example, was as variable within our subsampled 63 watersheds as it was across the full population of 235 watersheds (Figure 24, Panel B). Sub-surface connectivity in these watersheds also varied greatly within the subset, with the density of the stormwater pipe network density ranging from 2 to 28 times the stream network lengths in our subsample (as compared to 0.30 to 51.7 in the full dataset) (Figure 24, Panel C). The 15 watersheds selected represent a large amount of the variation in development characteristics within the 63 subset watersheds.

Within the 15 watersheds that originally fell between 45 and 55% developed, watershed redelineation to account for full sewersheds led to a final estimated range in development intensity from 42 to 58%, with watershed area ranging from 0.35 to 1.96 square kilometers (Table 9 and Appendix B Table 16). However, despite a small range of development, many other development characteristics varied hugely. The proportion imperviousness using high-resolution landcover data ranged from 19 to 41% in the 15 watersheds, showing that development and impervious cover are not completely synonymous (Table 9). The range in road densitiy was greater across the 15 watersheds (0 to 2.79 km km^{-2}) than across the forested and urban endpoint watersheds (1.01 to 2.54

km km^{-2}) (Appendix B Table 16). Further, one of the forested endpoints, dc_mt, had the third greatest road density in the population of watersheds despite being 96% vegetated (Appendix B Table 16). Mean development within 50 feet of the stream was greater in one of the subset watersheds (0.64) than in the urban endpoint (0.58), but much lower in the forested endpoints (both 0) than the minimum in the subset watersheds (0.23) (Appendix B Table 16).

In addition to watershed heatload metrics, the configuration of development varied greatly across the subset of watersheds, on par with the variation across forested and urban endpoints. Mean developed patch size showed a range of 0.02 to 0.3 km^2 within the selected watersheds, which is slightly greater than the range between the forested and urban endpoint watersheds: 0.03 to 0.2 km^2 (Appendix B Table 16). The watershed with the greatest percent of its area contained in the largest developed patch (32.7%) was only 50% developed, while the urban endpoint watershed had a largest patch index of 27% (Appendix B Table 16). Development aggregation also showed greater variation within the subset (0.90 to 0.96) than in the endpoint watersheds (0.91 to 0.92) (Appendix B Table 16).

Some delivery metrics showed similar levels of variation within the subset of watersheds. Watersheds with any amount of sub-surface infrastructure had comparable mean pipe lengths, and ranges in maximum pipe length were similar between the selected (0.08 to 0.16 km) and endpoint watersheds (0 to 0.18 km) (Appendix B Table 16).

Maximum pipe density in the subset watersheds (8.14 m km^{-2}) was similar to that in the urban endpoint (8.83 m km^{-2}) (Appendix B Table 16). Other delivery metrics varied less within the subset watersheds, with the range fully contained by the forested and urban endpoints (Appendix B Table 16).

How much do baseflow temperatures vary?

For the period June 7 to 13, 2012, the average daily minimum water temperatures across sites of similar development intensity ranged from 16.5 to 20.1°C (Table 11). Average maximum temperatures ranged from 19.9 to 25°C (Table 11). Average daily temperature was less variable across the 15 streams, ranging from 19.1 to 21.8°C (Table 11). The range of baseflow metrics across 15 sites of similar development intensity was similar to the range observed between our endpoint watersheds (Table 11). All of the urban streams were warmer than the most forested endpoint on average, but dc127, a site with 52% development showed cooler minimum temperatures. Dc064 (50% developed) was actually hotter on average than the highly urban endpoint, and dc157 (42% developed) showed greater maximum temperatures.

What drives differences in baseflow temperatures?

Multiple linear regressions revealed the metrics that best explained the differences in baseflow temperatures across the 15 watersheds of 45 to 55% development. The maximum R^2 (0.16) between explanatory metrics occurred between incision and the distance to the nearest upstream outlet, in describing the median

minimum baseflow temperature. Streams that had cooler minimum temperatures were more incised, had greater pipe lengths in the watershed, and were closer to upstream stormwater outfalls (Table 12). The incision of the channel and maximum pipe length in the watershed explained 53% of the variation in average minimum temperature (P = 0.03). The average maximum temperature of a stream, on the other hand, was controlled entirely by watershed-scale heatload metrics (Table 12). Streams with a higher proportion of older development in the watershed were likely to be cooler, while streams with greater traffic volume were likely to be hotter. Together, these variables explained 45% of the variation in average maximum temperature across the watersheds (P = 0.05). The best single predictor of average maximum temperature was the proportion of development in the watershed that existed before 1985 (P = 0.06; R^2 = 0.29).

As with average maximum temperature, streams in watersheds with greater pre-1985 development were likely to be cooler in terms of mean temperature (Table 12). As with average minimum temperature, streams in watersheds with greater maximum pipe lengths had cooler mean temperatures. These two variables explained 53% of the variation in average temperature (P = 0.03), and the maximum pipe length in the watershed alone was able to explain 38% (P = 0.03).

How much do stormflow temperatures vary?

Across all 15 sites, we captured water level and temperature records over 527 storms. From this dataset, we removed 33 storms for which our HEC-RAS models

estimated unreasonably high flows. The frequency of storms across each site varied greatly, ranging from 5 to 76 identified events per stream. Although this was partly due to data loss and inconsistent deployment periods across sites, the time period for data from the sites with 5 and 76 storm events was similar (129 days versus 109 days, respectively). The thermal impacts of storms varied both within and across streams, with some storms leading to warming events and other storms generating cooling events (Figures 25 and 26; Appendix B, Figure 29).

We observed the largest thermal amplitudes in both directions in the same stream (dc143), which drains a watershed with 50% development. In one storm, this stream increased in temperature by 4.7°C, while in another it decreased in temperature by 3.4°C. This range is greater than that observed across the endpoint watersheds: maximum increase in the urban endpoint was 3.2°C, while the maximum decrease in the forested endpoints was 1.4°C.

We also observed a wide range in maximum heating and cooling changes over 5 minutes (Figure 26; Appendix B, Figure 29). The greatest heating observed, a 3.8°C increase over 5 minutes, occurred at a site with 57% development. In contrast, the greatest thermal increase over 5 minutes in highly urban streams was only 2.2°C. The maximum cooling observed over 5 minutes was 3.2°C in a watershed with 51% development, while the greatest cooling at the two forested sites was 2.6°C.

What drives the differences in heat pulse amplitude and magnitude of heat transfer?

We assessed the ability of hierarchical models to explain the variation in both thermal amplitude and magnitude of heat transfer to air and flow metrics (the relationships between predictor variables and thermal amplitude at each site; $\beta_{1,j}$) (Figure 23, Arrows A and B; Appendix B, Figure 29). To do this, we compared hierarchical models without group-level predictors (i.e. a hierarchical model that allowed intercepts and slopes to vary by watershed) with models that used reach- and watershed-scale variables as group-level predictors. The group-level predictors that best explain variation in both thermal amplitude and magnitude of heat transfer provide the best indicators of why and how landcover modulates thermal responses to storms across streams.

For the 358 storms for which positive amplitude greater than 0°C was recorded, we found that mean air temperature for the two hours prior to the storm and the intensity of stormflow were the best predictors of the positive amplitude of storm heat pulses. Across all watersheds, a 1°C increase in air temperature before a rain event led to a 0.11°C increase in pulse amplitude, while an increase in maximum flow intensity of 1 $m^3\ s^{-1}$ led to a 0.45°C increase in pulse amplitude. Including reach- and watershed-scale variables in the model increased the amount of variation explained in magnitude of positive amplitude by only a small amount, from 28.5 to 29.5% (Table 13), but allowed

us to explain the variation in magnitude of heat transfer using reach- and watershed-scale variables.

The variation in both positive amplitude and magnitude of heat transfer to both air and flow metrics were best explained by delivery metrics (Figure 27). Both pre-1985 development and the distance to the nearest upstream outlet increased the magnitude of heat transfer to the stream. Specifically, the magnitude of heat transfer controlled by air temperature was best explained by pre-1985 development ($R^2 = 0.95$; $P < 0.001$) (Figure 27; Appendix B, Tables 17 and 18). The magnitude of heat transfer controlled by flow intensity was best explained by the distance to the nearest upstream outlet, with an R^2 of 0.55 ($P < 0.001$) (Figure 27; Appendix B, Tables 19 and 20). The final model includes both of these metrics, despite some correlation between air temperature and flow intensity ($r = 0.23$). Because of this, the variation explained by pre-1985 development decreases ($R^2 = 0.42$), while the variation explained by distance to nearest upstream outlet increase ($R^2 = 0.72$) (Table 13).

The counter-intuitive relationship between distance to outlet and magnitude of heat transfer means heat pulses are most likely to move far downstream of outlets during intense flows (Somers Chapter 2), so sites further from outlets are more thermally responsive to the flow intensity of a storm. The sites in this study varied from 5.7 to more than 643 m downstream of an outlet (Appendix B Table 16). Sites closer to outlets may more regularly receive heat pulses from stormwater runoff, regardless of

flow intensity; we could not confirm this with our data over 4 months, but Somers, *Chapter 3* showed this relationship with 12 months of data. These localized dampening effects mean that distance to nearest upstream outlet should be considered in determining the best location for monitoring equipment. Additionally, this relationship ($R^2 = 0.55$) was weak compared to the three other relationships between air and flow metrics and thermal response variables, which all showed an R^2 of 0.95 or greater. The slope of this relationship was estimated as 0.01 with the lower 90th percentile at 0, so increases in distance to nearest the upstream outlet resulted in only small increases in rate of heat transfer. Overall, the metrics describing the delivery of heat from the watershed to the stream network provided the best explanation of variation in heat pulse amplitude and rate of heat transfer controlled by both air and flow metrics.

What drives the differences in heat pulse intensity and rate of heat transfer?

As with heat pulse amplitude and magnitude of heat transfer, we also used hierarchical models to examine the variation in both heat pulse intensity (the maximum thermal change over 5 minutes) and rate of heat transfer (the relationships between predictor variables and heat pulse intensity at each site: $\beta_{1,j}$) (Figure 23, Arrows A and B; Appendix B, Figure 29). Again, we compared models without reach- and watershed-scale variables to those using reach- and watershed-scale variables as group-level predictors in order to assess the variables that best explained variation in heat pulse intensity and rate of heat transfer.

We analyzed 391 storm events that included an increase in temperature over 5 minutes. Mean air temperature over the two hours before the start of the storm event showed a positive correlation with heat pulse intensity, while antecedent flow was negatively correlated. Across all watersheds, an increase in average air temperature of 1°C led to a 0.04°C increase in heat pulse intensity, and an increase in antecedent flow of 1 $m^3 s^{-1}$ resulted in a 0.29°C decrease in heat pulse intensity.

Unlike heat pulse amplitude and magnitude of heat transfer, the category of metrics that best explained variation in heat pulse intensity and rate of heat transfer differed. Delivery metrics best explained variation in heat pulse intensity, with the inclusion of these variables as group-level predictors increasing the overall R^2 of the model at the data level from 0.228 to 0.269. Watershed-scale heatload metrics explained only 25.2% of the variation in heat pulse intensity but explained a much greater amount of variation in rate of heat transfer.

Heat pulse intensity was best explained by a positive relationship with delivery metrics overall, which also explained some variation in rate of heat transfer. The density of pipe-stream intersections explained 85% of variation in rate of heat transfer controlled by air temperature, while the ratio of stream-to-pipe length explained 84% of variation in rate of heat transfer controlled by antecedent flow.

Variation in rate of heat transfer was best explained using watershed heatload metrics: average development in the riparian zone explained the greatest amount of

variation in rate of heat transfer controlled by air temperature ($R^2 = 0.99$) (Figure 27; Appendix B, Tables 21 and 22). Despite its proximity, development in the riparian zone is not as efficiently connected to the stream network due to a lack of sub-surface connectivity. Watersheds with high amount of development are likely to have lower pipe-stream intersection densities ($r = -0.63$). Heat from development within the riparian buffer that is not connected via stormwater infrastructure transfer into stream networks less efficiently than development connected via subsurface piping. Rate of heat transfer controlled by antecedent flow was best explained by the proportion of coarse vegetation in the watershed ($R^2 = 0.99$; $P < 0.001$) (Figure 27; Appendix B, Tables 23 and 24). In watersheds of similar development intensity, those with greater proportions of forest have less aggregated development: proportion of coarse vegetation correlates negatively with development aggregation ($r = -0.52$), largest patch index ($r = -0.75$), and mean patch size ($r = -0.43$). These streams likely show lower rates of heat transfer due to protection from stormflow thermal pollution provided by coarse vegetation, as well as the lack of concentrated heat loads across the watershed.

Discussion

Watersheds that were 45 to 55% developed showed variation in development characteristics on par with watersheds ranging from 2 to 94% developed (Table 9 and Appendix B Table 16, Figure 24). By selecting watersheds of similar development intensity, we were able to assess the impacts of development characteristics separately

from development proportion. In these watersheds, proportion of pre-1985 development, maximum pipe length, and incision decreased baseflow temperatures (Table 12). Proportion of pre-1985 development and distance to nearest upstream outlet increased heat pulse amplitude and magnitude of heat transfer to stream, while average development in a 50-foot buffer and proportion of coarse vegetation decreased heat pulse intensity and rate of heat transfer to stream (Table 13). The large variability in development characteristics and the ability of these metrics to explain thermal variation in subsets of the urban gradient illustrate the need for more sophisticated measures of urbanization.

New metrics to capture variation in development characteristics

The use of higher resolution landcover data allowed us to calculate the aggregation and size of development patches and the location of development within riparian buffers and connected to streams via subsurface stormwater pipes. In addition to this 1-m landcover, future research should focus on delineating sewersheds to select a subset within a more accurate range of development. The importance of proportion of watershed imperviousness in some models implies that selecting watersheds based on impervious intensity, rather than development intensity, may provide further insight into urban watersheds. The use of infrastructure maps rather than satellite-derived landcover may further improve impervious estimations, as this will include paved areas

that may be obscured by canopy cover, and therefore would not be visible in satellite imagery.

Pre-1985 development was surprisingly predictive of stream temperatures at both baseflow and stormflow. In these watersheds, the proportion of the watershed developed in 1985 was positively correlated with maximum pipe length (r = 0.33), incision (r = 0.44), and proportion of forest (r = 0.55) and negatively correlated with proportion of fine vegetation (r = -0.53). Two example watersheds show the degree to which development age can influence piping and forest (Figure 28). Pipe length and incision serve to cool baseflow by shading, while the proportion forest in the watershed cools air temperatures and decreases urban heat island effects (Oke et al. 1989). Areas of fine vegetation in urban watersheds, like lawns and golf courses, are warmer than areas of coarse, forested vegetation, resulting in increased urban heat island effects. These watersheds that were more developed in 1985 have cooler baseflow temperatures, so thermal change caused by heated runoff during stormflow is likely to be greater. The delivery of heated runoff to streams is also faster in these watersheds, due to greater maximum pipe lengths (r = 0.33), corresponding with changes in stormwater management and NPDES permitting (US EPA 1999).

Controls on baseflow

For watersheds with approximately half their surface area developed, baseflow temperatures were warmer in watersheds with greater traffic and cooler in incised

streams and in watersheds where the majority of development was more than 2 decades old and where pipe networks were extensive. Traffic effects reflect the magnitude and extent of urban heat island effects across a watershed. Traffic across the watershed can increase urban heat island effects through roads, heat from automobile combustion, and localized greenhouse effects from automobile emissions (King et al. 2000, Saaroni et al. 2000). Alternately, the three variables that result in decreased baseflow temperature broadly reflect different levels and types of shading throughout a watershed. Longer pipe lengths result in lower temperatures due to lack of radiation (Natarajan and Davis 2010). The banks of highly incised channels may provide shading to urban streams, even where canopy closure is low. This cooling is one of the few ecological benefits of the incision caused by urban stormflow, because it also results in the disconnection of streams from their floodplains and decreases overall stream health. As described above, the cooling influence of pre-1985 development likely reflects greater subsurface connectivity and greater coarse vegetation (Figure 28).

Controls on stormflow

The wide range of reach- and watershed-scale variables and storm thermal metrics in watersheds within similar development intensity highlights the variation present within the USS. In one watershed, we observed only 5 storm events over the study, while in another watershed, we observed 76 storm events over a similar period of deployment. We did not observe a maximum amplitude greater 1°C during a storm in

the former watershed, while the latter showed a maximum amplitude of 3.5°C. Despite the large differences in flow and thermal metrics, both of these watersheds are 50% developed. The more thermally-responsive watershed had greater proportion impervious, development aggregation, and sub-surface connectivity. These outliers show the potential to explain variation in thermal metrics within a subset of development intensity by better understanding the characteristics of development in a watershed.

The positive influence of delivery metrics on magnitude and rate of heat transfer shows that watersheds with greater sub-surface connectivity route stormwater more efficiently into streams and increase the ability of stormwater to cause both greater overall and sudden thermal surges. Similarly, increased imperviousness and decreased coarse vegetation increase the rate and magnitude of heat transfer to streams by decreasing the stormwater infiltration of watersheds, while also increasing the temperature of stormwater runoff via urban heat island effects. Overall, the hydrologic connectivity of these watersheds determines the rate and amount of heat transferred from development throughout the watershed into the stream network, controlling the rate and magnitude of heat transfer to urban streams.

Managing thermal regimes in urban watersheds and future research

To manage thermal pollution, we must explicitly consider the interactions of baseflow and stormflow temperatures and the reach- and watershed-scale variables that

control them. For example, maximum pipe length and incised channels cool baseflow, which leads to greater stormflow heat surges. At the same time, streams with warmer baseflow temperatures respond less to heated runoff. Management of baseflow thermal regimes typically focuses on reach-scale interventions, overlooking the impacts of watersheds that become hyper-connected at stormflow. These two aspects of stream temperature must be considered in parallel, to understand their interactions and restore more natural thermal regimes at both baseflow and stormflow.

One meter of imperviousness anywhere in a watershed absorbs a similar amount of heat, but the impact of that heat varies depending on the location of the development and its connectivity to the stream network. The pathways by which this heat enters the stream have a greater effect on thermal pollution than the amount of heat absorbed across the watershed. By decreasing the sub-surface connectivity of urban watersheds and the point-source impacts of stormwater outfalls, managers can control the amount of thermal pollution that enters the stream network during storm events. The influence of pre-1985 development in controlling magnitude of heat transfer shows the large potential for retro-fitting aging stormwater infrastructure to reduce connectivity. Watershed-scale management should focus on decreasing the hyper-connectivity of urban watersheds and transmitting lower amounts of stormflow directly into streams.

To understand and protect stream ecosystems in developed landscapes, researchers and managers should explore how these patterns differ across other subsets

of development intensity, in other regions, and for other urban pollutants. Future studies can explicitly include the precision of instruments and use sensitivity analysis in order to provide managers with a known level of confidence in results and their implications. Researchers also need to explore the impacts of best management practices on these patterns, focusing on the potential to alter watershed-scale connectivity by identifying the most effective locations and types of engineered interventions. By redefining the development gradient based on connectivity of urban watersheds and the potential for impacts to streams, researchers and managers can move beyond documenting degradation to developing realistic and relevant management guidelines that focus on moderating urban impacts in an increasingly urban world.

Tables

Table 9. Summary of landcover metrics across all delineated, 45 to 55% developed, and selected watersheds. Note that these metrics were calculated using 30-m resolution landcover within the originally-delineated watersheds, not sewersheds.

	All delineated watersheds (n = 235)			**All watersheds 45 to 55% developed (n = 63)**			**Selected watersheds (n = 15)**		
	Min	Mean	Max	Min	Mean	Max	Min	Mean	Max
Area (km^2)	0.49	1.4	4.2	0.55	1.5	4.2	0.64	1.3	1.94
% Developed 2005	2	50	94	45	50	55	46	50	55
% Impervious 2006	0.53	19	58	6.7	17.5	36	9	19	36
Road density	0	2.2	8	0	1.77	5.4	0	1.6	5.3
Pipe density (km pipe/ km^2)	0.2	5.6	17.8	1.6	5.4	11.6	2	5.5	8.2
Pipe-stream ratio (km pipe / km stream)	0.3	9	52	2	8.9	27.6	2.4	9	18.6
Development aggregation	0.24	0.69	0.88	0.54	0.7	0.88	0.54	0.69	0.79
Correlation length	37	35.6	859	138	339.2	552.7	212	330.4	501.2

Table 10. Reach- and watershed-scale metrics calculated, including their associated category. Asterisks represent metrics considered in the transmission category during stormflow, but watershed-scale heatload at baseflow.

Direct radiation	Watershed-scale heatload	Heatload configuration	Heatload transmission
% Canopy closure from NAIP satellite photos	% Developed in 2005 (30 m)	Connectivity of development patches	Pipe density
Mean incision	% Impervious in 2006 (30 m)	Aggregation of development patches	Pipe-stream intersection density
Mean width	% Building impervious (1 m)	Largest patch index	Mean pipe length
	% Impervious (1 m)	Mean size of development patches	Maximum pipe length
	Road density		Upstream distance to nearest pipe-stream intersection
	Road length and traffic volume per area of watershed		Ratio of stream to pipe length
	% Transportation impervious (1 m)		% Developed in 1985 (30 m) *
	% Forest in 2005		% Developed in 1995 (30 m) *
	% Coarse vegetation (1 m)		% Development present in 2005 that was present in 1985*
	% Fine vegetation (1 m)		% Development in 2005 that has occurred since 1985*
	% Vegetation (1 m)		
	Mean inverse-distance weighted development connect to stream by pipes		
	Mean development within 50 feet of stream		

Table 11. Baseflow statistics in selected watersheds across one week in June 2012. Thermal logger accuracy is ± 0.54°C.

Site	Latitude	Longitude	Median daily mean temperature (°C)	Median daily minimum temperature (°C)	Median daily maximum temperature (°C)
dc021	36.064	-78.9204	19.31	18.43	19.95
dc025	36.0715	-78.9009	19.91	18.52	20.71
dc043	35.9674	-78.8821	19.74	17.76	22.05
dc044	35.9687	-78.8822	20.82	19.19	23.10
dc051	35.9734	-78.9213	19.68	18.43	20.62
dc064	35.9185	-78.9525	21.79	20.09	24.21
dc118	35.887	-78.6667	19.07	18.33	19.95
dc123	35.8863	-78.6388	19.28	17.67	20.42
dc127	35.8655	-78.6557	19.40	16.62	21.19
dc134	35.843	-78.702	19.60	18.33	21.00
dc148	35.816	-78.6688	19.72	18.62	20.71
dc157	35.7575	-78.7014	19.36	17.76	20.90
dc175	35.7561	-78.6292	20.31	17.86	25.03
dc_gc	35.9932	-78.8838	21.48	19.38	24.26
dc_mt	36.0041	-78.9714	19.11	17.95	20.19
dc_pb	35.8753	-78.7522	18.42	17.48	19.47
dc_rb	35.7862	-78.6801	19.78	18.81	20.81

Table 12. Regression equations for baseflow thermal metrics within each category and across all landcover metrics. Italic text shows a negative relationship, and bold text shows a positive relationship.

	Direct radiation	**Watershed-scale heatload**	**Heatload configuration**	**Heatload transmission**	**All**	**Stepped-down full model**
Median minimum temperature						
Best equation	*~ incision*	NS	NS	*~ maximum pipe length* + *distance to upstream outlet*	*~ maximum pipe length* + *distance to upstream outlet* + *incision*	*~ maximum pipe length* + *incision*
R^2	0.27			0.42	0.61	0.53
P	0.07			0.07	0.03	0.009
Median maximum temperature						
Best equation	NS	*~ pre-1985 development* + **traffic**	NS	NS	*~ pre-1985 development* + **traffic**	*~ pre-1985 development*
R^2		0.34			0.34	0.29
P		0.05			0.05	0.06
Median temperature						
Best equation	NS	*~ pre-1985 development*	NS	*~ maximum pipe length*	*~ maximum pipe length* + *pre-1985 development*	*~ maximum pipe length*
R^2		0.26		0.38	0.53	0.38
P		0.08		0.03	0.03	0.03

Table 13. The significance and explanatory power of final hierarchical models describing the relationships between storm and heat pulse metrics, and their relationships with landcover metrics. The first model in A and B shows no grouping by landcover metrics. The second model in A and B shows grouping using landcover metrics, and so includes three R^2 values: (1) data (amplitude or heat pulse intensity) and magnitude or rate of thermal change (as a relationship between amplitude or intensity and (2) air temperature and (3) flow metrics). Note that table B has two models that include landcover metrics: the first model best describes variation in rate of heat transfer, while the second model best describes variation in heat pulse intensity. Italic text shows a negative relationship, and bold text shows a positive relationship. All *P*-values were < 0.001

A	R^2 for amplitude	R^2 for magnitude of thermal change described by air temperature	R^2 for magnitude of thermal change described by flow intensity
Positive amplitude ~ air temperature + flow intensity	0.285	(no landcover metrics)	(no landcover metrics)
Positive amplitude ~ air temperature:**pre-1985 development** + flow intensity: **distance to nearest upstream outlet**	0.295	0.42	0.72
B	R^2 for change intensity	R^2 for rate of thermal change described by air temperature	R^2 for rate of thermal change described by flow intensity
Heat pulse intensity ~ air temperature + antecedent flow	0.228	(no landcover metrics)	(no landcover metrics)
Heat pulse intensity ~ air temperature:*average development in 50-ft butter* + antecedent flow:*% coarse vegetation*	0.252	0.99	0.97
Heat pulse intensity ~ air temperature:**pipe-stream intersection density** + antecedent flow:**pipe-stream ratio**	0.269	0.85	0.84

Figures

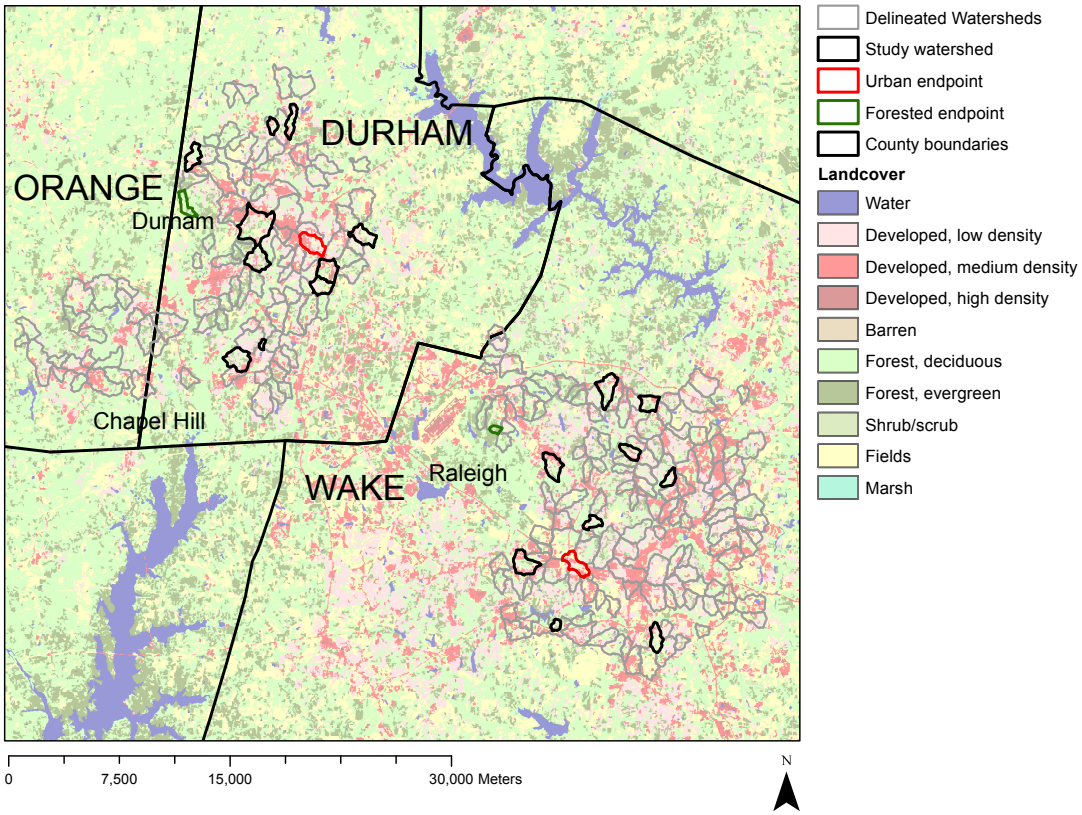

Figure 19. Delineated watersheds in the municipalities of Carrboro, Chapel Hill, Durham, and Raleigh, North Carolina. Watersheds within the subset of 45 to 55% development used in this study are outlined in grey, while endpoint watersheds are outlined in green (forested) or red (urban).

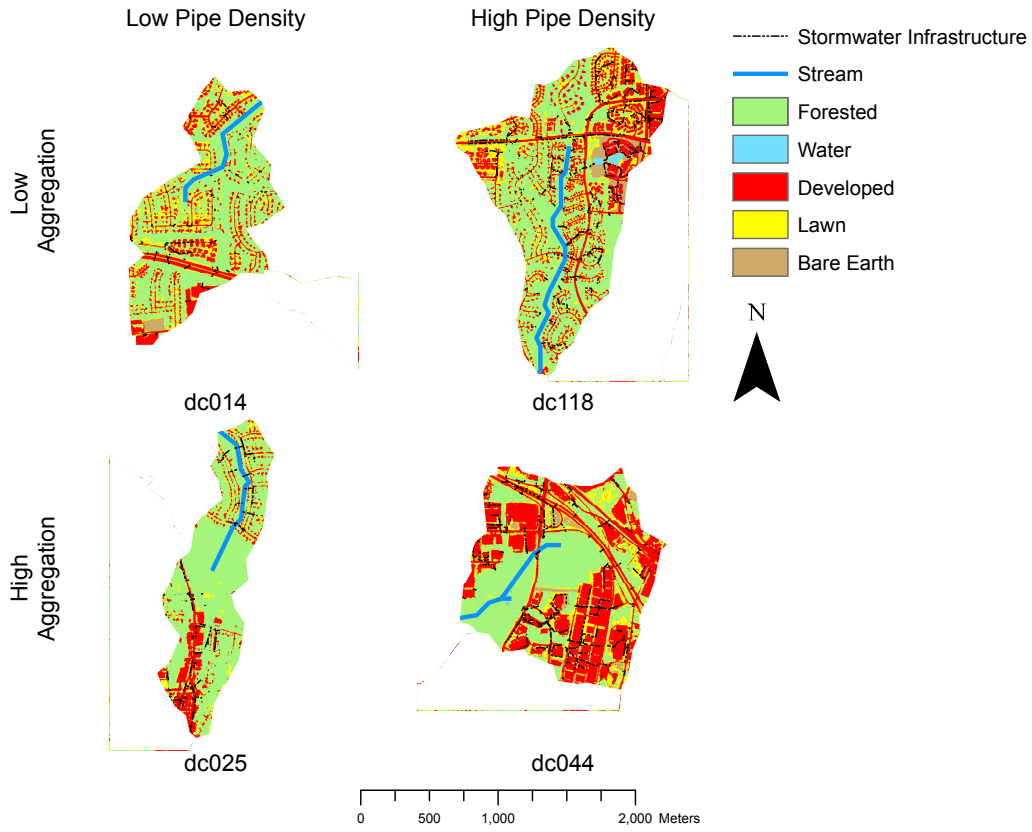

Figure 20. Four watersheds from the study, showing the potential for variation in stormwater infrastructure and development aggregation even within a narrow subset of proportion of development.

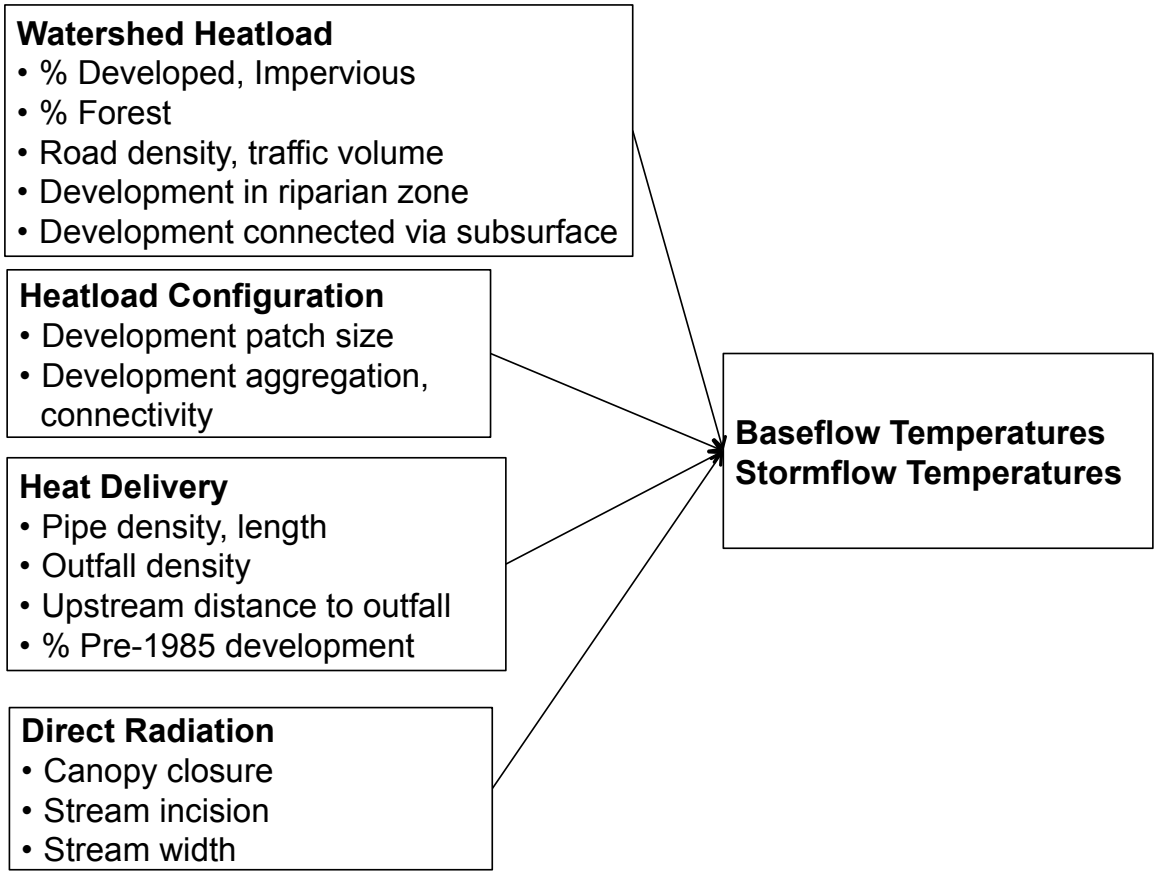

Figure 21. Conceptual diagram of different categories of heatload metrics at reach- and watershed-scale that potentially influence stream baseflow and stormflow thermal regimes.

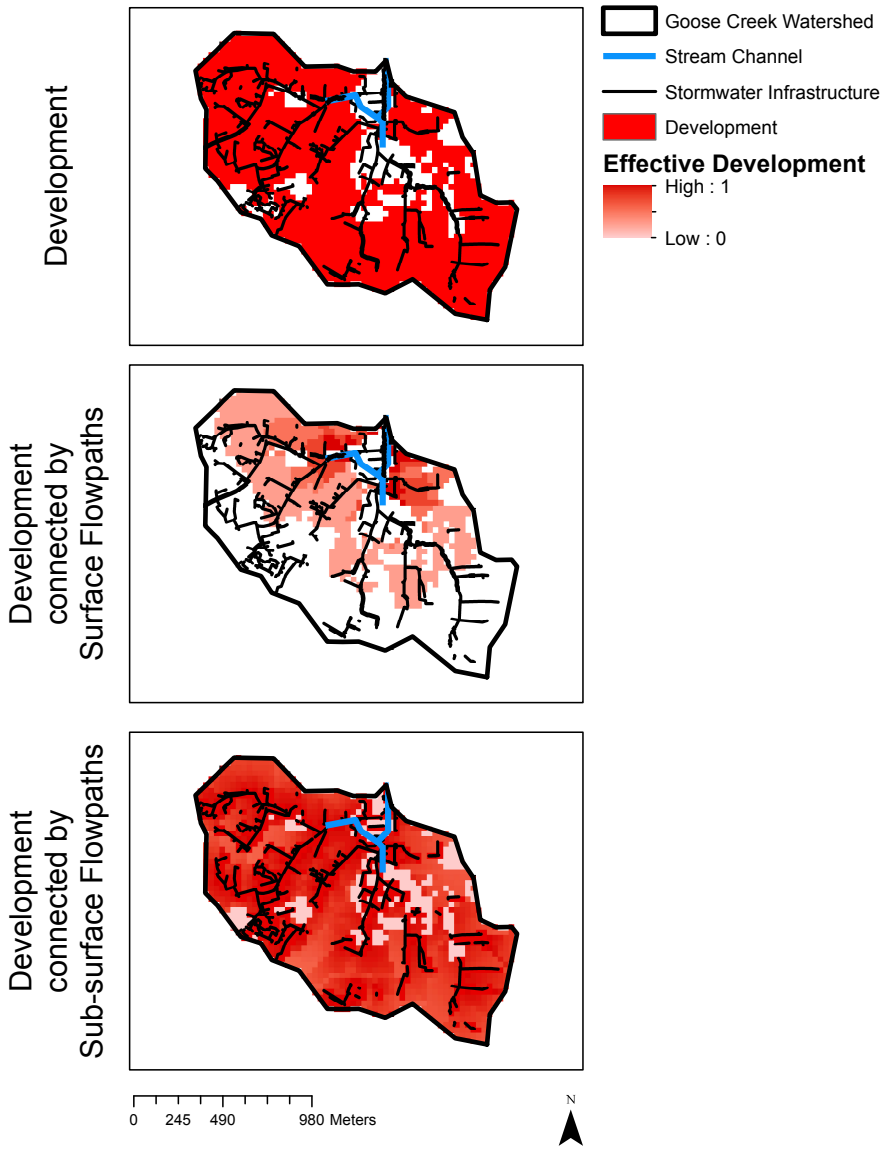

Figure 22. Development in a watershed can be calculated as the total proportion development across the watershed (A), the proportion of development connected to the stream via surface flowpaths and weighted by distance and intervening landcover (B), or the proportion of development connected to the stream via subsurface flowpaths and weighted by distance (C). This final option best describes the hydrological processes at work in urban watersheds, with nearly all development highly connected to the stream via subsurface infrastructure.

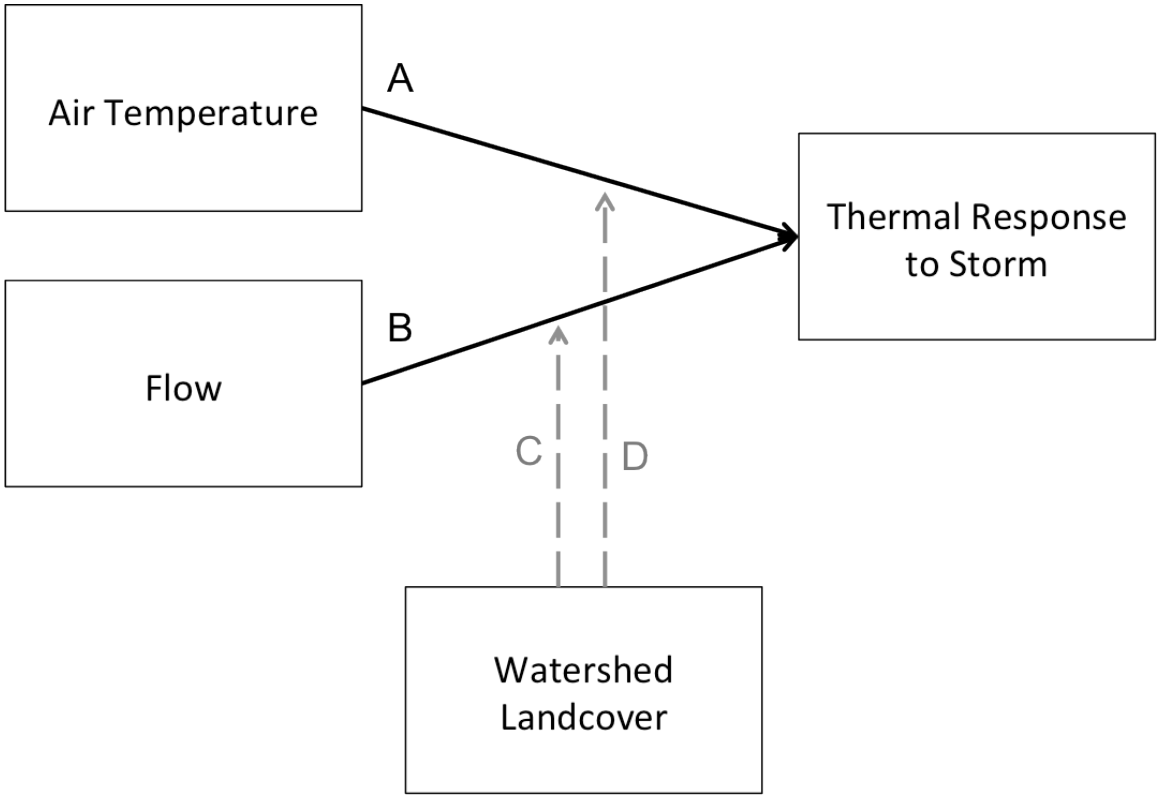

Figure 23. Conceptual model of motivation for hierarchical modeling of this dataset. The thermal response (amplitude or intensity) of a stream to a storm depends on the storm characteristics (air temperature and flow). This relationship is described as the magnitude or rate of thermal change: arrows A and B. Across many streams, the magnitude or rate of thermal change of each stream to a population of storms is modulated by the landcover of the watershed: arrows C and D.

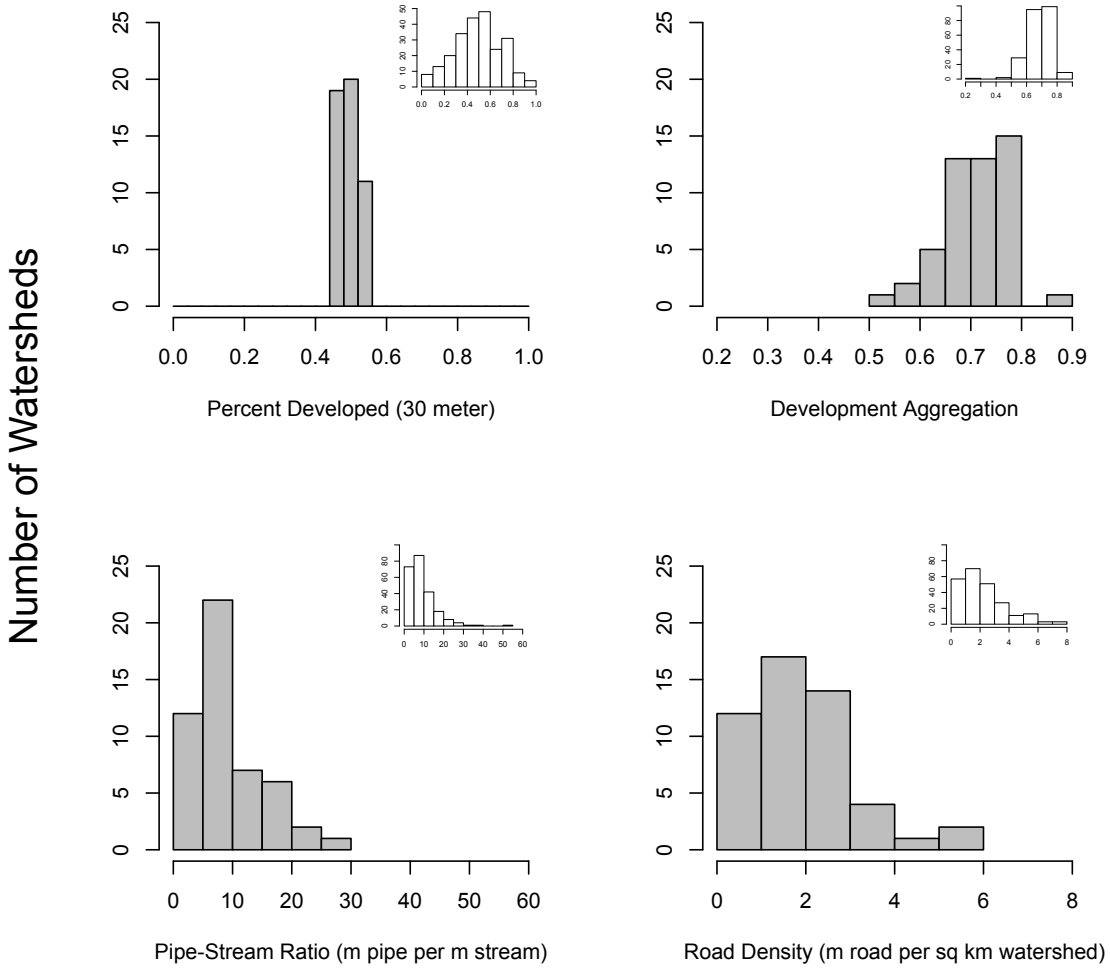

Figure 24. Histograms of development characteristics, North Carolina inset in white and histograms of the 63 watersheds within 45 to 55% developed in the main plot in grey. The variation in many of the development characteristics within the subset of development level is similar to the variation across all watersheds.

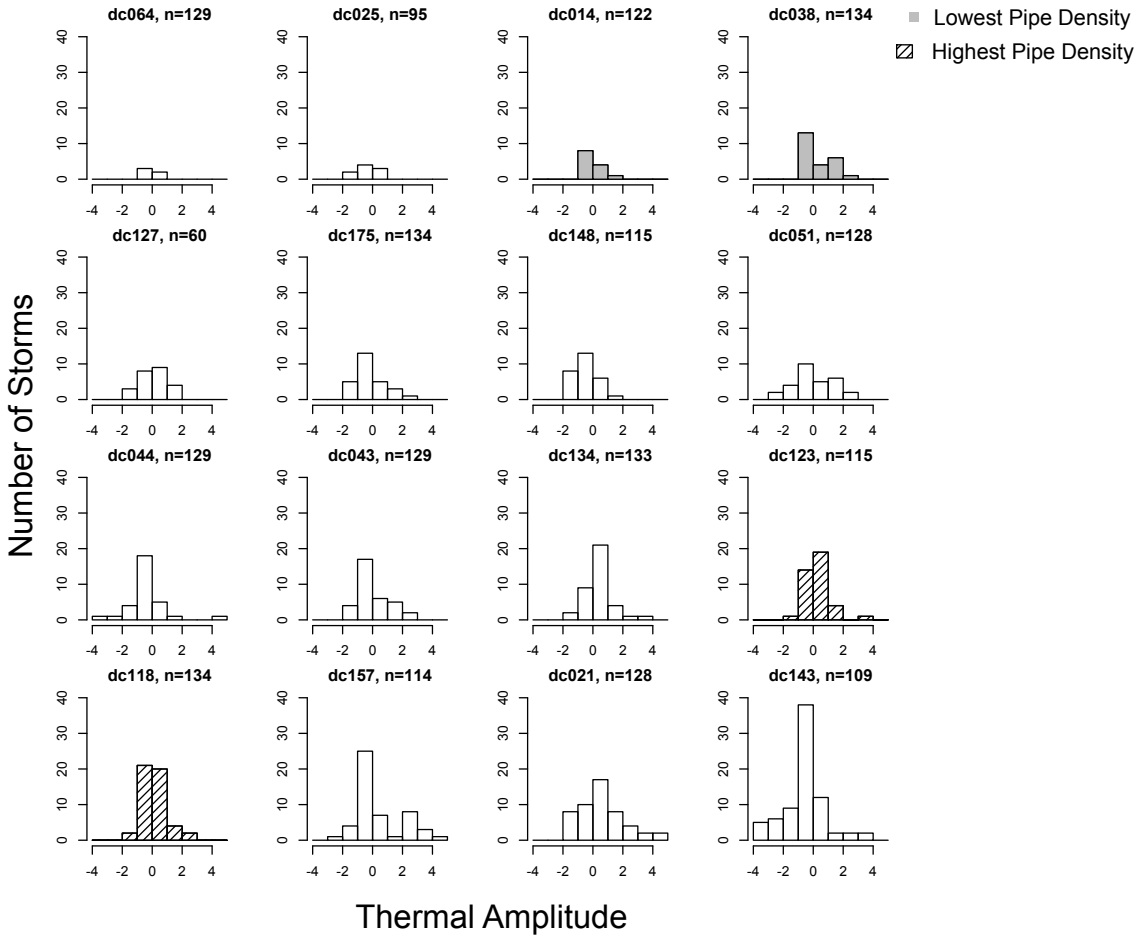

Figure 25. Histograms of amplitude observed across all storms at each site. The watersheds with lowest and highest pipe density are highlighted. Variations in amplitude at each site highlight the wide range the influence of storm characteristics. Thermal logger accuracy is ± 0.54°C.

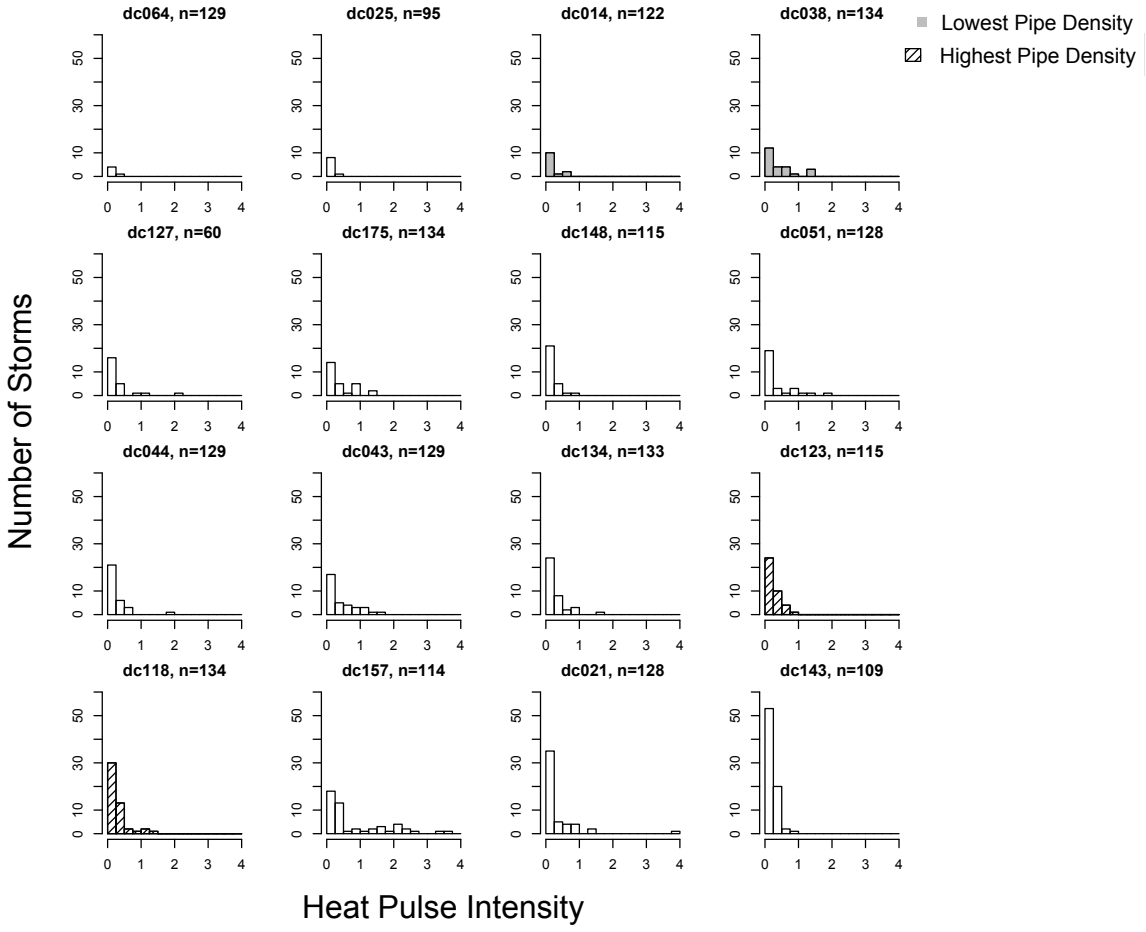

Figure 26. Histograms of maximum positive increase observed across all storms at each site. The watersheds with lowest and highest pipe density are highlighted. Variations in heat pulse intensity at each site highlight the wide range the influence of storm characteristics.

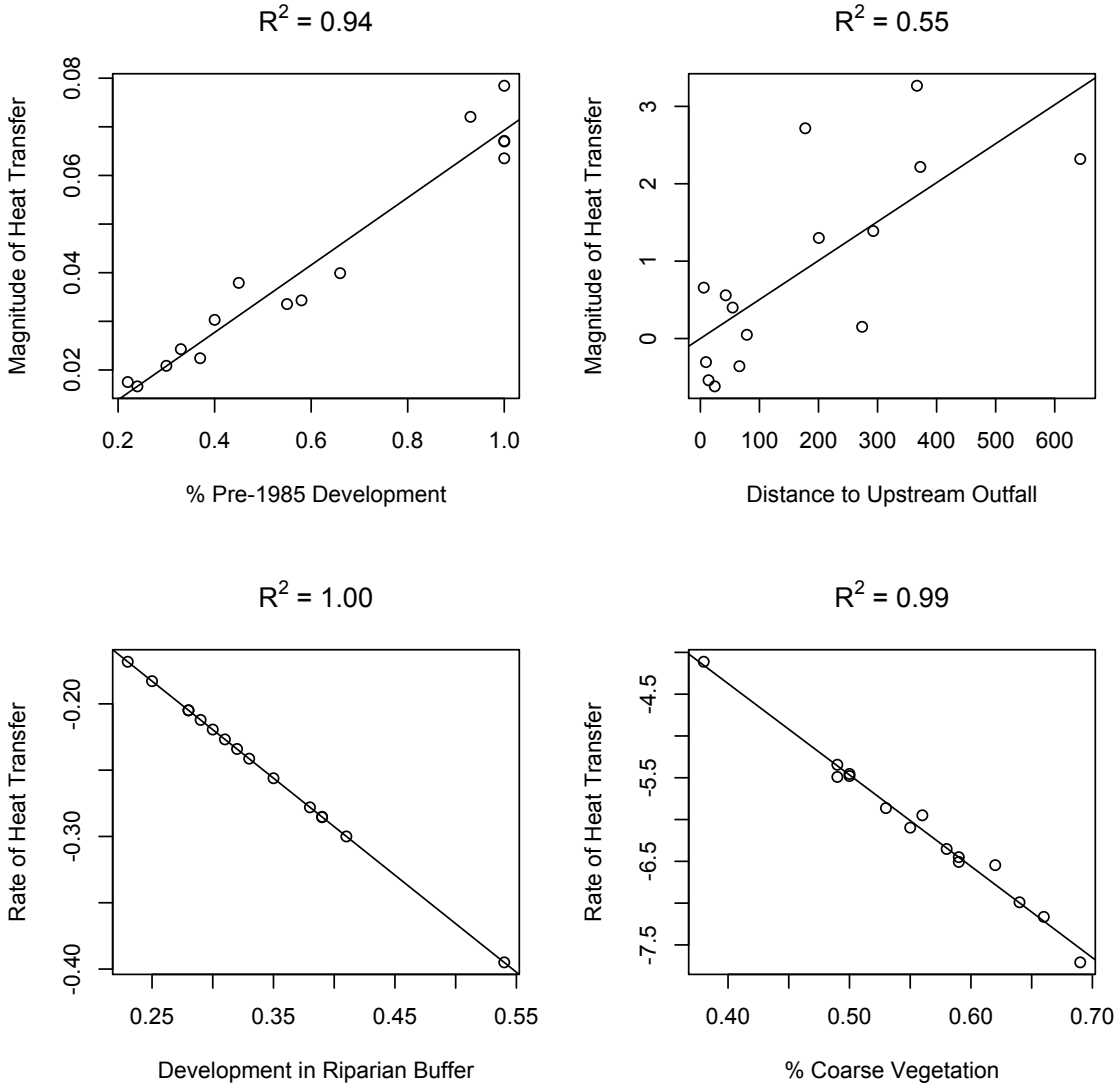

Figure 27. Relationships between the magnitude or rate of thermal change and the best predictor landcover metric, with a single predictor and landcover metric in each model. Panels A and B shows the magnitude of thermal change as the relationship between amplitude and air temperature (A) and flow intensity (B). Panels C and D shows the rate of thermal change as the relationship between heat pulse intensity and air temperature (C) and antecedent flow (D). Note that extremely high R^2 values to some degree reflect the model's inclusion of the given landcover metric in assessing the variation in relationships across sites.

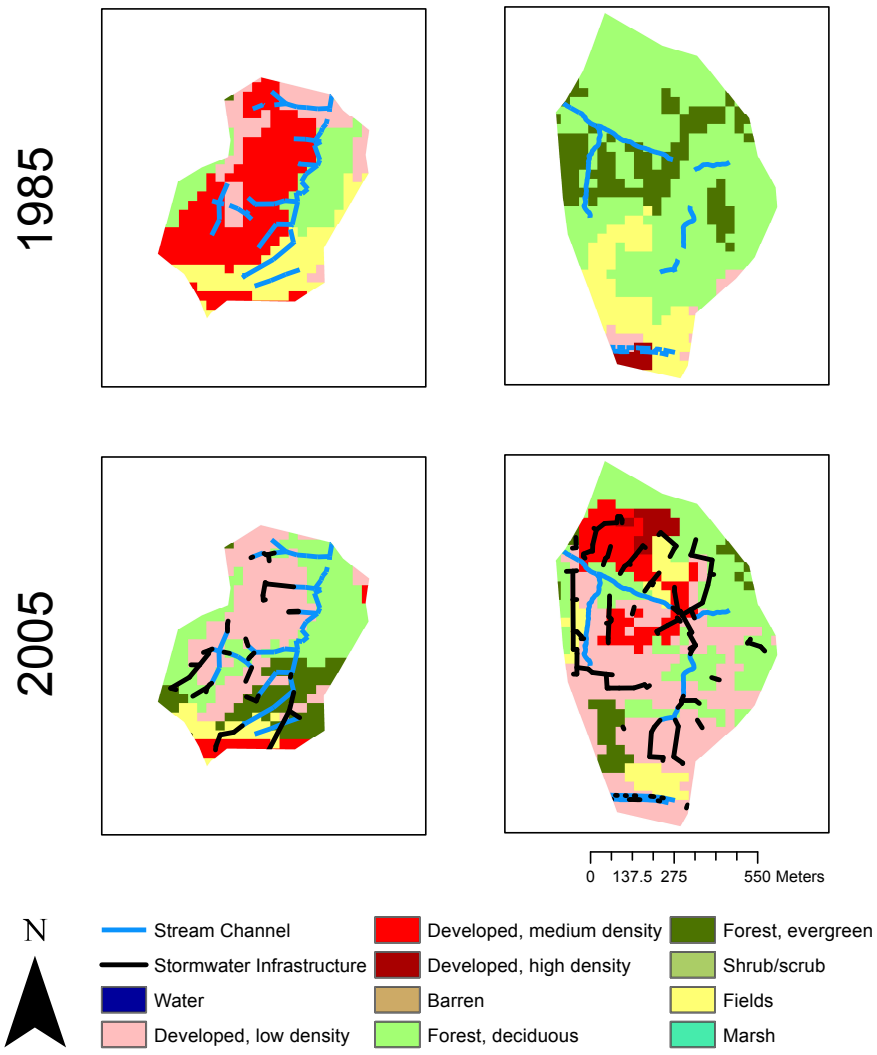

Figure 28. Differences in landcover change between 1985 and 2005 in two watersheds. On left, development in dc157 did not increase from 1985 to 2005. On right, development in dc021 increased from 4% in 1985 to 57% in 2005.

5. Conclusions

Heat is an important stressor in urban streams, acting as both a press disturbance during baseflow and a pulse disturbance during stormflow. The research in this dissertation documents the magnitude of thermal differences at baseflow and stormflow in streams across an urban landscape, reveals the different pathways through which heat is delivered from imperviousness in the watershed into the stream, and explores how these impacts propagate downstream. I also show the range of thermal differences in watersheds both across a gradient of development intensity and across a gradient of development configuration and connectivity, within similar development intensity. This research points to the importance of heat as a direct and indirect stressor in the USS and the need to include thermal effects in urban ecology and watershed management. Heat also provides an inexpensive, if conservative, tracer of urban impacts to stream ecosystems and provides a starting place for new questions to explore pathways between development and streams.

I found that, across a gradient of urbanization, the most urban streams are hotter at baseflow and show greater temperature increases during stormflow. However, this relationship varies along the gradient, partially due to reach-scale metrics controlling baseflow temperatures and the greater amount of thermal heterogeneity in urban reaches. Stormflow temperature changes are more directly controlled by catchment-scale metrics.

Although heat is not a conservative pollutant, thermal changes caused by urbanization are able to move far downstream of urban inputs before dissipating, especially during storm events. Other urban pollutants, such as heavy metals and polycyclic aromatic hydrocarbons (PAHs), will remain in stream ecosystems for much longer than heat pulses and have the potential to travel even further downstream of urban inputs. These longitudinal impacts emphasize the importance of addressing pollutant inputs at the source across a landscape, rather than managing at the reach scale, after the pollutant has entered the network. Even in moderately urbanized landscapes like Durham, North Carolina, nearly all stream ecosystems are likely to be regularly impacted by urban pollutants.

Within a narrow subset of development intensity, I found a range in other development characteristics and thermal metrics similar to those seen across the entire landscape and urban gradient. Within this subset of watersheds, baseflow temperatures are cooler in watersheds with longer pipe lengths, greater percentage of pre-1985 development, and greater channel incision. The thermal responsiveness of streams to storms was greater in watersheds with higher sub-surface connectivity and lower in watersheds with greater amounts of development within the riparian zone and forest across the catchment. All development is clearly not equal. In a constantly developing world, this research points to managing the ways in which development is connected to

stream ecosystems and the location and configuration of development in order to protect urban streams.

Heat as a Tracer for Urban Stressors

Heat serves as an inexpensive indicator of urban impacts to streams, but underestimates the impacts of the pulse/press dynamics of the USS because heat dissipates relatively quickly, compared to other urban pollutants. In future studies, we need to identify which aspects of the USS are highly correlated with heat surges, including amounts of scour and high flow, pollutants, and nutrients. By quantifying these relationships, heat surges can be used in other studies and by managers to assess stream health. This research shows that thermal pollution is an important part of the USS and must be addressed as such, in terms of understanding how urban watersheds function and how to protect urban streams. Scientists and managers need to better understand the impacts and implications of thermal pollution to urban streams and also to understand the additive effects of thermal pollution with other USS aspects. Thermal changes can also be used to cheaply assess urban impacts and as a first stage in answering cutting-edge questions in urban stream research. By explicitly incorporating temperature in urban stream research, we better understand the suite of factors at work in the USS and can use this symptom to move forward in the diagnosis and treatment of the USS.

Future Directions

Alterations of streams in urban watersheds, though predictable on a broad level, are complex and interwoven. Scientists and managers often focus on a single pathway of change that occurs in urban streams, but this view can result in overly simplistic models that do not take into account the interactions between urban stream processes and the variability in changes that occur.

The metrics influencing baseflow and stormflow temperatures of urban streams function at different spatial scales, but these pathways and temperatures interact. Cool baseflow temperatures from piped channel inputs paired with a highly developed watershed can result in large stormflow heat surges. Reach-scale restoration in urban watersheds focuses on re-engineering channels, which decreases incision and riparian canopy cover, both of which increase baseflow temperatures (Sudduth et al. 2011). These changes do not address stormflow surges explicitly, but warmer baseflow temperatures can decrease magnitude of heat pulse increases. Some best management practices (BMPs) focus more intentionally on stormflow impacts, including decreasing stormflow surges and allowing for settling of sediments out of the water column (US EPA 1999). These practices focus on delaying the delivery of stormwater flow to the stream network, but do not always consider the thermal impacts at baseflow. For example, wet detention basins and stormwater wetlands often lack canopy cover, trading decreases in heat flow surges for constant heat inputs (Herb et al. 2009, Jones and Hunt 2010).

Researchers and managers must include the interplay between baseflow and stormflow temperatures to understand the thermal changes observed and maintain more natural thermal regimes in urban streams. The spatial propagation of thermal pollution within the stream network also shows the importance of understanding the urban impacts that occur across a developing landscape, even in streams in protected, managed areas. The multiple spatial scales at which thermal pollution occurs emphasize the need to research and manage urban streams in a way that embraces the landscape-level effects of urbanization.

This focus on the processes by which thermal pollution propagates into urban streams and moves downstream led to the realization that all development in a watershed is not equal. One square meter of imperviousness absorbs an equal amount of heat anywhere in a watershed, but its location, configuration, and connectivity explain the pathways by which and the amount of heat that enters the stream network. Watersheds with greater shading via canopy, subsurface pipes, and incision receive less heat from this imperviousness at baseflow. However, imperviousness that is hydrologically closer to the stream network via subsurface connections or a part of a large aggregation of development will deliver greater heat at stormflow to stream networks. The importance of these aspects of development in explaining the changes observed in urban streams show that research focused on a forested-to-urban gradient can obscure important relationships and processes in urban systems. Moving beyond

simple metrics, like the percent impervious in a watershed, to the connection and arrangement of imperviousness extends our understanding of how urban watersheds function and provides realistic guidelines for management of streams that accept the presence of development on the landscape. Development is unlikely to decrease, so a mechanistic understanding of urban watersheds provides suggestions to protect streams by altering how development occurs in a watershed rather than controlling only the amount that occurs.

The research in this dissertation goes beyond documenting changes in urban streams to exploring the processes by which these changes occur and pointing the way to a new understanding of the urban gradient. This dissertation allowed me to compare the importance and strengths of thermal pollution pathways that occur at different spatial and temporal scales. The interactions between these metrics and pathways are often overlooked in urban stream research, but are an essential aspect of understanding the USS. By exploring the downstream propagation of thermal pollution, I found that stream ecosystems in urban landscapes are likely to be impacted regularly by urban inputs, even far downstream of the point source. Finally, this research points to a new interpretation of the urban gradient by recognizing the importance of the connectivity and arrangement of impervious surfaces across watersheds. These new metrics can better explain why and how urbanization affects stream ecosystems and provide

realistic guidelines for making development more sustainable and improving urban watershed management.

Appendix A

Table 14. Storm characteristics across 54 storms for which we collected air and stream temperature, precipitation, and flow data. 7 additional storms were identified from flow data, but lacked data necessary to evaluate differences in storm characteristics. Storms 57 to 61 were not analyzed within the SEM due to lack of air temperature data. Definitions of each metric are described in Table 5. Thermal logger accuracy is ± 0.54°C.

Storm	Start	End	Ant. flow (L/s)	Flow %	Flow diff. (L/s)	Mean flow (L/s)	Mean flow in 1st hour (L/s)	Max flow (L/s)
1	5/27/11 13:27	5/27/11 16:54	7.16	280987.31	20100.56	6762.65	4109.14	20107.72
2	5/27/11 16:54	5/27/11 22:33	982.31	240.92	1384.22	941.34	1868.93	2366.53
3	5/27/11 22:33	5/28/11 2:34	1201.78	21.78	-940.06	221.52	209.38	261.73
4	5/28/11 2:34	5/28/11 14:13	1237.64	36.10	-790.79	149.72	229.62	446.85
5	6/12/11 21:53	6/13/11 10:57	28.14	323.08	62.78	43.15	78.55	90.92
6	7/4/11 16:31	7/4/11 18:39	4.54	67662.15	3068.49	940.18	5.99	3073.03
7	7/4/11 18:39	7/5/11 3:38	88.30	322242.19	284437.45	31708.30	56582.15	284525.74
8	7/5/11 22:53	7/6/11 12:57	47.78	33.76	-31.65	13.28	11.94	16.13
14	8/13/11 10:17	8/13/11 11:57	1.44	3935.89	55.23	45.31	48.27	56.67
15	8/13/11 11:57	8/13/11 21:11	4.51	3235.39	141.35	43.00	109.33	145.86
18	9/6/11 5:08	9/6/11 9:06	3.86	65981.59	2546.06	592.46	5.73	2549.92
19	9/6/11 9:06	9/6/11 12:31	101.46	11043.94	11104.25	2873.48	5223.57	11205.71
20	9/6/11 12:35	9/6/11 13:28	512.49	81.93	-92.59	367.55	365.51	419.90
21	9/6/11 13:28	9/6/11 17:58	525.89	455.64	1870.26	729.53	444.96	2396.15
22	9/6/11 22:38	9/7/11 8:59	677.20	7835.22	52382.82	5669.69	7704.56	53060.02
23	9/21/11 19:08	9/22/11 13:58	9.10	22956.39	2080.60	195.49	1377.13	2089.71
24	9/23/11 13:58	9/24/11 0:45	24.76	4761.95	1154.38	281.53	775.85	1179.14
25	9/24/11 17:02	9/25/11 4:03	60.61	90.07	-6.02	42.05	34.39	54.59
26	9/28/11 4:18	9/28/11 15:06	20.13	790.48	139.00	69.93	111.32	159.13
27	10/12/11 9:45	10/13/11 3:42	5.82	1396.76	75.46	29.35	57.20	81.28
28	10/19/11 1:08	10/19/11 11:45	8.52	57839.40	4921.70	966.08	2577.40	4930.22
29	10/19/11 11:45	10/19/11 13:58	432.50	28.69	-308.42	112.36	105.42	124.08
30	10/19/11 13:58	10/19/11 22:26	442.20	38.29	-272.86	127.69	134.66	169.34
31	11/4/11 3:04	11/4/11 13:29	12.51	291972.20	36520.77	5178.90	3216.60	36533.28
32	11/4/11 13:29	11/4/11 18:45	2257.44	8.82	-2058.38	170.34	167.26	199.06
33	11/17/11 6:54	11/17/11 12:10	17.32	357.01	44.51	56.18	48.23	61.82
34	11/17/11 12:10	11/18/11 0:23	26.42	1891.47	473.36	146.25	294.61	499.79
35	11/23/11 3:52	11/23/11 14:11	17.76	965.18	153.69	80.76	142.34	171.46
36	11/29/11 2:26	11/30/11 10:02	17.16	39215.06	6711.55	636.98	19.51	6728.71

37	12/21/11 12:20	12/22/11 11:11	23.04	15483.85	3544.74	473.05	29.77	3567.78
38	12/22/11 16:07	12/23/11 9:02	390.24	75.95	-93.84	144.89	100.53	296.40
39	12/27/11 12:37	12/28/11 0:45	18.65	580.34	89.56	69.48	51.08	108.21
40	1/11/12 16:36	1/12/12 7:51	16.75	556.59	76.46	57.15	51.41	93.20
41	1/21/12 9:18	1/21/12 22:40	22.44	566.79	104.76	78.20	69.74	127.20
42	1/27/12 7:22	1/28/12 11:08	16.70	18866.35	3133.75	251.32	2082.88	3150.45
43	2/5/12 6:21	2/5/12 21:39	17.65	363.56	46.52	37.27	28.93	64.17
44	2/16/12 17:18	2/17/12 6:08	14.63	797.19	101.97	65.73	32.50	116.59
45	2/19/12 15:43	2/19/12 22:10	17.29	3038.69	508.00	228.22	19.19	525.28
46	2/19/12 22:10	2/20/12 12:10	74.01	324.15	165.89	140.20	211.92	239.90
47	2/23/12 2:35	2/23/12 11:54	22.16	610.95	113.21	79.21	67.43	135.37
48	2/24/12 17:48	2/25/12 10:53	29.69	10877.51	3200.12	378.00	1645.24	3229.81
49	2/27/12 12:54	2/28/12 10:58	22.90	438.55	77.53	57.40	27.15	100.43
50	3/1/12 1:16	3/1/12 15:27	29.12	380.96	81.81	68.83	34.60	110.93
51	3/3/12 3:10	3/4/12 4:38	29.71	103314.16	30664.18	1961.64	32.38	30693.89
52	3/4/12 4:38	3/4/12 10:08	2079.43	8.25	-1907.97	152.60	145.69	171.46
53	3/9/12 7:08	3/9/12 18:53	25.86	347.23	63.93	62.69	48.00	89.79
54	3/17/12 23:04	3/18/12 16:03	25.18	8402.73	2090.68	321.31	26.89	2115.87
55	3/20/12 23:28	3/21/12 10:32	37.18	576.91	177.31	123.47	64.59	214.49
56	4/4/12 18:12	4/5/12 10:34	22.78	319.09	49.90	43.24	27.23	72.67
57	4/21/12 22:06	4/22/12 9:03	16.81	9573.72	1592.47	261.82	18.98	1609.27
58	4/22/12 9:03	4/22/12 19:11	128.29	93.18	-8.76	83.30	56.69	119.53
59	4/22/12 19:11	4/23/12 8:38	156.67	83.24	-26.26	75.91	52.15	130.41
60	4/26/12 6:19	4/26/12 10:45	19.85	228.18	25.45	36.93	29.55	45.30
61	4/26/12 13:03	4/27/12 0:10	25.36	1356.77	318.75	104.66	148.76	344.12

Table 14, cont.

Storm	Max change in flow (L/s)	Duration of elevated flow (min.)	Area under flow curve	Max precip rate (in./ min.)	Total precip (in.)	Mean precip (in.)	Max precip rate over 1 hour (in.)	Precip in first hour (in.)
1	6910.73	203	1398821.54	0.27	0.79	0.98	1.39	1.39
2	308.38	163	60597.99	0.02	0.42	0.17	0.2	0.16
3	15.59	220	49459.80	0.01	0.07	0.03	0.04	0.02
4	26.30	349	24793.86	0.04	0.18	0.22	0.18	0.18
5	8.37	764	33298.55	0.06	0.13	0.22	0.13	0.13
6	619.41	54	503.56	0.29	1.22	0.86	1.19	1.19
7	113197.20	269	41526.81	0.4	2.36	0.36	2.36	2.36
8	1.16	822	10944.41	0.02	0.11	0.03	0.05	0.05

14	11.84	98	4488.79	0.21	0.61	0.32	0.53	0.53
15	10.45	274	4206.43	0.06	0.23	0.11	0.21	0.21
18	655.98	209	139776.98	0.36	0.92	0.50	0.84	0.84
19	2082.92	202	590290.95	0.28	1	0.92	0.62	0.62
20	16.91	50	18466.74	0.01	0.01	0.01	0.01	0.01
21	247.56	225	181282.38	0.23	0.38	0.17	0.37	0.37
22	7975.59	609	3525568.75	0.21	1.41	0.35	0.66	0.22
23	715.30	1096	219987.29	0.11	0.77	0.07	0.45	0.13
24	110.10	634	181760.00	0.1	0.6	0.06	0.34	0.02
25	3.21	658	27718.01	0.02	0.11	0.01	0.08	0.01
26	15.31	637	45089.06	0.06	0.32	0.21	0.22	0.22
27	21.73	1003	30223.50	0.15	0.29	0.03	0.18	0.02
28	461.26	624	615234.69	0.06	1.39	0.19	0.4	0.03
29	7.48	120	13380.67	0.06	0.24	0.04	0.11	0.11
30	7.39	492	63521.23	0.03	0.07	0.03	0.06	0.06
31	8746.97	403	3195184.42	0.09	1.75	0.31	0.61	0.19
32	11.28	315	53583.97	0.01	0.12	0.02	0.04	0.01
33	4.23	311	17451.58	0.06	0.16	0.02	0.06	0.05
34	35.95	724	106958.40	0.03	0.48	0.04	0.2	0.06
35	14.82	612	49747.62	0.12	0.37	0.10	0.32	0.32
36	1145.39	1895	1208255.97	0.05	1.34	0.04	0.38	0.02
37	355.02	1361	648331.38	0.04	0.76	0.03	0.22	0.07
38	19.54	965	143440.31	0.04	0.19	0.01	0.16	0.16
39	35.11	726	50504.53	0.02	0.31	0.05	0.09	0.06
40	4.85	882	51290.64	0.02	0.33	0.02	0.13	0.13
41	6.70	799	62574.62	0.05	0.52	0.02	0.13	0.05
42	883.68	1652	418567.31	0.12	0.4	0.22	0.36	0.36
43	14.75	917	34186.71	0.02	0.25	0.01	0.07	0.01
44	7.13	751	50079.99	0.03	0.35	0.04	0.16	0.16
45	31.00	375	86251.03	0.03	0.47	0.05	0.18	0.03
46	14.11	429	39438.90	0.01	0.06	0.04	0.03	0.03
47	7.86	557	44224.76	0.12	0.21	0.42	0.21	0.21
48	943.10	1020	387410.44	0.24	0.39	0.78	0.39	0.39
49	6.06	1313	75716.76	0.01	0.27	0.04	0.08	0.08
50	6.88	842	58310.56	0.06	0.17	0.04	0.1	0.1
51	5936.91	1509	2997161.61	0.18	1.11	0.16	0.69	0.17

52	11.88	325	49683.47	0.01	0.07	0.06	0.06	0.06
53	5.77	703	44166.51	0.02	0.22	0.04	0.09	0.09
54	557.91	986	325517.17	0.11	0.72	0.20	0.59	0.59
55	44.42	660	81763.62	0.02	0.29	0.07	0.1	0.08
56	7.25	979	42367.99	0.11	0.22	0.02	0.17	0.17
57	385.39	631	170710.74	0.19	0.54	0.32	0.53	0.53
58	8.60	585	49423.53	0.01	0.29	0.03	0.08	0.07
59	6.25	663	53993.90	0.01	0.26	0.04	0.1	0.05
60	2.20	244	9107.67	0.07	0.16	0.05	0.04	0.04
61	30.84	602	67134.87	0.12	0.3	0.11	0.28	0.28

Table 14, cont.

Storm	Mean air temp over 30 minutes (˚C)	Mean air temp over 60 minutes (˚C)	Mean air temp over 120 minutes (˚C)	Sum of air temp DH over 2 hours	Sum of air temp DH over 3 hours	Sum of air temp DH over 4 hours	Sum of air temp DH over 5 hours	Sum of air temp DH over 6 hours	Sum of air temp DH over 24 hours	Max. amp. (˚C)	Distance of dissipation (m)
1	22.62	23.21	23.93	52.56	76.42	98.98	120.53	141.24	287.99	3.16	1212.37
2	18.80	18.88	18.91	38.93	63.01	90.10	114.51	137.52	327.06	0.86	0.00
3	18.27	18.33	18.44	37.28	56.30	75.12	93.76	112.76	458.60	0.86	0.00
4	18.04	18.04	18.06	36.23	54.42	72.83	91.45	110.25	36.24	1.14	0.00
5	26.34	26.46	27.03	56.86	86.65	116.98	146.58	174.74	454.16	5.20	1108.20
6	28.96	30.47	31.61	72.11	104.93	137.40	167.55	195.79	54.80	6.06	2168.06
7	22.16	22.07	22.13	45.34	74.56	111.98	146.67	179.34	522.56	2.22	0.00
8	23.85	23.95	24.19	49.62	75.30	101.91	129.30	157.56	546.44	1.63	0.00
14	22.17	22.09	22.05	44.23	66.33	88.42	110.56	132.44	176.96	3.28	792.14
15	23.76	23.44	23.12	46.59	69.06	91.32	113.37	135.41	247.32	1.64	429.00
18	20.98	20.95	20.91	42.07	63.03	83.90	104.64	125.48	125.63	2.69	2168.06
19	21.06	20.96	20.84	42.05	63.13	84.33	105.20	126.16	188.66	1.26	0.00
20	20.87	20.75	20.94	42.19	63.16	83.83	104.96	126.14	209.77	0.19	0.00
21	22.26	22.09	21.61	43.55	64.70	86.22	107.06	128.10	254.07	1.85	294.11
22	21.00	21.04	21.18	42.89	64.77	86.94	109.02	131.09	473.07	1.45	375.61
23	23.49	23.72	24.21	50.60	75.16	99.66	123.39	145.58	361.27	4.30	2168.06
24	22.38	22.26	22.08	44.41	66.00	87.36	108.66	129.99	257.68	2.21	1735.25
25	20.27	20.14	19.86	39.65	58.81	77.85	96.89	116.06	212.51	5.59	1648.77

26	22.70	22.72	22.51	46.51	68.60	91.05	114.00	137.50	45.59	2.48	1648.77
27	16.93	16.91	16.89	33.79	50.63	67.45	84.26	101.08	101.21	1.52	482.82
28	18.96	19.39	19.86	41.36	63.59	87.40	113.21	141.08	397.25	3.90	2168.06
29	16.20	16.12	15.96	32.00	47.59	63.45	79.73	96.59	163.96	1.33	375.65
30	16.88	16.86	16.79	33.55	49.76	65.74	81.41	97.00	214.62	1.71	294.11
31	9.01	8.92	8.70	7.65	26.95	35.86	45.62	57.76	186.45	2.82	721.95
32	8.58	8.53	8.48	17.08	26.24	35.05	44.00	53.43	25.77	3.21	2168.06
33	18.28	18.78	18.58	39.03	56.91	74.69	91.93	108.04	263.83	3.14	488.04
34	12.62	12.88	13.25	28.77	45.55	62.42	78.61	94.63	26.66	2.11	375.65
35	15.51	15.60	15.46	31.47	46.27	60.63	74.05	87.53	31.73	5.79	1602.30
36	15.07	14.92	14.76	29.90	44.28	57.85	71.35	85.32	15.35	3.06	2168.06
37	6.11	6.08	6.16	12.39	18.87	25.13	31.54	38.02	50.58	4.51	2168.06
38	10.40	10.52	10.60	21.83	32.95	43.87	53.89	63.03	143.03	2.30	390.86
39	2.80	2.77	2.65	5.42	7.78	9.88	11.73	13.27	15.46	2.94	390.86
40	6.10	6.11	6.14	12.57	18.33	23.63	28.42	33.04	65.36	1.77	439.27
41	5.37	5.60	5.96	13.14	21.03	29.63	37.66	45.52	69.15	1.80	390.86
42	9.66	9.66	9.70	20.21	30.04	39.85	49.39	58.20	68.08	4.28	429.00
43	4.63	4.66	4.69	9.57	14.67	20.16	25.83	31.51	83.30	1.67	429.00
44	7.38	8.17	8.22	18.81	27.77	35.29	40.47	44.19	74.28	3.04	792.14
45	2.98	3.01	3.12	6.86	10.77	15.72	20.99	26.26	62.56	1.69	0.00
46	1.92	1.95	2.02	4.81	7.58	10.67	4.05	17.66	69.45	2.63	0.00
47	5.24	5.16	5.22	10.66	16.53	22.12	28.80	37.29	5.39	1.77	429.00
48	13.46	13.57	13.80	9.72	44.17	59.59	75.98	2.54	185.03	4.48	2168.06
49	2.87	2.78	2.38	4.79	6.22	7.11	6.98	6.37	6.83	4.25	390.86
50	10.10	10.10	10.03	20.50	30.31	41.02	52.21	63.39	168.05	2.70	390.86
51	6.99	7.00	7.03	14.20	21.44	28.57	35.73	42.85	14.01	2.41	2168.06
52	5.48	5.47	5.59	11.93	17.72	23.59	29.75	36.18	17.20	1.07	0.00
53	8.32	8.40	8.45	17.15	26.10	35.12	44.33	53.26	25.96	1.64	429.00
54	10.78	10.86	10.83	22.14	33.25	45.13	58.30	72.75	281.48	1.81	1648.77
55	2.67	12.87	13.33	28.86	45.60	62.92	81.62	100.18	266.06	2.28	375.65
56	0.00	0.00	0.00	0.00	0.00	0.00	0.00	0.00	0.00	4.68	1134.06
57	0.00	0.00	0.00	0.00	0.00	0.00	0.00	0.00	0.00	2.95	2168.06
58	0.00	0.00	0.00	0.00	0.00	0.00	0.00	0.00	0.00	2.48	0.00
59	0.00	0.00	0.00	0.00	0.00	0.00	0.00	0.00	0.00	1.91	0.00
60	0.00	0.00	0.00	0.00	0.00	0.00	0.00	0.00	0.00	2.97	375.65

61	0.00	0.00	0.00	0.00	0.00	0.00	0.00	0.00	0.00	4.19	2168.06

Table 15. Significant (α = 0.05) correlations between all storm metrics.

	Max. amp. (˚C)	Dist of diss (m)	Ant flow (L/s)	Flow diff (L/s)	Mean flow (L/s)	Mean flow 1st hr (L/s)	Max flow (L/s)	Max flow ch (L/s)	Flow dur. (min.)	Flow AUC	Flow %	Max precip 5 min. (in.)
Max. amp. (˚C)	1	0.65	0	0.43	0	0	0.39	0.45	0	0	0.41	0
Dist of diss (m)		1	0	0.61	0.52	0	0.56	0.59	0	0	0.74	0.62
Ant flow (L/s)			1	0	0	0	0	0	0	0	0	0
Flow diff (L/s)				1	0.8	0.62	0.99	0.95	0	0.65	0.8	0.7
Mean flow (L/s)					1	0	0.84	0.64	-0.39	0	0.77	0.77
Mean flow 1st hr (L/s)						1	0.62	0.71	0.51	0.9	0	0
Max flow (L/s)							1	0.94	0	0.66	0.77	0.7
Max flow ch (L/s)								1	0	0.69	0.77	0.61
Flow dur. (min.)									1	0.55	0	-0.46
Flow AUC										1	0	0
Flow %											1	0.78
Max precip 5 min. (in.)												1

Table 15, cont.

	Total precip (in.)	Mean precip (in. / min)	Max precip rate (in / hr)	Precip 1st hr (in.)	Air 30 min. (°C)	Air 60 min. (°C)	Air 120 min. (°C)	Air DH tot.	Air DH 2 hr	Air DH 3 hr	Air DH 4 hr	Air DH 5 hr	Air DH 6 hr
Max. amp. (°C)	0.4	0.44	0.48	0.45	0.43	0.45	0.46	0.45	0.5	0.49	0.48	0.47	0.45
Dist of diss (m)	0.79	0.56	0.77	0.6	0.59	0.61	0.62	0.46	0.63	0.62	0.61	0.6	0.59
Ant flow (L/s)	0	0	0	0	0	0	0	0	0	0	0	0	0
Flow diff (L/s)	0.75	0.63	0.79	0.69	0.42	0.43	0.44	0.33	0.46	0.45	0.45	0.44	0.43
Mean flow (L/s)	0.73	0.72	0.82	0.8	0.5	0.52	0.53	0.43	0.56	0.55	0.54	0.53	0.52
Mean flow 1st hr (L/s)	0	0	0	0	0	0	0	0	0	0	0	0	0
Max flow (L/s)	0.71	0.61	0.77	0.68	0.44	0.45	0.46	0.35	0.48	0.47	0.46	0.45	0.44
Max flow ch (L/s)	0.68	0.54	0.7	0.61	0.35	0.36	0.37	0	0.39	0.38	0.37	0.37	0.36
Flow dur. (min.)	0	-0.44	-0.39	-0.46	-0.54	-0.54	-0.54	-0.36	-0.53	-0.53	-0.53	-0.53	-0.53
Flow AUC	0	0	0	0	0	0	0	0	0	0	0	0	0
Flow %	0.85	0.81	0.9	0.87	0.45	0.47	0.49	0.35	0.52	0.51	0.5	0.49	0.48
Max precip 5 min. (in.)	0.73	0.79	0.88	0.85	0.6	0.6	0.6	0	0.6	0.59	0.58	0.58	0.58
Total precip (in.)	1	0.7	0.92	0.78	0.45	0.47	0.49	0	0.52	0.51	0.51	0.5	0.49
Mean precip (in. / min)		1	0.89	0.92	0.47	0.48	0.5	0.37	0.54	0.53	0.52	0.51	0.51
Max precip rate (in			1	0.94	0.59	0.61	0.62	0.41	0.65	0.64	0.63	0.62	0.61

/ hr)													
Precip 1st hr (in.)				1	0.49	0.51	0.42	0	0.55	0.54	0.53	0.52	0.5
Air 30 min. (˚C)					1	0.99	0.97	0.83	0.99	0.99	0.98	0.98	0.98
Air 60 min. (˚C)						1	1	0.86	1	0.99	0.99	0.99	0.99
Air 120 min. (˚C)							1	0.84	0.99	0.99	0.99	0.99	0.99
Air DH total								1	0.86	0.86	0.86	0.86	0.86
Air DH 2 hr									1	1	1	0.99	0.99
Air DH 3 hr										1	1	1	1
Air DH 4 hr											1	1	1
Air DH 5 hr												1	1
Air DH 6 hr													1

Appendix B

Table 16. Landcover metrics for all re-delineated sewersheds in study.

Site	Largest patch index (%)	Mean patch size (km^2)	Develop-ment aggrega-tion	Correl-ation length	Pipe density (m pipe km^{-2})	Pipe-stream ratio (m pipe / m stream)	Pipe-stream intersection density (km^{-2})	Mean pipe length (km)	Max pipe length (km)
dc_gc	26.97	0.10	0.92	283.98	8.83	6.38	36.29	0.02	0.18
dc_mt	0.66	0.04	0.91	63.94	0.00	0.00	0.00	0.00	0.00
dc_pb	1.05	0.03	0.92	33.70	0.03	0.01	5.56	0.00	0.00
dc_rb	19.82	0.21	0.94	290.89	6.04	1.49	24.31	0.02	0.10
dc014	3.20	0.03	0.92	85.02	2.22	0.33	13.57	0.02	0.13
dc021	16.42	0.04	0.91	164.11	5.62	2.16	14.38	0.02	0.10
dc025	8.86	0.03	0.92	126.60	5.07	2.27	12.12	0.02	0.11
dc038	3.46	0.02	0.90	81.40	2.86	0.54	23.13	0.02	0.10
dc043	4.56	0.03	0.93	106.71	4.38	0.72	18.43	0.02	0.13
dc044	32.70	0.07	0.95	416.96	6.86	1.92	14.97	0.03	0.13
dc051	7.51	0.02	0.91	134.28	3.89	0.97	18.83	0.02	0.13
dc064	8.65	0.02	0.92	101.39	5.46	1.09	24.57	0.02	0.08
dc118	14.85	0.11	0.92	248.54	7.54	1.39	21.63	0.02	0.13
dc123	11.19	0.09	0.94	142.93	8.14	2.27	20.79	0.03	0.12
dc127	7.37	0.07	0.94	97.09	7.30	1.70	28.11	0.02	0.14
dc134	27.40	0.15	0.95	282.51	6.55	1.87	20.78	0.03	0.13
dc143	11.63	0.30	0.96	201.99	5.76	1.33	17.29	0.03	0.14
dc148	5.48	0.06	0.91	58.35	4.47	1.85	28.25	0.03	0.16
dc157	2.26	0.10	0.93	39.04	3.55	0.61	10.84	0.03	0.14
dc175	13.46	0.10	0.93	317.28	5.75	1.58	15.17	0.02	0.12

Site	Distance to nearest upstream pipe-stream intersection (m)	Propor-tion canopy closure	Mean incision	Mean width (m)	Propor-tion develo-pment in 1985	Propor-tion develo-pment in 1995	Propor-tion develo-pment in 2005	Proportion impervious in 2006
dc_gc	6	0.7	0.62	0.55	0.93	0.95	0.82	0.39
dc_mt	1017.7	1	0.44	2.18	0.03	0.03	0.04	0.01
dc_pb	438.6	1	0.32	0.42	0	0.02	0.03	0.01
dc_rb	85.7	1	0.63	1.01	0.37	0.51	0.59	0.35
dc014	643.2	1	0.33	0.18	0.26	0.55	0.58	0.17
dc021	366.7	0.85	0.26	1.55	0.04	0.26	0.57	0.17
dc025	59.6	0.9	0.57	2.08	0.61	0.69	0.59	0.18
dc038	42.9	0.85	0.23	2.51	0.26	0.62	0.47	0.17
dc043	200.6	1	0.38	1.24	0.34	0.52	0.51	0.21
dc044	372.4	1	0.36	1.20	0.35	0.4	0.5	0.36
dc051	54.6	1	0.31	3.82	0.56	0.49	0.51	0.17
dc064	292.7	0.95	0.37	1.33	0.38	0.49	0.5	0.15
dc118	273.9	1	0.53	1.19	0.19	0.52	0.55	0.17
dc123	78.7	0.95	0.92	0.66	0.4	0.54	0.51	0.22
dc127	9.5	0.95	0.88	0.30	0.65	0.57	0.52	0.24
dc134	66.1	0.95	0.88	0.30	0.68	0.54	0.52	0.25
dc143	24.3	0.95	0.41	1.81	0.21	0.34	0.5	0.28
dc148	13.8	0.9	0.24	3.71	0.32	0.26	0.51	0.09
dc157	177.6	0.9	0.32	0.79	0.62	0.59	0.42	0.14
dc175	5.7	0.8	0.84	0.48	0.28	0.49	0.47	0.15

Site	Proportion building impervious (1 m)	Proportion impervious (1 m)	Proportion development present in 2005 that was present in 1985	Proportion development in 2005 that has occurred since 1985	Road density (m road km^{-2})	Traffic volume effects
dc_gc	0.18	0.43	1	0	1.46	1202700
dc_mt	0.01	0.04	0.34	0.01	2.54	192484
dc_pb	0.01	0.03	1	0.03	1.01	790
dc_rb	0.09	0.34	0.38	0.23	2.17	3202000
dc014	0.07	0.24	0.55	0.32	2.66	2951800
dc021	0.05	0.22	0.93	0.53	0.46	108000
dc025	0.05	0.19	1	0	1.93	2198900
dc038	0.06	0.22	0.45	0.22	0.82	437100
dc043	0.08	0.29	0.33	0.17	1.09	235100
dc044	0.12	0.41	0.3	0.15	2.79	5188600
dc051	0.07	0.21	1	0	2.13	1386300
dc064	0.06	0.24	0.24	0.12	0.73	1026140
dc118	0.11	0.28	0.66	0.36	2.02	771724
dc123	0.07	0.21	0.22	0.11	1.43	1451000
dc127	0.09	0.25	0	1	0.60	52000
dc134	0.1	0.37	1	0	1.38	3174000
dc143	0.08	0.31	0.58	0.29	2.40	1322730
dc148	0.09	0.22	0.37	0.19	0.00	0
dc157	0.07	0.2	1	0	2.24	575900
dc175	0.06	0.21	0.4	0.19	1.00	3485000

Site	Proportion transportation impervious (1 m)	Proportion forest in 2005	Proportion coarse vegetation (1 m)	Proportion fine vegetation (1 m)	Proportion vegetation (1 m)	Mean inverse-distance weighted development connect to stream by pipes	Mean development within 50 ft of stream
dc_gc	0.24	0.06	0.28	0.27	0.55	0.83	0.58
dc_mt	0.02	0.82	0.85	0.11	0.96	0.03	0
dc_pb	0.02	0.93	0.85	0.11	0.97	0.02	0
dc_rb	0.25	0.02	0.34	0.29	0.63	0.58	0.55
dc014	0.18	0.31	0.56	0.18	0.75	0.54	0.54
dc021	0.16	0.35	0.59	0.18	0.77	0.51	0.41
dc025	0.14	0.35	0.71	0.1	0.81	0.51	0.64
dc038	0.16	0.26	0.58	0.19	0.78	0.43	0.28
dc043	0.21	0.31	0.49	0.19	0.68	0.47	0.35
dc044	0.29	0.26	0.38	0.17	0.55	0.46	0.3
dc051	0.15	0.48	0.64	0.14	0.78	0.48	0.38
dc064	0.18	0.49	0.66	0.1	0.76	0.44	0.28
dc118	0.17	0.4	0.5	0.17	0.67	0.5	0.33
dc123	0.14	0.42	0.62	0.16	0.78	0.42	0.32
dc127	0.16	0.33	0.55	0.19	0.74	0.51	0.25
dc134	0.27	0.41	0.5	0.11	0.61	0.48	0.23
dc143	0.23	0.32	0.49	0.19	0.67	0.46	0.39
dc148	0.13	0.39	0.53	0.21	0.75	0.49	0.29
dc157	0.13	0.51	0.69	0.1	0.79	0.39	0.39
dc175	0.15	0.34	0.59	0.16	0.75	0.42	0.31

Table 17. Differing slopes ($\beta_{1,j}$) at each site between amplitude and air temperature.

Site	Magnitude of heat transfer: slope of amplitude regressed on air temperature
dc014	0.10
dc021	0.15
dc038	0.13
dc043	0.11
dc044	0.11
dc051	0.12
dc064	0.11
dc118	0.10
dc123	0.11
dc127	0.12
dc134	0.11
dc143	0.10
dc148	0.10
dc157	0.15
dc175	0.11

Table 18. Explanatory power and significance of simple hierarchical models, exploring the ability of a given landcover metric to explain variability in the relationship between air temperature and positive amplitude. All *P*-values < 0.001.

Landcover metric	R^2 of amplitude	R^2 of magnitude of heat transfer	Coefficient	Coefficient: lower 90th percentile	Coefficient: upper 90th percentile	Sign
Mean patch size (km^2)	0.23	0.00	0.00	-0.35	0.35	overlaps 0
% Development in 1995	0.23	0.00	0.00	-0.23	0.23	overlaps 0
Distance to nearest upstream pipe-stream intersection (m)	0.23	0.00	0.00	0.00	0.00	overlaps 0
% Vegetation (1 m)	0.23	0.01	-0.02	-0.41	0.38	overlaps 0
% Building impervious (1 m)	0.23	0.02	-0.12	-1.42	1.17	overlaps 0
% Canopy closure	0.23	0.10	-0.08	-0.47	0.30	overlaps 0
% Impervious (1 m)	0.23	0.13	0.13	-0.33	0.58	overlaps 0
Mean incision	0.23	0.22	0.04	-0.06	0.15	overlaps 0
Mean width (m)	0.23	0.28	-0.01	-0.04	0.02	overlaps 0
Road density (m road km^{-2})	0.23	0.28	0.00	-0.03	0.04	overlaps 0
% Development in 2005 that has occurred since 1985	0.23	0.29	-0.07	-0.22	0.09	overlaps 0
% Coarse vegetation (1 m)	0.22	0.31	0.10	-0.23	0.44	overlaps 0
Pipe density (m pipe km^{-2})	0.24	0.33	0.01	-0.01	0.03	overlaps 0
Mean pipe length (km)	0.23	0.38	4.97	-6.35	16.29	overlaps 0
% Transportation impervious (1 m)	0.23	0.49	0.11	-0.41	0.63	overlaps 0
Mean development within 50 ft of stream	0.23	0.49	-0.26	-0.72	0.19	overlaps 0
% Development in 2005	0.23	0.50	-0.15	-0.69	0.39	overlaps 0
% Development in 1985	0.23	0.52	0.08	-0.05	0.21	overlaps 0
Pipe-stream ratio (m pipe / m stream)	0.24	0.56	0.04	-0.01	0.08	overlaps 0
Largest patch index (%)	0.24	0.59	0.00	0.00	0.01	overlaps 0
Correlation length	0.23	0.61	0.00	0.00	0.00	overlaps 0
% Forest in 2005	0.23	0.64	0.10	-0.22	0.43	overlaps 0
Mean inverse-distance weighted development connect to stream by pipes	0.23	0.66	-0.20	-0.78	0.38	overlaps 0
Development aggregation	0.23	0.69	0.54	-0.99	2.07	overlaps 0
Pipe-stream intersection density (km^{-2})	0.22	0.72	0.00	-0.01	0.00	overlaps 0
% Fine vegetation (1 m)	0.23	0.84	-0.62	-1.39	0.15	overlaps 0
Traffic volume effects	0.23	0.88	0.00	0.00	0.00	overlaps 0
% Impervious in 2006	0.23	0.94	0.34	-0.07	0.75	overlaps 0
% Development present in 2005 that was present in 1985	0.23	0.95	0.07	-0.02	0.15	overlaps 0

Table 19. Differing slopes ($\beta_{1,j}$) at each site between amplitude and flow intensity.

Site	Magnitude of heat transfer: slope of amplitude regressed on flow intensity
dc014	0.85
dc021	3.72
dc038	2.36
dc043	2.10
dc044	2.02
dc051	1.91
dc064	1.59
dc118	0.75
dc123	1.28
dc127	0.91
dc134	0.76
dc143	0.55
dc148	0.73
dc157	4.30
dc175	2.87

Table 20. Explanatory power and significance of simple hierarchical models, exploring the ability of a given landcover metric to explain variability in the relationship between flow intensity and positive amplitude. All *P*-values < 0.001.

Landcover metric	R^2 of amplitude	R^2 of magnitude of heat transfer	Co-efficient	Co-efficient: lower 90th percentile	Co-efficient: upper 90th percentile	Sign
Road density (m road km^{-2})	0.18	0.00	-0.06	-1.07	0.96	overlaps 0
% Development in 1995	0.18	0.00	-0.68	-7.61	6.25	overlaps 0
Traffic volume effects	0.18	0.00	0.00	0.00	0.00	overlaps 0
Pipe density (m pipe km^{-2})	0.18	0.01	0.06	-0.47	0.59	overlaps 0
% Vegetation (1 m)	0.18	0.01	1.79	-12.85	16.43	overlaps 0
% Impervious (1 m)	0.18	0.02	-2.82	-18.82	13.19	overlaps 0
% Transportation impervious (1 m)	0.18	0.03	-4.56	-22.82	13.69	overlaps 0
% Impervious in 2006	0.18	0.03	-3.43	-18.20	11.33	overlaps 0
% Development in 1985	0.18	0.04	-1.30	-5.17	2.56	overlaps 0
Mean development within 50 ft of stream	0.18	0.05	3.51	-7.00	14.02	overlaps 0
Mean inverse-distance weighted development connect to stream by pipes	0.18	0.06	-6.40	-29.48	16.68	overlaps 0
Mean width (m)	0.18	0.08	-0.33	-1.11	0.44	overlaps 0
Pipe-stream ratio (m pipe / m stream)	0.18	0.09	0.58	-0.93	2.08	overlaps 0
Mean incision	0.18	0.10	-1.49	-4.54	1.55	overlaps 0
% Development in 2005 that has occurred since 1985	0.18	0.10	2.37	-2.19	6.92	overlaps 0
% Development in 2005	0.18	0.11	7.69	-16.25	31.64	overlaps 0
% Development present in 2005 that was present in 1985	0.18	0.11	1.33	-1.54	4.19	overlaps 0
% Forest in 2005	0.18	0.12	5.26	-9.31	19.83	overlaps 0
Development aggregation	0.18	0.13	-24.44	-70.37	21.49	overlaps 0
Correlation length	0.19	0.15	0.01	-0.01	0.02	overlaps 0
% Building impervious (1 m)	0.18	0.16	-24.42	-72.31	23.48	overlaps 0
Largest patch index (%)	0.19	0.17	0.07	-0.05	0.19	overlaps 0
Mean patch size (km^2)	0.18	0.18	-6.64	-15.71	2.43	overlaps 0
% Fine vegetation (1 m)	0.18	0.22	-17.57	-43.79	8.65	overlaps 0
% Coarse vegetation (1 m)	0.18	0.23	6.90	-7.04	20.83	overlaps 0
Mean pipe length (km)	0.19	0.31	380.71	-157.30	918.72	overlaps 0
% Canopy closure	0.18	0.43	-12.81	-28.96	3.34	overlaps 0
Pipe-stream intersection density (km^{-2})	0.18	0.50	-0.17	-0.32	-0.03	negative
Distance to nearest upstream pipe-stream intersection (m)	0.19	0.55	0.01	0.00	0.01	positive

Table 21. Differing slopes ($\beta_{1,j}$) at each site between heat pulse intensity and air temperature.

Site	Rate of heat transfer: slope of heat pulse intensity regressed on air temperature
dc014	0.12
dc021	0.10
dc038	0.12
dc043	0.08
dc044	0.13
dc051	0.11
dc064	0.12
dc118	0.13
dc123	0.12
dc127	0.13
dc134	0.13
dc143	0.10
dc148	0.13
dc157	0.10
dc175	0.11

Table 22. Explanatory power and significance of simple hierarchical models, exploring the ability of a given landcover metric to explain variability in the relationship between air temperature and maximum thermal increase. All *P*-values < 0.001.

Landcover metric	R^2 of heat pulse intensity	R^2 of rate of heat transfer	Co-efficient	Co-efficient: lower 90th percentile	Co-efficient: upper 90th percentile	Sign
% Development in 2005	0.23	0.01	-0.07	-0.81	0.68	overlaps 0
Mean inverse-distance weighted development connect to stream by pipes	0.23	0.02	0.06	-0.69	0.82	overlaps 0
Mean pipe length (km)	0.23	0.02	1.13	-11.85	14.10	overlaps 0
% Canopy closure	0.23	0.02	-0.05	-0.48	0.38	overlaps 0
% Transportation impervious (1 m)	0.23	0.02	-0.06	-0.66	0.55	overlaps 0
% Coarse vegetation (1 m)	0.23	0.03	-0.04	-0.41	0.34	overlaps 0
% Impervious in 2006	0.22	0.04	-0.05	-0.53	0.42	overlaps 0
Development aggregation	0.23	0.07	-0.30	-2.13	1.52	overlaps 0
Mean width (m)	0.23	0.09	0.00	-0.03	0.02	overlaps 0
% Development present in 2005 that was present in 1985	0.23	0.11	0.02	-0.08	0.13	overlaps 0
% Vegetation (1 m)	0.23	0.13	-0.09	-0.51	0.33	overlaps 0
% Impervious (1 m)	0.23	0.14	0.10	-0.37	0.57	overlaps 0
Mean patch size (km^2)	0.23	0.19	-0.12	-0.50	0.25	overlaps 0
% Forest in 2005	0.23	0.21	0.12	-0.26	0.50	overlaps 0
Distance to nearest upstream pipe-stream intersection (m)	0.23	0.23	0.00	0.00	0.00	overlaps 0
Road density (m road km^{-2})	0.23	0.25	-0.01	-0.05	0.03	overlaps 0
Correlation length	0.23	0.45	0.00	0.00	0.00	overlaps 0
% Development in 2005 that has occurred since 1985	0.23	0.47	-0.13	-0.32	0.06	overlaps 0
% Fine vegetation (1 m)	0.22	0.52	-0.60	-1.44	0.25	overlaps 0
% Development in 1985	0.23	0.55	0.13	-0.02	0.28	overlaps 0
% Development in 1995	0.22	0.61	0.16	-0.08	0.41	overlaps 0
Pipe-stream ratio (m pipe / m stream)	0.23	0.61	0.03	-0.02	0.08	overlaps 0
Traffic volume effects	0.23	0.64	0.00	0.00	0.00	overlaps 0
Mean incision	0.23	0.77	0.08	-0.03	0.19	overlaps 0
% Building impervious (1 m)	0.23	0.86	1.18	-0.12	2.47	overlaps 0
Largest patch index (%)	0.22	0.89	0.00	0.00	0.01	overlaps 0
Pipe density (m pipe km^{-2})	0.21	0.92	0.01	0.00	0.03	overlaps 0
Pipe-stream intersection density (km^{-2})	0.22	0.93	0.01	0.00	0.01	positive
Mean development within 50 ft of stream	0.23	1.00	-0.73	-1.15	-0.31	negative

Table 23. Differing slopes ($\beta_{1,j}$) at each site between thermal change intensity and antecedent flow.

Site	Rate of heat transfer: slope of heat pulse intensity regressed on antecedent flow
dc014	-0.18
dc021	-0.58
dc038	-0.56
dc043	-0.64
dc044	-0.27
dc051	-0.64
dc064	-0.43
dc118	-0.42
dc123	-0.19
dc127	-0.63
dc134	-0.41
dc143	-0.36
dc148	-0.65
dc157	-1.10
dc175	-0.57

Table 24. Explanatory power and significance of simple hierarchical models, exploring the ability of a given landcover metric to explain variability in the relationship between antecedent flow and maximum thermal increase. All *P*-values < 0.001.

Landcover metric	R^2 of heat pulse intensity	R^2 of rate of heat transfer	Co-efficient	Co-efficient: lower 90th percentile	Co-efficient: upper 90th percentile	Sign
Mean pipe length (km)	0.11	0.00	1.64	-284.53	287.81	overlaps 0
Mean patch size (km^2)	0.15	0.05	6.14	-14.14	26.41	overlaps 0
Mean development within 50 ft of stream	0.11	0.08	0.99	-4.61	6.58	overlaps 0
Road density (m road km^{-2})	0.15	0.18	-0.90	-2.49	0.69	overlaps 0
Development aggregation	0.11	0.19	8.34	-13.51	30.19	overlaps 0
Pipe-stream intersection density (km^{-2})	0.15	0.23	0.16	-0.10	0.42	overlaps 0
Mean width (m)	0.11	0.26	-0.13	-0.48	0.22	overlaps 0
Distance to nearest upstream pipe-stream intersection (m)	0.11	0.31	0.00	0.00	0.00	overlaps 0
% Development in 1995	0.15	0.33	-10.07	-22.39	2.26	overlaps 0
Mean incision	0.11	0.33	0.64	-0.96	2.23	overlaps 0
% Building impervious (1 m)	0.11	0.42	14.23	-14.00	42.46	overlaps 0
Traffic volume effects	0.11	0.46	0.00	0.00	0.00	overlaps 0
% Development in 2005 that has occurred since 1985	0.16	0.50	10.28	0.68	19.87	positive
% Forest in 2005	0.11	0.52	-2.93	-9.57	3.71	overlaps 0
Pipe density (m pipe km^{-2})	0.15	0.53	0.67	-0.08	1.42	overlaps 0
% Canopy closure	0.11	0.53	4.10	-4.43	12.62	overlaps 0
% Transportation impervious (1 m)	0.11	0.62	5.24	-2.15	12.63	overlaps 0
% Impervious in 2006	0.11	0.62	3.63	-1.47	8.73	overlaps 0
% Development present in 2005 that was present in 1985	0.11	0.65	-0.73	-2.24	0.78	overlaps 0
% Fine vegetation (1 m)	0.11	0.66	7.30	-4.77	19.37	overlaps 0
% Development in 1985	0.11	0.79	-1.47	-3.19	0.25	overlaps 0
Correlation length	0.11	0.82	0.00	0.00	0.01	overlaps 0
% Impervious (1 m)	0.11	0.82	5.51	-1.68	12.71	overlaps 0
Mean inverse-distance weighted development connect to stream by pipes	0.14	0.84	45.42	18.64	72.19	positive
Pipe-stream ratio (m pipe / m stream)	0.14	0.86	2.63	0.73	4.53	positive
Largest patch index (%)	0.11	0.86	0.04	-0.01	0.09	overlaps 0
% Vegetation (1 m)	0.11	0.90	-6.06	-13.06	0.94	overlaps 0
% Development in 2005	0.14	0.92	52.30	24.56	80.05	positive
% Coarse vegetation (1 m)	0.11	0.99	-10.93	-19.94	-1.93	negative

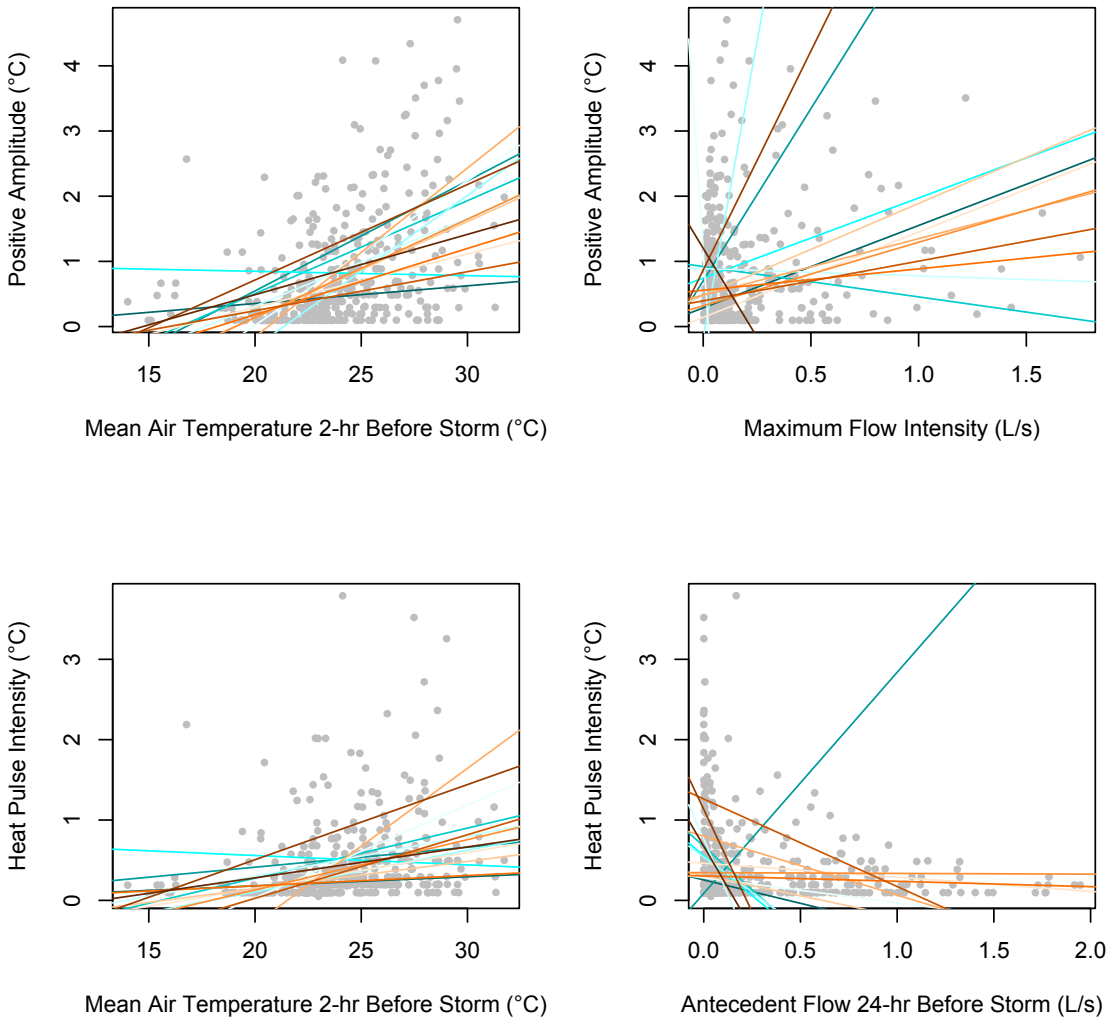

Figure 29. Variation in relationships between air and flow metrics and positive amplitude and thermal change intensity across all sites (points in grey) and within each site (colored lines).

References

Allen, J. 1995. Stream ecology: Structure and function of running waters. Page 388. . Chapman & Hall, New York.

Arbuckle, J. L. 2007. Amos 16.0 User's Guide. . SPSS Inc.

Arnold, C. L., and C. J. Gibbons. 1996. Impervious surface coverage - The emergence of a key environmental indicator. Journal of the American Planning Association 62:243–258.

Asaeda, T., V. Ca, and A. Wake. 1996. Heat storage of pavement and its effect on the lower atmosphere. Atmospheric environment 30:413–427.

Barrett, M. 2008. Comparison of BMP performance using the International BMP Database. Journal of Irrigation and Drainage Engineering:556–561.

Bates, D., M. Maechler, and B. Bolker. 2012. lme4: Linear mixed-effects models using S4 classes.

Beaulieu, J., J. Tank, S. K. Hamilton, W. Wollheim, R. Hall, P. J. Mulholland, B. J. Peterson, L. R. Ashkenas, L. W. Cooper, C. N. Dahm, W. K. Dodds, N. B. Grimm, S. L. Johnson, W. H. Mcdowell, G. C. Poole, H. M. Valett, C. P. Arango, M. J. Bernot, A. J. Burgin, C. L. Crenshaw, A. M. Helton, L. T. Johnson, J. M. O'Brien, J. D. Potter, R. W. Sheibley, D. J. Sobota, and S. M. Thomas. 2011. Nitrous oxide emission from denitrification in stream and river networks. Proceedings of the National Academy of Sciences of the United States of America.

Beck, S., M. McHale, and G. Hess. (n.d.). Beyond Impervious: Urban Landcover Pattern Variation and Implications for Water Quality.

Beitinger, T. L., W. A. Bennett, and R. W. McCauley. 2000a. Temperature tolerances of North American freshwater fishes exposed to dynamic changes in temperature. Environmental Biology of Fishes 58:237–275.

Beitinger, T. L., W. A. Bennett, and R. W. McCauley. 2000b. Temperature tolerances of North American freshwater fishes exposed to dynamic changes in temperature. Environmental Biology of Fishes 58:237–275.

Berdahl, P., and S. Bretz. 1997. Preliminary survey of the solar reflectance of cool roofing materials. Energy and Buildings 25:149–158.

Bernhardt, E. S., L. E. Band, C. J. Walsh, and P. E. Berke. 2008. Understanding, managing, and minimizing urban impacts on surface water nitrogen loading. Year in Ecology and Conservation Biology 2008 1134:61–96.

Bernhardt, E. S., and M. A. Palmer. 2007. Restoring streams in an urbanizing world. Freshwater Biology 52:738–751.

Bernhardt, E. S., E. B. Sudduth, M. A. Palmer, J. D. Allan, J. L. Meyer, G. Alexander, J. Follastad-Shah, B. Hassett, R. Jenkinson, R. Lave, J. Rumps, and L. Pagano. 2007. Restoring rivers one reach at a time: Results from a survey of US river restoration practitioners. Restoration Ecology 15:482–493.

Bernot, M. J., D. J. Sobota, R. O. Hall, P. J. Mulholland, W. K. Dodds, J. R. Webster, J. L. Tank, L. R. Ashkenas, L. W. Cooper, C. N. Dahm, S. V. Gregory, N. B. Grimm, S. K. Hamilton, S. L. Johnson, W. H. Mcdowell, J. L. Meyer, B. Peterson, G. C. Poole, H. M. Valett, C. Arango, J. J. Beaulieu, A. J. Burgin, C. Crenshaw, A. M. Helton, L. Johnson, J. Merriam, B. R. Niederlehner, J. M. O'Brien, J. D. Potter, R. W. Sheibley, S. M. Thomas, and K. Wilson. 2010. Inter-regional comparison of land-use effects on stream metabolism. Freshwater Biology 55:1874–1890.

Bernstein, L., P. Bosch, O. Canziani, Z. Chen, R. Christ, O. Davidson, W. Hare, D. Karoly, V. Kattsov, Z. Kundzewicz, J. Liu, U. Lohmann, M. Manning, T. Matsuno, B. Menne, B. Metz, M. Mirza, N. Nicholls, L. Nurse, R. Pachauri, J. Palutikof, D. Qin, N. Ravindranath, A. Reisinger, J. Ren, K. Riahi, C. Rosenzweig, S. Schneider, Y. Sokona, S. Solomon, P. Stott, R. Stouffer, T. Sugiyama, R. Swart, D. Tirpak, C. Vogel, and G. Yohe. 2007. Climate Change 2007 : Summary for Policymakers:12–17.

Booth, D. B. 1990. Stream-channel incision following drainage-basin urbanization. Journal of the American Water Resources Association 26:407–417.

Booth, D. B., and C. R. Jackson. 1997. Urbanization of aquatic systems: Degradation thresholds, stormwater detection, and the limits of mitigation. Journal of the American Water Resources Association 33:1077–1090.

Boughton, D. A., C. Hatch, and E. Mora. 2012. Identifying distinct thermal components of a creek. Water Resources Research 48:W09506.

Bowler, K. 1963. A Study of the Factors Involved in Acclimatization to Temperature and Death at High Temperatures in Astacus pallipes. Journal of Cellular and Comparative Physiology 62:119–132.

Branham, J. M., A. R. Gaufin, and R. L. Traver. 1975. Growth of Plecoptera (stonefly) nymphs at constant, abnormally high temperatures. Great Basin Naturalist 35:51–61.

Breiman, L., J. H. Friedman, R. A. Olshen, and C. J. Stone. 1984. Classification and regression trees. . Wadsworth and Brooks/Cole, Monterey, CA.

Van Buren, M. A., W. E. Watt, J. Marsalek, and B. C. Anderson. 2000. Thermal enhancement of stormwater runoff by paved surfaces. Water Research 34:1359–1371.

Caissie, D. 2006. The thermal regime of rivers: a review. Freshwater Biology 51:1389–1406.

Caissie, D., M. G. Satish, and N. El-Jabi. 2007. Predicting water temperatures using a deterministic model: Application on Miramichi River catchments (New Brunswick, Canada). Journal of Hydrology 336:303–315.

Carolli, M., and M. Bruno. 2012. Responses of benthic invertebrates to abrupt changes of temperature in flume simulations 691:678–691.

Chadwick, M., D. Dobberfuhl, A. Benke, A. Huryn, K. Suberkropp, and J. Thiele. 2006. Urbanization affects stream ecosystem function by altering hydrology, chemistry, and biotic richness. Ecological Applications 16:1796–807.

Chae, G.-T., S.-T. Yun, B.-Y. Choi, S.-Y. Yu, H.-Y. Jo, B. Mayer, Y.-J. Kim, and J.-Y. Lee. 2008. Hydrochemistry of urban groundwater, Seoul, Korea: the impact of subway tunnels on groundwater quality. Journal of Contaminant Hydrology 101:42–52.

Chow, V. T. 1959. Open-channel hydraulics. . McGraw-Hill Book Co., New York.

City of Carrboro. 2009. Stormwater Features. . City of Carrboro, Carrboro, NC.

City of Chapel Hill. 2011. Stormwater Features. . City of Chapel Hill, Chapel Hill, NC.

City of Raleigh Public Works. 2009. Raleigh Storm Water Inventory. . City of Raleigh, Raleigh, NC.

Clarke, A., and K. Fraser. 2004. Why does metabolism scale with temperature? Functional Ecology 18:243–251.

Cochran, B., and C. Logue. 2011. A Watershed Approach to Improve Water Quality: Case Study of Clean Water Services' Tualatin River Program1. JAWRA Journal of the American Water Resources Association 47:29–38.

Coutant, C. 1970. Biological Aspects of Thermal Pollution: 1. Entrainment and Discharge Canal Effects. CRC Critical Reviews in Environmental Controls 1:341–381.

Coutant, C. C. 1973. Effect of thermal shock on vulnerability of juvenile salmonids to predation. Journal of the Fisheries Research Board of Canada 30:965–975.

Cuffney, T., R. Brightbill, J. T. May, and I. Waite. 2010. Responses of benthic macroinvertebrates to environmental changes associated with urbanization in nine metropolitan areas. Ecological Applications 20:1384–401.

Deitchman, R., and S. P. Loheide. 2012. Sensitivity of thermal habitat of a trout stream to potential climate change, Wisconsin, United States 48:1091–1103.

Department of Environmental and Natural Resources. 2012. North Carolina Natural Heritage Program.

Diefenderfer, B. 2006. Model to predict pavement temperature profile: Development and validation. Journal of Transportation Engineering 132:162–167.

Dietz, M. E. 2007. Low impact development practices: A review of current research and recommendations for future directions. Water Air and Soil Pollution 186:351–363.

Dunne, T., and L. B. Leopold. 1978. Water in environmental planning., 16th edition. W.H. Freeman and Company, San Francisco, CA.

Durham Storm Water. 2007. Durham Storm Water GIS Layers.

Environmental Systems Research Institute. 2008. ArcGIS. . ESRI, Redlands, California.

Fry, J., G. Xian, S. Jin, J. Dewitz, C. Homer, L. Yang, C. Barnes, N. Herold, and J. Wickham. 2011. Completion of the 2006 National Land Cover Database for the Conterminous United States. Photogrammetric Engineering and Remote Sensing 77:858–864.

Fuka, D., M. Walter, J. Archibald, T. Steenhuis, and Z. Easton. 2012. EcoHydRology v.0.4.5.

Galli, F. J. 1991. Thermal Impacts Associated with Urbanization and Stormwater Management Best Management Practices. . Metropolitan Washington Council of Governments, Washington, D.C.

Gardner, R. H., B. T. Milne, M. G. Turner, and R. V O'Neill. 1987. Neutral models for the analysis of broad-scale land- scape pattern. Landscape Ecology 1:19–28.

Gardner, R. H., and D. L. Urban. 2007. Neutral models for testing landscape hypotheses. Landscape Ecology 22:15–29.

Gelman, A., and J. Hill. 2006. Data Analysis Using Regression and Multilevel/Hierarchical Models. . Cambridge University Press.

Gelman, A., and I. Pardoe. 2006. Bayesian measures of explained variance and pooling in multilevel (hierarchical) models. Technometrics:1–22.

Gibbons, J. W. 1970. Reproductivedynamics of a turtle (Pseudemys scripta) population in a reservoir receiving heated effluent from a nuclear reactor. Candian Journal of Zoology 49:881–885.

Gibbons, J. W., and R. R. Sharitz (Eds.). 1974. Thermal Ecology. Thermal Ecology. . Nat. Tech. Inform. Serv., Oak Ridge, TN.

Goslee, S. C., and D. L. Urban. 2007. The ecodist package for dissimilarity-based analysis of ecological data. Journal of Statistical Software 22:1–19.

Gotelli, N. J., and A. M. Ellison. 2004. A Primer Of Ecological Statistics. . Sinauer Associates.

Grace, J. B. 2006a. Structural Equation Modeling and Natural Systems. . Cambridge University Press, Cambridge.

Grace, J. B. 2006b. SEM and Natural Systems. . Cambridge University Press, Cambridge.

Grace, J. B., T. M. Anderson, H. Olff, and S. M. Scheiner. 2010. On the specification of structural equation models for ecological systems. Ecological Monographs 80:67–87.

Grace, J. B., D. R. Schoolmaster, G. R. Guntenspergen, A. M. Little, B. R. Mitchell, K. Miller, and E. Schweiger. 2012. Guidelines for a graph-theoretic implementation of structural equation modeling. Ecosphere 3.

Grimm, N. B., R. W. Sheibley, and W. J. Roach. 2005. N Retention and Transformation in Urban Streams. Journal of the North American Benthological Society 24:626–642.

Groffman, P. M., D. J. Bain, L. E. Band, K. T. Belt, G. S. Brush, J. M. Grove, R. V Pouyat, I. C. Yesilonis, and W. C. Zipperer. 2003. Down by the riverside: urban riparian ecology. Frontiers in Ecology and the Environment 1:315–321.

Groffman, P. M., N. J. Boulware, W. C. Zipperer, R. V Pouyat, L. E. Band, and M. F. Colosimo. 2002. Soil nitrogen cycle processes in urban Riparian zones. Environmental Science & Technology 36:4547–4552.

Herb, W., O. Mohseni, and H. Stefan. 2009. Simulation of Temperature Mitigation by a Stormwater Detention Pond1. JAWRA Journal of the … 45:1164–1178.

Herb, W. R., B. Janke, O. Mohseni, and H. G. Stefan. 2008. Thermal pollution of streams by runoff from paved surfaces. Hydrological Processes 22:987–999.

Hester, E., and K. Bauman. 2013. Stream and Retention Pond Thermal Response to Heated Summer Runoff From Urban Impervious Surfaces1. Journal of the American Water Resources Association:1–15.

Hester, E. T., and M. W. Doyle. 2011. Human Impacts to River Temperature and their Effects on Biological Processes: A Quantitative Synthesis. Journal of the American Water Resources Association 46:1–17.

Hill, B. H., R. K. Hall, P. Husby, A. T. Herlihy, and M. Dunne. 2000a. Interregional comparisons of sediment microbial respiration in streams. Freshwater Biology 44:213–222.

Hill, B. H., R. K. Hall, P. Husby, A. T. Herlihy, and M. Dunne. 2000b. Interregional comparisons of sediment microbial respiration in streams. Freshwater Biology 44:213–222.

Holmes, R. M., J. B. Jones, S. G. Fisher, and N. B. Grimm. 1996. Denitrification in a nitrogen-limited stream ecosystem. Biogeochemistry 33:125–146.

Homer, C., C. Q. Huang, L. M. Yang, B. Wylie, and M. Coan. 2004. Development of a 2001 National Land-Cover Database for the United States. Photogrammetric Engineering and Remote Sensing 70:829–840.

Hongve, D. A. G. 1987. A revised procedure for discharge measurement by means of the salt dilution method 1:267–270.

Imberger, S. J., C. J. Walsh, and M. R. Grace. 2008. More microbial activity, not abrasive flow or shredder abundance, accelerates breakdown of labile leaf litter in urban streams. Journal of the North American Benthological Society 27:549–561.

Imholt, C., C. Soulsby, I. a. Malcolm, and C. N. Gibbins. 2012. Influence of contrasting riparian forest cover on stream temperature dynamics in salmonid spawning and nursery streams. Ecohydrology:n/a–n/a.

Inwood, S. E., J. L. Tank, and M. J. Bernot. 2005. Patterns of denitrification associated with land use in 9 midwestern headwater streams. Journal of the North American Benthological Society 24:227–245.

Johnson, S. L. 2004. Factors influencing stream temperatures in small streams: substrate effects and a shading experiment. Canadian Journal of Fisheries and Aquatic Sciences 61:913–923.

Jones, J. A., F. J. Swanson, B. C. Wemple, and K. U. Snyder. 2000. Effects of Roads on Hydrology, Geomorphology, and Disturbance Patches in Stream Networks. Conservation Biology 14:76–85.

Jones, K. L., G. C. Poole, J. L. Meyer, W. Bumback, and E. A. Kramer. 2006. Quantifying expected ecological response to natural resource legislation: a case study of riparian buffers, aquatic habitat, and trout populations. Ecology and Society 11:-.

Jones, M., and W. Hunt. 2009. Bioretention impact on runoff temperature in trout sensitive waters. Journal of Environmental Engineering:577–585.

Jones, M., and W. Hunt. 2010. Effect of Storm-Water Wetlands and Wet Ponds on Runoff Temperature in Trout Sensitive Waters. Journal of Irrigation and Drainage …:656–661.

Joreskog, K. G. 1982. The LISREL approach to causal model-building in the social sciences. Pages 81–100 *in* K. G. Joreskog and H. O. Wold, editors. Systems under indirect observation, Part I. . North-Holland, Amsterdam.

Julian, J. P., M. W. Doyle, and E. H. Stanley. 2008. Empirical modeling of light availability in rivers. Journal of Geophysical Research 113:1–16.

Kalnay, E., and M. Cai. 2003. Impact of urbanization and land-use change on climate. Nature 423:528–531.

Kaushal, S. S., and K. T. Belt. 2012. The urban watershed continuum: evolving spatial and temporal dimensions. Urban Ecosystems 15:409–435.

Kaushal, S. S., G. E. Likens, N. A. Jaworski, M. L. Pace, A. M. Sides, D. Seekell, K. T. Belt, D. H. Secor, and R. L. Wingate. 2010. Rising stream and river temperatures in the United States. Frontiers in Ecology and the Environment 8:461–466.

Keitt, T. H., D. L. Urban, and B. T. Milne. 1997. Detecting critical scales in fragmented landscapes. Conservation Ecology 1.

Kelleher, C., T. Wagener, M. Gooseff, B. McGlynn, K. McGuire, and L. Marshall. 2011. Investigating controls on the thermal sensitivity of Pennsylvania streams. Hydrological Processes.

King, R., K. Nunnery, and C. Richardson. 2000. Macroinvertebrate assemblage response to highway crossings in forested wetlands: implications for biological assessment. Wetlands Ecology and …:243–256.

King, R. S., M. E. Baker, D. F. Whigham, D. E. Weller, T. E. Jordan, P. F. Kazyak, and M. K. Hurd. 2005a. Spatial considerations for linking watershed land cover to ecological indicators in streams. Ecological Applications 15:137–153.

King, R. S., M. E. Baker, D. F. Whigham, D. E. Weller, T. E. Jordan, P. F. Kazyak, and M. K. Hurd. 2005b. Spatial considerations for linking watershed land cover to ecological indicators in streams. Ecological Applications 15:137–153.

Kingsolver, J., and R. Huey. 2008. Size, temperature, and fitness: three rules. Evolutionary Ecology Research:251–268.

Kirby, J. T. 2006. Mockingbird song : ecological landscapes of the South. Page xx, 361 p. University of North Carolina Press, Chapel Hill.

Kite, G. 1993. Computerized streamflow measurement using slug injection 7:227–233.

Konrad, C., and D. Booth. 2005. Hydrologic changes in urban streams and their ecological significance. American Fisheries Society Symposium:157–177.

Kratzer, E. B., J. K. Jackson, D. B. Arscott, A. K. Aufdenkampe, C. L. Dow, L. A. Kaplan, J. D. Newbold, and B. W. Sweeney. 2006. Macroinvertebrate distribution in relation to land use and water chemistry in New York City drinking-water-supply watersheds. Journal of the North American Benthological Society 25:954–976.

Krause, C. W., B. Lockard, T. J. Newcomb, D. Kibler, V. Lohani, and D. J. Orth. 2004. Predicting influences of urban development on thermal habitat in a warm water stream. Journal of the American Water Resources Association 40:1645–1658.

Lake, P. S., N. Bond, and P. Reich. 2007. Linking ecological theory with stream restoration. Freshwater Biology 52:597–615.

LeBlanc, R. T., R. D. Brown, and J. E. FitzGibbon. 1997. Modeling the effects of land use change on the water temperature in unregulated urban streams. Journal of Environmental Management 49:445–469.

Lemmon, P. E. 1957. A new instrument for measuring forest overstory density. Journal of Forestry 55:667–669.

Lygren, E., E. Gjessing, and L. Berglind. 1984. Pollution Transport from a Highway. Science of the Total Environment 33:147–159.

Matthews, K., and N. Berg. 1997. Rainbow trout responses to water temperature and dissolved oxygen stress in two southern California stream pools. Journal of Fish Biology:50–67.

Mayer, T., Q. Rochfort, J. Marsalek, J. Parrott, M. Servos, M. Baker, R. McInnis, A. Jurkovic, and I. Scott. 2011. Environmental characterization of surface runoff from three highway sites in Southern Ontario, Canada: 2. Toxicology. Water Quality Research Journal of Canada 46:121–136.

McCullough, D. a., J. M. Bartholow, H. I. Jager, R. L. Beschta, E. F. Cheslak, M. L. Deas, J. L. Ebersole, J. S. Foott, S. L. Johnson, K. R. Marine, M. G. Mesa, J. H. Petersen, Y. Souchon, K. F. Tiffan, and W. a. Wurtsbaugh. 2009a. Research in Thermal Biology: Burning Questions for Coldwater Stream Fishes. Reviews in Fisheries Science 17:90–115.

McCullough, D. A., J. M. Bartholow, H. I. Jager, R. L. Beschta, E. F. Cheslak, M. L. Deas, J. L. Ebersole, J. S. Foott, S. L. Johnson, K. R. Marine, M. G. Mesa, J. H. Petersen, Y. Souchon, K. F. Tiffan, and W. a. Wurtsbaugh. 2009b. Research in Thermal Biology:

Burning Questions for Coldwater Stream Fishes. Reviews in Fisheries Science 17:90–115.

McGarigal, K., S. A. Cushman, M. C. Neel, and E. Ene. 2002. FRAGSTATS: Spatial Pattern Analysis Program for Categorical Maps. . University of Massachusetts, Amherst.

Mesa, M. G., L. K. Weiland, and P. Wagner. 2002. Effects of acute thermal stress on the survival, predator avoidance, and physiology of juvenile fall chinook salmon. Northwest Science 76:118–128.

Meyer, J. L., M. J. Paul, and W. K. Taulbee. 2005. Stream ecosystem function in urbanizing landscapes. Journal of the North American Benthological Society 24:602–612.

Mohseni, O., H. G. Stefan, and T. R. Erickson. 1998. A nonlinear regression model for weekly stream temperatures. Water Resources Research 34:2685–2692.

Moore, A. A., and M. A. Palmer. 2005. Invertebrate biodiversity in agricultural and urban headwater streams: Implications for conservation and management. Ecological Applications 15:1169–1177.

Natarajan, P., and A. P. Davis. 2010. Thermal Reduction by an Underground Storm-Water Detention System. Journal of Environmental Engineering 136:520–526.

Nathan, R., and T. McMahon. 1990. Evaluation of automated techniques for base flow and recession analyses. Water Resources Research 26:1465–1473.

National Agriculture Imagery Program (NAIP). 2008. NAIP Imagery. . U.S. Department of Agriculture, Farm Service Agency.

Nebeker, A., and A. Lemke. 1968. Preliminary Studies on the Tolerance of Aquatic Insects to Heated Waters. Journal of Kansas Entomological Society 41:413–418.

Nelson, K. C., and M. A. Palmer. 2007. Stream temperature surges under urbanization and climate change: Data, models, and responses. Journal of the American Water Resources Association 43:440–452.

North Carolina Department of Environment and Natural Resources. 1999. Riparian Buffer Protection Rules for the Neuse and Tar-Pamlico River Basins 1:6–7.

North Carolina Department of Transportation. 2007. NCDOT GIS Data Layers.

North Carolina Department of Transportation. 2009. NCDOT GIS Data Layers.

Oke, T. 1973. City size and the urban heat island. Atmospheric Environment 7:769–779.

Oke, T. R., J. M. Crowther, K. G. McNaughton, J. L. Monteith, and B. Gardiner. 1989. The Micrometeorology of the Urban Forest [and Discussion]. Philosophical Transactions of the Royal Society B: Biological Sciences 324:335–349.

Olden, J. D., and R. J. Naiman. 2010. Incorporating thermal regimes into environmental flows assessments: modifying dam operations to restore freshwater ecosystem integrity. Freshwater Biology 55:86–107.

Paul, M. J., and J. L. Meyer. 2001. Streams in the urban landscape. Annual Review of Ecology and Systematics 32:333–365.

Pickett, S. T. A., M. L. Cadenasso, J. M. Grove, C. H. Nilon, R. V Pouyat, W. C. Zipperer, and R. Costanza. 2001. Urban ecological systems: Linking terrestrial ecological, physical, and socioeconomic components of metropolitan areas. Annual Review of Ecology and Systematics 32:127–157.

Pluhowski, E. 1970. Urbanization and its effects on the temperature of the streams on Long Island, New York. Geological Survey professional paper.

Poole, G. C., and C. H. Berman. 2001. An ecological perspective on in-stream temperature: Natural heat dynamics and mechanisms of human-caused thermal degradation. Environmental Management 27:787–802.

Population Reference Bureau. 2012. Population Data Sheet:1–20.

Qian, S., T. Cuffney, and I. Alameddine. 2010. On the application of multilevel modeling in environmental and ecological studies. Ecology 91:355–361.

R Development Core Team. 2008a. R: A language and environment for statistical computing. R Foundation for Statistical Computing, Vienna, Austria.

R Development Core Team. 2008b. R: A language and environment for statistical computing. R Foundation for Statistical Computing, Vienna, Austria.

Reckhow, K. H., S. S. Qian, and R. D. Harmel. 2009. A Multilevel Model of the Impact of Farm-Level Best Management Practices on Phosphorus Runoff. JAWRA Journal of the American Water Resources Association 45:369–377.

Ripley, B. 2009. tree: Classification and regression trees.

Roltsch, W., F. Zalom, and A. Strawn. 1999. Evaluation of several degree-day estimation methods in California climates. International Journal of … 42:169–176.

Roy, a. H., M. C. Freeman, B. J. Freeman, S. J. Wenger, W. E. Ensign, and J. L. Meyer. 2005. Investigating hydrologic alteration as a mechanism of fish assemblage shifts in urbanizing streams. Journal of the North American Benthological Society 24:656.

Roy, A. H., A. L. Dybas, K. M. Fritz, and H. R. Lubbers. 2009. Urbanization affects the extent and hydrologic permanence of headwater streams in a midwestern US metropolitan area. Journal of the North American Benthological Society 28:911–928.

Saaroni, H., E. Ben-Dor, A. Bitan, and O. Potchter. 2000. Spatial distribution and microscale characteristics of the urban heat island in Tel-Aviv, Israel. Landscape and Urban Planning 48:1–18.

Salmela, J. A., and R. L. Anderson. 1978. Thermal shock effects on larvae of caddis fly Brachycentrus americanus. The Journal of the Minnesota Academy of Science 44:25–27.

Seto, K. C., M. Fragkias, and B. Gu. 2011. A Meta-Analysis of Global Urban Land Expansion 6.

Sevacherian, V., V. M. Stern, and A. J. Mueller. 1977. Heat Accumulation for Timing Lygus (Hemiptera-(Heteroptera)-Miridae) Control Measures in a Safflower-Cotton Complex. Journal of Economic Entomology 70:399–402.

Sexton, J. O., D. L. Urban, M. J. Donohue, and C. Song. 2013. Landcover dynamics by multi-temporal classification across the Landsat-5 record. Remote Sensing of Environment 128:246–258.

Sherberger, F. F., E. F. Benfield, K. L. Dickson, and J. Cairns J. 1977. Effects of thermal shocks on drifting aquatic insects: a laboratory simulation. Journal fo the Fisheries Research Board of Canada 34:529–536.

Shields, F. D., R. E. Lizotte, S. S. Knight, C. M. Cooper, and D. Wilcox. 2010. The stream channel incision syndrome and water quality. Ecological Engineering 36:78–90.

Soil Survey Staff United States Department of Agriculture, N. R. C. S. 2010. Soil Survey Geographic (SSURGO) Database for Piedmont Region of North Carolina.

Somers, K. A., E. S. Bernhardt, J. B. Grace, B. A. Hassett, E. B. Sudduth, S. Wang, and D. L. Urban. 2013. Streams in the urban heat island: spatial and temporal variability in temperature. Freshwater Science.

Somers, K. A., E. S. Bernhardt, M. Losordo, and D. L. Urban. (n.d.). Downstream propagation of thermal pollution in urban streams.

Sponseller, R. A., E. F. Benfield, and H. M. Valett. 2001. Relationships between land use, spatial scale and stream macroinvertebrate communities. Freshwater Biology 46:1409–1424.

SPSS. 2007. IBM SPSS Amos. . IBM, Chicago, IL.

Sudduth, E. B., B. A. Hassett, P. Cada, and E. S. Bernhardt. 2011. Testing the Field of Dreams Hypothesis: functional responses to urbanization and restoration in stream ecosystems. Ecological Applications 21:1972–1988.

Sun, G., S. G. Mcnulty, J. A. M. Myers, and E. C. Cohen. 2009. Impacts of Multiple Stresses on Water Demand and Supply across the Southeastern United States 44.

Tischendorf, L., D. J. Bender, and L. Fahrig. 2003. Evaluation of patch isolation metrics in mosaic landscapes for specialist vs. generalist dispersers. Landscape Ecology 18:41–50.

Tsihrintzis, V. A., and R. Hamid. 1997. Modeling and management of urban stormwater runoff quality: A Review. Water Resources Management 11:137–164.

U.S. Army Corps of Engineers. 2010. HEC-RAS. . Davis, California.

U.S. Department of Agriculture, S. C. S. (USDA S. 1986. Technical Release (TR-55). . Natural Resources Conservation Service, Conservation Engineering Division.

United Nations Population Division. 2012. World Urbanization Prospects: The 2011 Revision.

United States Census Bureau. 2013. State and County QuickFacts. Data derived from Population Estimates, American Community Survey, Census of Population and Housing, County Business Patterns, Economic Census, Survey of Business Owners, Building Permits, Consolidated Federal Funds Report, Ce.

United States Department of Agriculture. 2009. NAIP Imagery. . U.S. Department of Agriculture, Farm Service Agency.

United States Environmental Protection Agency. 1999. Preliminary Data Summary Urban Storm Water Best Management Practices.

United States Environmental Protection Agency. 2006. NHDPlus Version1.

Urban, D. L. 2002. Tactical monitoring in landscapes. Pages 294–311 *in* J. Liu and W. Taylor, editors. Integrating landscape ecology into natural resource management. Cambridge University Press, Cambridge, UK.

Vannote, R. L., and B. W. Sweeney. 1980. Geographic Analysis of Thermal Equilibria - a Conceptual-Model for Evaluating the Effect of Natural and Modified Thermal Regimes on Aquatic Insect Communities. American Naturalist 115:667–695.

Violin, C. R., P. Cada, E. B. Sudduth, B. A. Hassett, D. L. Penrose, and E. S. Bernhardt. 2011. Effects of urbanization and urban stream restoration on the physical and biological structure of stream ecosystems. Ecological Applications 21:1932–1949.

Walsh, C. J., T. D. Fletcher, and A. R. Ladson. 2005a. Stream restoration in urban catchments through redesigning stormwater systems: looking to the catchment to save the stream. Journal of the North American Benthological Society 24:690–705.

Walsh, C. J., A. H. Roy, J. W. Feminella, P. D. Cottingham, P. M. Groffman, and R. P. Morgan. 2005b. The urban stream syndrome: current knowledge and the search for a cure. Journal of the North American Benthological Society 24:706–723.

Wang, L. H., and P. Kanehl. 2003. Influences of watershed urbanization and instream habitat on macroinvertebrates in cold water streams. Journal of the American Water Resources Association 39:1181–1196.

Wang, S.-Y., E. B. Sudduth, M. D. Wallenstein, J. P. Wright, and E. S. Bernhardt. 2011. Watershed urbanization alters the composition and function of stream bacterial communities. PloS one 6:e22972.

Ward, J., and J. Stanford. 1995. Ecological connectivity in alluvial river ecosystems and its disruption by flow regulation. Regulated Rivers: Research & Management 11:105–119.

Ward, J. V, and J. A. Stanford. 1982. Thermal Responses in the Evolutionary Ecology of Aquatic Insects. Annual Review of Entomology 27:97–117.

Weaver, J., S. Terziotti, K. Kolb, and C. Wagner. 2012. StreamStats in North Carolina: A Water-Resources Web Application. pubs.usgs.gov.

Webb, B. W., D. M. Hannah, R. D. Moore, L. E. Brown, and F. Nobilis. 2008. Recent advances in stream and river temperature research. Hydrological Processes 22:902–918.

Webb, B., and Y. Zhang. 1997. Spatial and seasonal variability in the components of the river heat budget. Hydrological Processes.

Wenger, S. J., A. H. Roy, C. R. Jackson, E. S. Bernhardt, T. L. Carter, S. Filoso, C. A. Gibson, W. C. Hession, S. S. Kaushal, E. Marti, J. L. Meyer, M. A. Palmer, M. J. Paul, A. H. Purcell, A. Ramirez, A. D. Rosemond, K. A. Schofield, E. B. Sudduth, and C. J. Walsh. 2009. Twenty-six key research questions in urban stream ecology: an assessment of the state of the science. Journal of the North American Benthological Society 28:1080–1098.

Winston, R., W. Hunt, and W. Lord. 2011. Thermal Mitigation of Urban Storm Water by Level Spreader–Vegetative Filter Strips. Journal of Environmental …:707–716.

Biography

Kayleigh Somers was born in Cocoa Beach, Florida, United States of America on the ninth of September, in the year 1986 to Robert Jay Somers and Valerie Ann Crawford. She went on to attend the University of Maryland, Baltimore County, graduating in 2008, *summa cum laude,* with a Bachelor of Science in Environmental Science and a Bachelor of Arts in English Literature. Somers has published one article: "Streams in the urban heat island: spatial and temporal variability in temperature" in the March 2013 issue of *Freshwater Science*. She is a member of Phi Beta Kappa and has received a number of accolades, including the National Science Foundation Doctoral Dissertation Improvement Grant ($15,000); the Center for Transformative Environmental Monitoring Program's Pilot Program Grant (equipment rental worth $42,000); the North American Benthological Society's Simpson Award ($600); the American Society for Limnology and Oceanography's Student Travel Award ($250); and the James B. Duke Fellowship (additional stipend support of $20,000). Somers looks forward to a career in urban watershed science and management.